UNIVERSIDADE DE LISBOA
FACULDADE DE CIÊNCIAS
DEPARTAMENTO DE QUÍMICA E BIOQUÍMICA

Diagnosis, Prognosis and Personalized Treatment of Cystic Fibrosis

Raquel Martins Centeio

Mestrado em Bioquímica
Especialização em Bioquímica Médica

Dissertação orientada por:
Professora Drª. Margarida Amaral,
Professor Dr. Karl Kunzelmann

2018

This page was intentionally left blank.

Acknowledgements and Dedication

First, I would like to thank my supervisors. Prof. Margarida Amaral, for the opportunity of joining her lab and starting my career in science in such a demanding work environment that allowed me to contact head on with innovative techniques in the translational medicine field. For the knowledge shared and for corrections to this thesis. Prof. Karl Kunzelmann, for receiving me in his lab, for acknowledging my hard work and being supportive, for the knowledge shared, for constructive criticism and for teaching me to "work smart". And Iris Silva, for all the guidance throughout this year, for shared early mornings and late nights of work, for showing me the good and the bad of working in a scientific research environment, for teaching me so so much and always being available to answer my questions, for the fruitful discussions, for the support and help and revision of all my progress reports, for so very thorough corrections to this thesis and for being a driving force for its improvement!

A special thanks goes to my lab colleagues (past and present) who have shared this experience with me and in some way, shape, or form helped build this thesis and the professional I am today.

From Portugal, to Miquéias for being supportive of my struggle, for all the reality checks, for sharing your experience with me and for saving me a position in your future lab (I will not forget this!). To Madalena, for all the conversations about our cloned families, for all the advices and suggestions and for having a work ethic I admire. To Margarida for always carefully but surely speaking her mind, for the readiness to teach and for having a hilarious twisted humour. To João for all the "it's none of my business but"s, for sharing your work experience and advices, for being another example of work ethics and for some laughs! To Aires for all the pivot tables, keyboard shortcuts, pipelines, codes, macros and micros you taught me about that helped make this thesis so much easier to put together. Also for all the chilled and open-minded talks! To Joana P for having such a mood-upbringing fashion style and for career talks. To Luís M for knowing and sharing so much about microscopy and always being available to help. To Luís S for the never-ending goofiness that make the heavy work lighter. To Filipa for always offering to lend a hand. To Tiago for being my first fellow Carnaxidense in science and for sharing some like-minded ideas. To André, Violeta and Ricardo for joining our team (although one year too late!) and for the thoughts and laughs we've shared already. Finally, to Sofia C, Sofia R, Susana, Hugo, Ines, Joana L, Sara, Arsénia, Prof. Carlos Farinha, Prof. Margarida Ramos and Prof. Luka Clarke for the knowledge and help shared. And to Tereza (from Prague) for trusting a newbie with her patients' samples. Ay caramba!

From Germany, I would like to thank Ji and Prof. Rainer for answering all my "but why"s and always being available to share their knowledge and experience. To Tini for all the 20 L batches of Ringer made last minute for me, for so many help offers and for being so interested in my work and my results. To Patricia for all the times I started my day off with a warming "You smell so good!". To Silvia for always being available to help me with lab bureaucracies. A very very special thanks goes out to Inês and Robi for taking me in so kindly, for being my German mommas and teaching me general home and life hacks, for forcing me out of my comfort zone and for all the conversations, picnics, parties and trips. Also to Filipe for showing me what true and genuine teamwork is, for all the help and for having my back!

I would also like to thank FCUL in general for becoming my second home, for the great professionals that guided me throughout these five amazing years spent in these facilities, for the friends made and the experience gained, for making a professional out of an unsure teen that thought that five years would be a hell to go through, and now they have flown by, unnoticed. Thank you sincerely.

Aos meus amigos!!! À Cláu e à Jana por participarem nesta jornada de cinco anos comigo, pelas ambições e sonhos partilhados, pela torcida mútua, pelos almoços, jantares e risadas e por tornarem esta experiência e os seus momentos mais difíceis, tão mais fáceis. À Gata por ser o meu maior exemplo de ambição, persistência e organização e por mostrar-me que há sempre tempo para tudo, se as prioridades estiverem bem ordenadas. À Valente por percorrer comigo todas as Padarias Portuguesas de Lisboa e tomar em cada uma delas aquele pequeno-almoço longo onde os desabafos são muitos e a paciência e os ouvidos incansáveis. Ao Sebas por lembrar-me constantemente que aconteça o que acontecer, podia sempre ser pior! À Baltas por ser o *yang* para o meu *yin*, por saber ler-me melhor que ninguém, por estar ao meu lado há já 11 anos e ainda não se ter atirado de um penhasco. Ao B por estar sempre pronto a ir, seja onde for! Por todas as viagens planeadas e não concretizadas (é desta!). Ao Du pela alegria e animação constantes, irritantes e contagiantes, e por conseguir sempre tirar-me a cara feia. Ao Gui pela amizade leal, sincera e companheira que um dia serei capaz de retribuir. A todos os meus amigos pelos almoços, cafés e jantares que falhei porque estava a trabalhar ou porque estava a trabalhar, ou porque, quando não estava a trabalhar, estava a trabalhar. Por me conhecerem, por me compreenderem, por me respeitarem e por continuarem sempre aqui, a aguentar-me de pé!

Ao Miguel por ser o meu amuleto da sorte, pelo carinho e apoio incondicionais, pela paciência inumana, pelo verdadeiro companheirismo nos bons e nos maus momentos e por ser feliz com a minha felicidade.

À minha família!!! À minha prima Vânia por ser um exemplo de determinação, luta e conquista, pelos conselhos, pelo apoio e pela motivação. "Yes we can"! E ao Tio Neto, à Tia Alice, à Vanessa e ao Valter (e novos membros!), ao Tio João e família, por torcerem sempre por mim e celebrarem todos os meus pequenos sucessos. Ao meu irmão por puxar-me e empurrar-me sempre para fora da minha zona de conforto, por ser um exemplo de um espírito independente e aventureiro e por pôr sempre a família em primeiro lugar. À minha mãe por desejar o melhor para mim, por fazer-se sentir nas alturas mais difíceis e por estar sempre orgulhosa dos meus pequenos passos para um futuro maior. À minha maninha por assistir ao treino de todas as minhas apresentações "super técnicas", por aguentá-las até ao fim e criticá-las sempre construtivamente, apesar de não ter uma veia científica no corpo! Pelo carinho e apoio, por ser uma pequena mulher e por ser uma artista inspiradora!!!

Por fim, ao meu pai. À pessoa que sempre acreditou em mim mais do que eu alguma vez acreditei em mim mesma, pelo amor e apoio incondicionais, inquestionáveis e incansáveis nos bons e nos maus momentos, por estar sempre aqui. Por ensinar-me a conhecer o meu valor, a lutar pelo que quero e pelo que mereço, a celebrar humildemente as minhas vitórias, a não gozar louros do que não ganhei pelo meu próprio mérito e a reconhecer e agradecer sempre a contribuição de outros para o meu sucesso. Por ser a matriz do meu carácter, das minhas ambições e do meu empenho. Por querer mais do que tudo a minha felicidade. Espero fazer-te eternamente orgulhoso!

A todos, o meu mais sincero obrigada.

Dedico o fim deste capítulo à Vóvó e à Titi

Summary

Cystic Fibrosis (CF) is the most common lethal autosomal recessive genetic disorder in Caucasian populations. CF is caused by over 2000 mutations in the *Cystic Fibrosis Transmembrane conductance Regulator* (*CFTR*) gene, that encodes a cAMP-activated and phosphorylation-regulated chloride (Cl^-) and bicarbonate (HCO_3^-) channel expressed at the apical membrane of epithelial cells. Malfunction of mutant CFTR leads to dysregulation of ion and fluid homeostasis across several epithelia, resulting in dehydration and obstruction of ducts, atrophic epithelia, gland hypertrophy, inflammation and tissue fibrosis. The airways disease, characterized by an impaired mucociliary clearance and recurrent cycles of infection, inflammation and scarring, that cause progressive loss of lung function, remains the major cause of morbidity and mortality among CF patients. A classification system of *CFTR* mutations according to the respective functional defect elicited on the CFTR protein has been proposed and these classes (I-VII) have been evolving as theratypes, i.e., groups of mutations that are expected to be rescued by the same therapeutic strategy. Small-molecule drugs have recently been approved for treatment of CF patients carrying selected mutations, namely VX-770 (or ivacaftor, marketed as Kalydeco®), a potentiator of the CFTR channel, and combinations of this potentiator with correctors of the folding/ trafficking defects of the most frequent mutant (F508del-CFTR), namely VX-809 (lumacaftor, which in combination with ivacaftor is known as Orkambi®) and VX-661 (tezacaftor, known as Symdeco® when combined with ivacaftor). However, for patients carrying orphan mutations – very rare and un- or mischaracterized variants – it is unknown whether they can benefit from already approved therapies and it is unlikely that further therapeutic efforts will be made towards correction of these mutants. Against this background and given the fact that CF severity is also partially dependent on other non-*CFTR* related genetic modifiers and non-genetic factors such as environmental determinants, patient-personalized approaches are becoming the gold standard for CF diagnosis, prognosis and therapeutic advice.

In this MSc project, we first aimed to assess CFTR function in native tissues and primary cultures from CF/CF-suspicion patients carrying different (rare) mutations through (i) Ussing chamber measurements of CFTR-mediated Cl^- secretion in rectal biopsies, (ii) Forskolin(Fsk)-induced swelling (FIS) assays of 3D-intestinal organoids derived from these biopsies and (iii) Ussing chamber measurements in isolated human nasal epithelial cells (HNECs) to establish a CF diagnosis and possible prognosis for the studied patients. Our second goal was to repurpose the approved CFTR modulator drugs by testing them in the patient-derived primary cultures and using the above approaches to assess CFTR rescue after incubation with these drugs. Finally, we aimed to identify which among the CFTR function parameters used provide the best correlations with CF-relevant outcomes from patients, so as to further establish them as robust biomarkers for CF diagnosis, prognosis and personalized treatment.

We were able to support a diagnosis for 25/26 studied patients, with 14 being CF (mild) (i.e., with residual CFTR function) and 8 being CF (severe) (i.e., no residual CFTR function). For the remainder 3 patients, a non-CF diagnosis was proposed due to detection of high levels of Cl^- secretion and presentation of a normal or inconclusive clinical phenotype. We were also able to detect rescue of CFTR function by at least one of the current CF-approved drugs, with potential for clinical benefit, for 7/13 patients' samples assessed, some of which carry mutations outside of the approved drug labels (e.g. S955P). In the end, the cAMP and cholinergic co-activated CFTR-mediated current measured in rectal biopsies correlated best with donor-matched CFTR-dependent organoid swelling at 0.8 µM Fsk, and both these parameters also correlated strongly with more established CF biomarkers, namely the sweat chloride and fecal elastase E1 values. Overall, our results further validate the use of CFTR function measurements in rectal biopsies and 3D-intestinal organoids as personalized predictive tools for CF.

Key-words: Cystic Fibrosis; CFTR; Orphan mutations; Personalized medicine; CFTR modulators.

Resumo

A Fibrose Quística (FQ) é a doença autossómica recessiva letal mais comum em populações de origem Caucasiana, e afeta cerca de 85.000 pessoas em todo o mundo. Esta doença é causada por mais de 2000 mutações no gene *CFTR* (*Cystic Fibrosis Transmembrane conductance Regulator*), que codifica para um canal de cloreto (Cl^-) e bicarbonato (HCO_3^-) expresso na membrana apical das células epiteliais e que é ativado pelo cAMP e regulado por fosforilação. A CFTR atua também na regulação de outros canais epiteliais como o canal epitelial de sódio (Na^+) ENaC (*Epithelial sodium channel*). A disfunção da proteína CFTR leva à desregulação da homeostase iónica e hídrica em vários tecidos epiteliais, resultando na desidratação e obstrução de ductos, atrofia epitelial, hipertrofia de glândulas, inflamação crónica e fibrose dos tecidos. No caso particular das vias respiratórias, a deficiente secreção de Cl^- pela CFTR e a hiperabsorção de Na^+ pela ENaC leva à desidratação do líquido que reveste as superfícies respiratórias, aumentando a viscosidade das secreções e comprometendo o mecanismo de limpeza mucociliar, levando à mucoestase. Isto resulta em colonizações bacterianas recorrentes, obstrução das vias áereas, inflamação crónica e deterioração do tecido, que levam à perda progressiva da função pulmonar, que continua a ser a maior causa de morbilidade e mortalidade para os pacientes com FQ. O elevado número de mutações descritas no gene *CFTR* tem sido categorizado com base no respetivo defeito funcional causado ao nível da proteína em sete classes, numeradas de I-VII, que têm evoluído para teratipos, i.e., conjuntos de mutações que poderão ser corrigidas pela mesma estratégia terapêutica. Mutações de classe I originam tipicamente um codão *stop* prematuro no mRNA do *CFTR*, levando à sua degradação e à redução da expressão duma variante truncada da proteína CFTR; mutações de classe II resultam num defeito do enrolamento tridimensional da proteína (*misfolding)*, levando à sua retenção e degradação no retículo endoplasmático, resultando na sua ausência na membrana apical; mutações de classe III interferem com a regulação do canal da CFTR, reduzindo drasticamente a sua probabilidade de abertura e transporte de iões; mutações de classe IV levam a constrangimentos no poro do canal com a consequente redução da respetiva condutância; mutações de classe V são tipicamente associadas a mecanismos de *splicing* alternativo que levam à produção de transcritos normais e aberrantes do gene *CFTR* em diferentes rácios, levando a uma significativa redução dos níveis de proteína normal; mutações de classe VI desestabilizam a CFTR na membrana plasmática, reduzindo assim sua função; mutações de classe VII são chamadas de "irrecuperáveis", uma vez que causam defeitos tão significativos no *CFTR* que não podem ser farmacologicamente corrigidos, como, por exemplo, grandes deleções do gene. Estas últimas resultam na ausência de transcritos do *CFTR* e consequentemente não existe qualquer expressão da proteína. Recentemente, foram desenvolvidas e aprovadas pequenas moléculas para o tratamento de pacientes com FQ que possuem mutações específicas no *CFTR*, nomeadamente o VX-770 (ou ivacaftor), um potenciador da CFTR que leva ao aumento da probabilidade de abertura do canal, e tratamentos combinatórios deste potenciador com as moléculas VX-809 (ou lumacaftor) ou VX-661 (ou tezacaftor), corretoras de defeitos do tráfego do canal. Estes medicamentos estão comercializados como Kalydeco® (VX-770), Orkambi® (VX-809/770) e Symdeco® (VX-661/770), respetivamente. No entanto, para pacientes que possuem mutações órfãs – mutações raras cujo defeito funcional causado na CFTR é indefinido ou está mal caracterizado – ainda não se sabe se poderão beneficiar das terapias já aprovadas. Além disso, não é expectável que venham a ser desenvolvidos esforços direcionados para o desenvolvimento de terapias específicas para estas mutações, devido ao baixo número de pacientes que as expressam, associado à sua elevada distribuição geográfica. Dado isto, e o facto de que a gravidade da FQ é também parcialmente dependente doutros fatores genéticos não associados ao *CFTR* (p.ex., genes modificadores) e fatores não-genéticos (p.ex., ambientais), as abordagens personalizadas ao paciente individual, que têm em conta além do genótipo do *CFTR* e do defeito funcional que é causado na proteína, têm-se tornado no padrão-ouro para o

diagnóstico, prognóstico e aconselhamento terapêutico da FQ. Um conjunto de metodologias inovadoras têm vindo a ser desenvolvidas na área da FQ, permitindo a análise laboratorial de células/tecidos derivados do próprio paciente para seleção pré-clínica de pacientes que respondam positivamente a tratamentos já aprovados.

O primeiro objetivo deste projeto de Mestrado foi avaliar a função da CFTR em tecidos nativos e culturas primárias de pacientes com FQ ou suspeita de FQ, apresentando diferentes mutações no gene *CFTR*, com principal foco em pacientes com mutações raras ou ultra-raras. Isto foi realizado através de (i) medições electrofisiológicas da secreção de Cl^- mediada pela CFTR em biópsias rectais de pacientes usando a câmara de Ussing, (ii) ensaios do inchamento induzido por Forscolina (FIS – *Forskolin(Fsk)-induced swelling*), um ativador da CFTR que atua no aumento dos níveis intracelulares de cAMP, em culturas primárias de organóides intestinais 3D derivados destas biopsias rectais e (iii) medições electrofisiológicas da atividade da CFTR em culturas primárias de células epiteliais nasais isoladas dos pacientes, usando também a câmara de Ussing, a fim de estabelecermos um diagnóstico e possível prognóstico de FQ para os pacientes estudados. O nosso segundo objetivo foi reaproveitar os fármacos já aprovados para a correção de defeitos na CFTR, testando-os nas culturas primárias dos pacientes e usando novamente as metodologias supramencionadas para avaliar o resgate da função da CFTR após incubação com estas moléculas. Através disto, pretendíamos determinar qual a melhor terapia para cada paciente, de uma forma personalizada, bem como identificar mutações órfãs que respondessem positivamente aos tratamentos já aprovados. Finalmente, o nosso último objetivo foi identificar qual/quais de entre os parâmetros de avaliação da função da CFTR usados correlacionaria melhor com os resultados clínicos dos pacientes, permitindo validá-lo(s) como biomarcadores robustos para o diagnóstico, prognóstico e tratamento personalizado da FQ.

Através da nossa análise pudemos apoiar um diagnóstico para 25/26 pacientes estudados, tendo classificado 14 como pacientes com FQ não-clássica (i.e., com função residual da CFTR) e 8 com FQ clássica/severa (i.e., sem função da CFTR). Para os restantes 3 pacientes, propusemos a exclusão de um diagnóstico de FQ, devido à detecção de níveis elevados de secreção de Cl^- mediada pela CFTR nas suas biópsias rectais (i.e., função normal), a par de uma apresentação clínica não sugestiva de FQ. A análise por FIS dos organóides intestinais 3D dos pacientes, após incubação com os fármacos aprovados para a correção de disfunções da CFTR mutada, permitiu determinar a ocorrência do resgate da função da CFTR por pelo menos um desses fármacos (VX-770, VX-809/770 ou VX-661/770), com baixo, médio ou elevado potencial para benefício clínico, para 7/13 pacientes analisados, permitindo o reaproveitamento destas terapias para estes pacientes, alguns dos quais possuem mutações para as quais os fármacos não estão (ainda) aprovados (p.ex., S955P). Por fim, os nossos resultados da análise de correlações entre os parâmetros da função da CFTR usados neste projecto, mostraram ser a corrente dependente da CFTR, co-activada pelo cAMP e estímulos colinérgicos, detetada na análise de biópsias rectais em câmara de Ussing, o parâmetro que melhor se correlaciona com o inchamento dependente da CFTR dos organóides intestinais 3D, induzido por uma concentração de Fsk de 0.8 µM. Além disso, estes dois parâmetros funcionais também correlacionaram mais significativamente com outros biomarcadores de FQ melhor estabelecidos na área, nomeadamente as concentrações de Cl^- no suor e os valores de elastase fecal E1. Globalmente, os nossos resultados validam o uso das medições da função da CFTR em biópsias rectais e organóides intestinais 3D como ferramentas personalizadas preditivas para a FQ.

Palavras-chave: Fibrose Quística; CFTR; Mutações órfãs, Medicina personalizada; Moduladores da CFTR.

Table of Contents

Index of Figures and Tables

List of Acronyms and Abbreviations

#

2D	Two-dimensional
3D	Three-dimensional

A

ABC	ATP-binding cassette
AC	Adenyl cyclase
ALI	Air-liquid interface
Amil	Amiloride
AMP	Adenosine monophosphate
ANOVA	Analysis of variance
ASL	Airway surface liquid
ATP	Adenoside triphosphate
AUC	Area under the curve

C

Ca^{2+}	Calcium ion
cAMP	Cyclic adenosine monophosphate
CCH	Carbachol
CF	Cystic Fibrosis
CFBE	Cystic Fibrosis Bronchial Epithelia
CFTR	Cystic Fibrosis Transmembrane conductance Regulator
$CFTR_{inh}$-172	CFTR-inhibitor 172
CFTR-RD	CFTR-related disorders
Cl^-	Chloride ion

D

DMSO	Dimethyl sulfoxide

E

EMA	European Medicines Agency
ENaC	Epithelial sodium channel
ER	Endoplasmic reticulum
ERQC	Endoplasmic reticulum quality control

F

$F12^{ghp}$	Advanced DMEM/F12 + 1% Pen/Strep + 1% GlutaMax + 1% HEPES
FBS	Fetal bovine serum
FEE	Fecal elastase E1
FEV_1	Forced expiratory volume in 1 s
FDA	Food and Drug Administration
FIS	Forskolin-induced swelling
FRT	Fischer Rat Thyroid
Fsk	Forskolin

G

Gen	Genistein

H

HBECs	Human bronchial epithelial cells
HNECs	Human nasal epithelial cells
HCO_3^-	Bicarbonate

I

I/F	IBMX/Fsk
IBMX	3-isobutyl-1-methylxanthine
I_{eq-sc}	Equivalent short circuit current
ICL	Intracytoplasmic loop
ICM	Intestinal current measurements
IF	Immunofluorescence
Indo	Indomethacin
IRT	Immunoreactive trypsinogen

K

K^+	Potassium ion

N

Na^+	Sodium ion
NBD	Nucleotide binding domain
NBS	Newborn screening
NMD	Nonsense-mediated decay
NPD	Nasal potential difference
N-term	Amino-terminal

P

PBS	Phosphate-buffered saline
Pen/Strep	Penicilline/Streptomycin
PI	Pancreatic insufficiency/insufficient
PKA	Protein kinase A
PM	Plasma membrane
PS	Pancreatic sufficiency/sufficient
PTC	Premature stop codon

R

RD	Regulatory domain
rF508del	Rescued F508del
RT	Room temperature
R_{te}	Transepithelial resistance

S

SEM	Standard error of mean

T

t	Time
TEER	Transepithelial electrical resistance
TMD	Transmembrane domain

V

V_{te}	Transepithelial voltage

W

WT	Wild-type

1. Introduction

1.1. Cystic Fibrosis – An Overview

Cystic Fibrosis (CF) is the most common life-limiting rare disease, affecting around 85,000 people worldwide with prevalence rates significantly higher among Caucasian populations. This genetic condition has an autosomal recessive inheritance and it is caused by mutations in a single gene, the *Cystic Fibrosis Transmembrane conductance Regulator* (*CFTR*). The *CFTR* gene encodes for a cyclic AMP (cAMP)-dependent and phosphorylation-regulated chloride (Cl^-) and bicarbonate (HCO_3^-) channel, mostly expressed at the apical membrane of epithelial cells, that is responsible for the regulation of ion and fluid homeostasis across epithelia[1–3]. Besides functioning mainly as an ion channel, CFTR also plays a major role in the regulation of other epithelial channels, such as the epithelial sodium (Na^+) channel (ENaC)[4].

CF is a multisystem disease that is manifested in the epithelial-lined organs and tissues where CFTR is expressed, such as in the respiratory, reproductive and gastrointestinal tracts, including the biliary system, and the sweat glands. In these tissues, the malfunction of mutant CFTR leads to electrolyte and fluid transport disorders that result in obstructed ducts, atrophic epithelia, gland hypertrophy and ultimately inflammation and fibrosis[2,5].

The major cause of morbidity and mortality in CF is pulmonary disease, due to deficient CFTR-mediated Cl^- secretion and Na^+ hyperabsorption by ENaC. This leads to airway surface liquid (ASL) dehydration, which in turn results in impaired mucociliary clearance and mucostasis, recurrent bacterial colonization, airflow obstruction, chronic inflammation, progressive tissue damage and finally respiratory impairment (Figure 1.1)[6–8]. The impaired HCO_3^- secretion by mutant CFTR has also been shown to acidify the ASL, increasing its viscosity and mucus density – thus strengthening mucostasis – and inhibiting the activity of antimicrobial peptides there present[9–11].

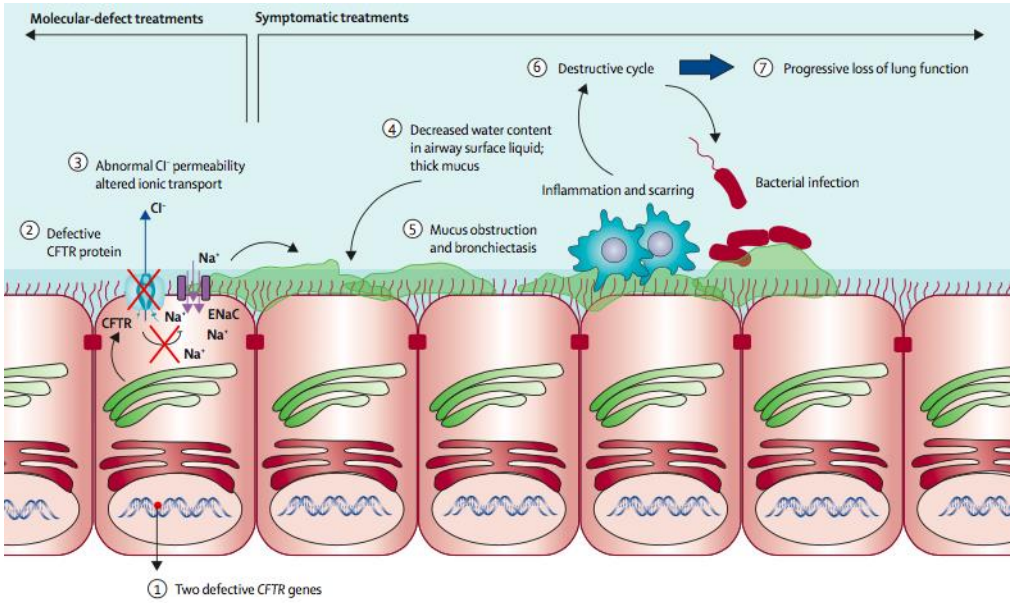

Figure 1.1 – Cystic Fibrosis pathophysiology. Lung disease is the main cause of death amongst CF patients. CF is caused by mutations in each of the two *CFTR* genes (1), which lead to absent or defective CFTR protein expression at the apical membrane of epithelial cells (2), causing abnormal electrolyte (3) and fluid (4) transport in epithelial-lined tissues. Airway surface liquid dehydration leads to thickened mucus (4), which causes obstruction of the airways and impaired mucociliary clearance (5). This results in recurrent cycles of airway infection, inflammation and scarring (6) that cause progressive lung damage and eventually loss of lung function (7). **Retrieved from De Boeck & Amaral (2016)[1].**

Despite progressive lung disease being the major cause of death for CF patients, noteworthy comorbidities caused by CFTR dysfunction occur in other affected organs. Namely, obstruction of pancreatic ducts and subsequent scarring and loss of exocrine function in the pancreas leads to pancreatic insufficiency, which results in nutrient malabsorption and poor growth; obstruction of the vas deferens in the embryonic male reproductive tract leads to their deterioration before birth and male infertility; excessive absorption in the baby's bowel leads to dehydration of the first stool and intestinal obstruction – a condition known as meconium ileus, that can also be present *in utero* –, while older CF patients also suffer from chronic constipation and rectal prolapse; in the sweat glands, the mechanism of NaCl reabsorption in the sweat ducts of CF patients is compromised, which results in sweat emerging from these glands with abnormally high salt concentrations, which may lead to acute dehydration, chronic salt depletion and electrolyte imbalance[8,12–15].

When CF was first described in the 1930s[16], the prognosis for a child diagnosed with CF was of infant/early childhood death, with meconium ileus and malnutrition related to pancreatic insufficiency being the main causes[2,12]. Today, median life expectancy for patients born after 2000 is estimated to be greater than 40 years old in developed countries. This improvement has been achieved mainly due to the early advent of therapies designed to treat the symptomatology of the disease, such as the administration of pancreatic enzyme supplements to replace pancreatic function, mucolytic and hydrator therapies to dissolve thick mucus and improve airway clearance, antibiotics to prevent and treat infections and anti-inflammatory drugs to lessen chronic inflammation[1,17]. The improved understanding of the disease also contributed to earlier and more accurate diagnoses with detection of milder and atypical forms of CF, culminating in better disease outcomes[18].

However, these therapies work in the downstream treatment of CF, i.e., at the level of the symptoms, and not in correcting the basic defect that leads to the disease pathophysiology. Also, although these symptomatic treatments have led to a significant increase in the patients' lifespan, progressive complications of the disease still emerge and the quality of life deteriorates. Moreover, the burden and cost of treatment become very significant for patients, their family and the health care systems that support them[19,20]. Thus, to further increase both the lifespan and the life quality of CF patients, therapies designed to correct the underlying molecular CFTR defects that cause CF are of utmost importance.

Since the cloning of the *CFTR* gene in 1989[21] and the new insights on the molecular alterations that lead to abnormal ion and fluid transport in epithelia and ultimately to CF clinical manifestations, research has been focused on developing new therapies directed to rescuing the lost CFTR function. For this, an intricate understanding of this gene and its products is essential.

1.2. CFTR

CFTR is one of the largest genes in the human genome, located in the long (q) arm of chromosome 7, at position 31.2[22]. This gene spans around 190 kb of genomic DNA and encodes an approximately 6.5 kb mRNA that comprises 27 exons and translates into a 1,480 amino-acids transmembrane glycoprotein with a molecular mass of 180 kDa[23].

The CFTR protein is a member of the ATP-binding cassette (ABC) membrane transporter superfamily, which make use of ATP hydrolysis to transport substrates across cellular membranes, normally against a concentration gradient[24]. This protein presents the typical ABC transporter architecture, consisting of two homologous halves that comprise in total two transmembrane domains

(TMD1/2) that form the channel pore, and two nucleotide binding domains (NBD1/2) that bind and hydrolyse ATP, regulating the gating of the channel. Unique to CFTR is an additional regulatory domain (RD), that links the two halves, with multiple phosphorylation sites[25] (Figure 1.2 and Figure 7.1 in Appendix I). Alike other secretory pathway proteins, CFTR biogenesis starts with its synthesis and folding in the endoplasmic reticulum (ER), where it undergoes co-translational core-glycosylation. After efficient folding is assessed by the ER quality control (ERQC) system, this immature form of CFTR is allowed to exit the ER and migrate through the Golgi complex, where it undergoes further processing to reach its mature fully-glycosylated form and is then delivered to the plasma membrane (PM)[26]. However, CFTR is the only known member of this family that acts as an ion channel, since, differently from other ABC transporters, it moves ions down their concentration gradient[24]. ATP binding favours the NBDs dimerization and channel opening after cAMP activation of protein kinase A (PKA) and RD phosphorylation, and ATP hydrolysis favours the NBDs dissociation and channel closing[27,28].

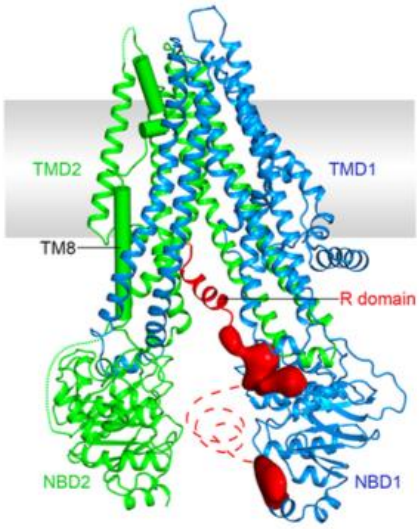

Figure 1.2 – CFTR structure determined by electron cryomicroscopy (cryo-EM). 3.9 Å molecular structure of human CFTR determined in the dephosphorylated, ATP-free conformation. CFTR is a 1,480 amino-acids transmembrane glycoprotein belonging to the ATP-binding cassette (ABC) superfamily of membrane transporters that uniquely works as a channel, moving ions down their concetration gradient. CFTR possesses two transmembrane domains (TMD1/2) that form the channel pore, each containing six hydrophobic alpha-helices which cross the cell surface lipid bilayer, joined by two intracellular loops and three extracellular loops; two nucleotide-binding domains (NBD1/2) with ATP-binding locations where hydrolysis occurs; and one unique regulatory domain (R domain) with protein kinase A (PKA) phosphorylation sites. CFTR channel opening is favoured by ATP binding and PKA phosphorylation and channel closing is favoured by ATP hydrolysis. The EM densities shown in red correspond to unstructured regions and dashed lines represent unresolved regions in the structure. Also depicted is a recently identified feature that distinguishes CFTR from all other ABC transporters – a helix-loop transition in transmembrane helix 8 (TM8) – which is thought to form the structural basis for CFTR's channel function. **Retrieved from Liu *et al*. (2017)[28].**

As mentioned previously, mutations in the *CFTR* gene often disrupt CFTR expression and/or function and if two dysfunctional mutations occur in both *CFTR* alleles, they ultimately lead to CF. To date, more than 2,000 mutations have been described, most presumed to be CF-causing. These consist of 39.30% missense, 15.68% frameshift, 13.26% sequence variation, 11.29% splicing, 8.33% nonsense, 2.61% large and 2.07% in-frame insertions/deletions, 0.84% promoter and 6.61% unknown significance mutations, that span all across the different CFTR protein domains[29].

F508del (previously ΔF508), is a deletion of three nucleotides that leads to the absence of the amino-acid phenylalanine at position 508 of the CFTR protein (in NBD1), and it is by far the most common CF-causing mutation, being present in about 70% of patients worldwide on at least one allele, with some geographic variations[30]. Other mutations have varying frequencies that also differ significantly among ethnic populations[2].

In general, all mutations that are CF-causing ultimately lead to defective Cl^- and HCO_3^- secretion by epithelial cells and consequent disruption of normal salt and water transport across epithelia. However, disease severity depends on how a specific mutation affects the *CFTR* gene products. Therefore, the elucidation of the pathologic molecular mechanisms elicited by each mutation is very informative, not only for structure-function studies of the CFTR channel but also for the development of small-molecule compounds (so-called modulators) that target these underlying defects, in a mutation-specific corrective therapy approach[1,31].

In 1993, it was proposed to classify these mutations according to the functional defect elicited on CFTR[32], in an attempt to allow for class-specific prognosis of CF-related cellular and clinical phenotypes. These functional classes have more recently evolved into theratypes, with the expectation that the same therapeutic strategies will be suitable to all mutations of the same class[1].

1.2.1. Functional classification of *CFTR* mutations and theratypes

This classification system underwent several improvements throughout the years and today *CFTR* mutations can be grouped according to their elicited functional defect into seven classes[1,31–33], for which some functional defect-specific corrective therapies have been proposed[1,2,33] (Figure 1.3).

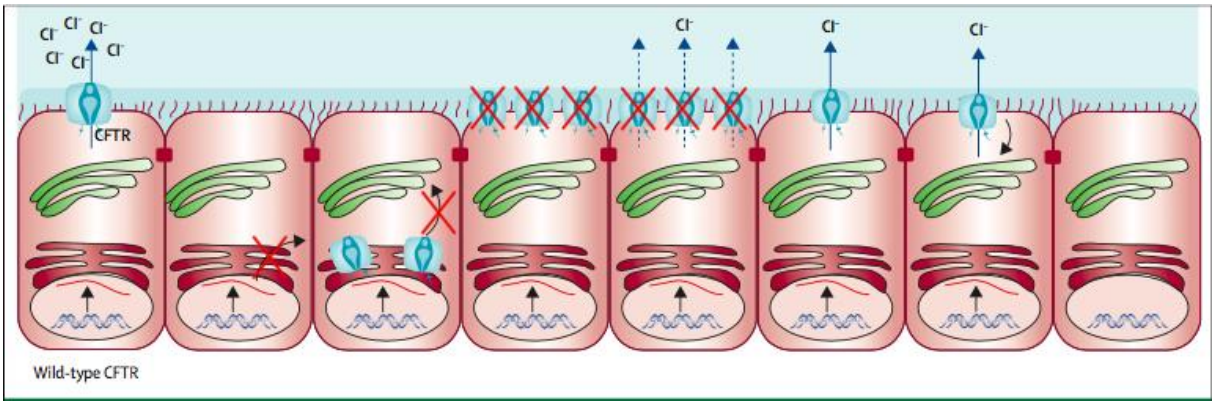

	Class I	Class II	Class III	Class IV	Class V	Class VI	Class VII
CFTR defect	No protein	No traffic	Impaired gating	Decreased conductance	Less protein	Less stable	No mRNA
Mutation examples	Gly542X, Trp1282X	Phe508del, Asn1303Lys, Ala561Glu	Gly551Asp, Ser549Arg, Gly1349Asp	Arg117His, Arg334Trp, Ala455Glu	Ala455Glu, 3272-26A→G, 3849+10 kg C→T	c. 120del23, rPhe508del	dele2,3(21 kb), 1717-1G→A
Corrective therapy	Rescue synthesis	Rescue traffic	Restore channel activity	Restore channel activity	Correct splicing	Promote stability	Unrescuable
Drug (approved)	Read-through compounds (no)	Correctors (yes)	Potentiators (yes)	Potentiators (no)	Antisense oligonucleotides, correctors, potentiators? (no)	Stabilisers (no)	Bypass therapies (no)

Figure 1.3 – Functional classification of CFTR mutations and theratype-specific CFTR modulators. *CFTR* mutations can be grouped into seven classes (I-VII), according to the functional defect elicited on the CFTR protein. Classes I-III and VII mutations confer absent or severe loss of CFTR production and function by different mechanisms and are associated with no residual function. Classes IV-VI mutations are less severe and associated with some residual, although highly variable, CFTR function. Functional defect-specific corrective therapies have been proposed to be applicable to all mutations belonging to the same class (theratypes). Mutation examples are presented. Gly = Glycine; X = Stop codon; Trp = Trypthophan; Phe = Phenylalanine; del(e) = deletion; Asn = Asparagine; Lys = Lysine; Ala = Alanine; Glu = Glutamine; Asp = Aspartate; Ser = Serine; Arg = Arginine; His = Histidine; r = rescued. **Retrieved from De Boeck & Amaral (2016)[1].**

I. **Class I** mutations cause a defect in protein production; these are generally nonsense mutations, i.e., those originating a premature stop codon (PTC), which often lead to mRNA degradation by nonsense-mediated decay (NMD), resulting in severely reduced or absent CFTR expression; e.g. G542X. These synthesis defects have been proposed to be corrected by read-through compounds, such as aminoglycoside antibiotics, that read through the PTC allowing for translation to continue to produce the full-length protein;

II. **Class II** mutations cause a defect in CFTR trafficking due to protein misfolding and subsequent retention at the ER and premature degradation by the ERQC system. This results in impaired normal biogenesis by preventing the protein from migrating to the cell membrane, leading to a severely reduced number of CFTR proteins at the cell surface; e.g. F508del. These processing defects can be rescued by chemical or pharmacological chaperones that promote protein folding, allowing for the mutant CFTR to escape degradation and to reach the cell surface. Such compounds have been named correctors; e.g. VX-809 (also known as lumacaftor);

III. **Class III** mutations impair the regulation of the CFTR channel, resulting in abnormal gating characterized by a reduced open probability; e.g. G551D. These defects can be restored by activators that increase this probability, which have been termed potentiators; e.g. VX-770 (also known as ivacaftor);

IV. **Class IV** mutations lead to a reduced channel conductance, i.e., flow of Cl^- and HCO_3^- ions; e.g. R334W. Conductance defects should be restored by increasing the overall cell surface amount of the mutant proteins, by the usage of CFTR correctors, or by increasing the level of activation of the already existing membrane channels, by using CFTR potentiators;

V. **Class V** mutations lead to a substantial decrease in the levels of normal CFTR being expressed. Usually, they affect the transcription factors' binding in the promoter or, more often, an alternative splicing that generates both aberrant and normal mRNA in different ratios; e.g. 3849+10kbC>T. This may be overcome by the usage of antisense oligonucleotides for the correction of mis-splicing and promoter sequence changes, while correctors and potentiators may also enhance the functional levels of mutant CFTR;

VI. **Class VI** mutations destabilize CFTR at the PM, either by reducing its conformational stability, increasing its endocytosis or decreasing its recycling back to the cell surface. This results in an accelerated turnover of CFTR and thus reduced expression at the membrane; e.g. rescued F508del. Stability defects have been proposed to be corrected by compounds that enhance CFTR retention at the cell surface, such as activators of Rac1 signaling like the hepatocyte growth factor;

VII. **Class VII** mutations are the so-called unrescuable CFTR mutations and include newly re-categorized mutations from class I that lead to the absence of mRNA production, and that cannot be pharmacologically rescued. These include large deletions such as the dele2,3(21kb) mutation. This class of defects requires bypass therapeutic strategies that can involve, for example, the stimulation of alternative Cl^- channels or gene editing/therapy – these are also suitable for all other mutation classes and are thus called 'mutation agnostic' therapies.

CFTR mutations are associated with a wide spectrum of clinical phenotypes but, in general, a homozygous or compound heterozygous genotype enclosing mutations belonging to classes I-III and VII – which should confer total absence of CFTR function by different mechanisms[12] – are associated with earlier and more severe manifestations of the disease (referred to as classical/severe CF), such as pancreatic insufficiency (PI). Mutations from classes IV-VI, on the other hand, are associated with some residual function, albeit variable, and patients bearing these mutations on at least one allele normally display milder forms of CF (called non-classic/mild/atypical CF), such as commonly being pancreatic

sufficient (PS)[34]. However, it is noteworthy to mention that this classification system encloses some oversimplifications since the same mutation might cause more than just one functional defect[2,12].

Nevertheless, recently, some of these above proposed therapeutics have been developed and approved for the treatment of CF patients bearing specific *CFTR* mutations, based on positive findings from clinical studies in which they demonstrate sustained improvements in lung function and sweat chloride levels, weight gain, and improvement in other CF-relevant parameters, when compared to placebo[35–37].

VX-770 (or ivacaftor, marketed as Kalydeco® by Vertex Pharmaceuticals Incorporated, Boston) is a potentiator molecule that was approved by the United States Food and Drug Administration (FDA) in January 2012, for the treatment of CF patients with the G551D gating mutation. This potentiator has later been approved to treat a larger number of residual function mutations (such as D1152H, S1251N, 3849+10kbC>T, 2789+5G>A, among others; 38 in total)[38]. VX-809 (or lumacaftor) and VX-661 (or tezacaftor) are corrector compounds that have both been approved in combination therapy with VX-770 (corrector/potentiator combo) to treat patients with the F508del mutation in both CFTR alleles, the most common genotype in CF (VX-809/770 combo, marketed as Orkambi® by Vertex Pharmaceuticals Inc., FDA approved in July 2015; VX-661/770 combo, marketed as Symdeko® by Vertex Pharmaceuticals Inc., FDA approved in February 2018)[38]. Symdeko® has also been approved for patients who have at least one of 26 residual function mutations in the *CFTR* gene that were shown to be responsive to treatment[38]. Both Kalydeco® and Orkambi® have also received approval for European marketing by the European Medicines Agency (EMA)[39].

1.2.1.1. Orphan mutations

While the most common *CFTR* mutations, such as F508del and G551D (frequencies of 0.70 and 0.02, respectively)[30] have already been extensively characterized, both molecularly and in terms of the disease liability[40], few data are available for a large number of so-called orphan *CFTR* mutations. These are rare variants for which prediction of the potential disease outcome is difficult, due to the low numbers of patients worldwide that carry them and also because the respective CFTR functional defect remains undefined or might be mischaracterized. Also, in general, therapeutic efforts are not directed towards correction of these mutants. For these reasons, it is unknown whether some orphan mutations can benefit from already approved CFTR therapies. Thus, it becomes extremely important to characterize them at the molecular, cellular and functional levels, and in regards to their specific response to CFTR modulators, in order to improve the diagnosis and prognosis of CF for all patients, while also providing insight into mutation-specific correction.

1.3. Current Diagnosis Methods

In general, diagnosis of CF traditionally combines several aspects, such as: presentation of one or more characteristic clinical manifestations of the disease, a history of CF in a sibling or a positive newborn screening test and laboratory evidence of CFTR dysfunction, whether through *CFTR* genotyping or by assessing CFTR function through sweat Cl^- or nasal potential difference (NPD) measurements[41,42].

1.3.1. Sweat Cl^- and Nasal Potential Difference measurements

Classically, measurements of the sweat Cl^- concentration in patients (pathologic if $[Cl^-] > 60$ mmol/L) have been the gold standard to support a CF diagnosis. Sweat Cl^- abnormalities occur early and can be measured in patients at any age, since sweat glands do not appear to sustain secondary damage from progressive CF. Plus, the method is highly convenient and rather uncostly[43]. However, despite the diagnosis of the more classic cases of CF being easy and established early in life, asymptomatic/less severe patients remain difficult to diagnose, due to limited clinical features of CF and inconclusive diagnostic tests[41]. Therefore, new laboratory diagnostic methods have been emerging to fight the current limitations. The ultimate goal is to establish a robust approach with more feasible readout thresholds, to better discriminate between non-CF subjects and mild or severe CF patients.

In order to support doubtful CF diagnoses, some centers also perform measurements of NPD[44], a technique that evaluates Na^+ and Cl^- transport in the nasal airway epithelium through the estimation of transepithelial bioelectrical properties[45]. NPD is the only direct *in vivo* measurement capable of separating and detecting specific CFTR-dependent Cl^- transport, since the nasal cavity provides a rather accessible site to examine the ion transport in the airways[45]. However, this method requires a highly experienced operator and results yield a high variability, even between the two nostrils of the same patient[46]. Moreover, NPD is unreliable in patients who have suffered nasal epithelium damage, such as infection or polyp formation, which are common secondary effects in late CF. Sweat Cl^- measurements on the other hand, also have low reproducibility and often lead to false positives, as they depend highly on technical, dermatologic and environmental conditions, among others[46,47]. More recently, *ex vivo* measurements of CFTR-mediated Cl^- secretion in rectal biopsies have emerged as a new laboratory diagnostic aid in the CF field[48,49].

1.3.2. Intestinal current measurements in rectal biopsies

Ussing chamber intestinal current measurements (ICM) of CFTR-mediated Cl^- secretion in human rectal biopsies have been established as a sensitive and robust biomarker for CF diagnosis and prognosis[48,49] (Figure 1.4). This indirect *ex vivo* measure of CFTR function in native colonic epithelia has been used to confirm/exclude a CF diagnosis in individuals with a clinical suspicion of CF, through comparison of the obtained values with CF reference groups and non-CF control groups[50]. Furthermore, these measurements have shown a significant correlation with more established CF biomarkers and clinical parameters, such as pulmonary function[50]. Also, it has been reported that these measurements alone or in combination with sweat Cl^- and fecal elastase E1 (FEE) values, measured to assess the patient's exocrine pancreatic function (sufficient if > 200 µg/g stool), provide the best tool so far for a discriminative diagnosis among non-CF individuals and patients with classic or non-classic CF[50].

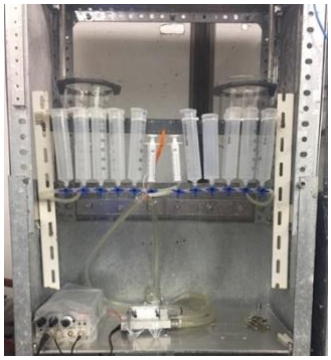

Figure 1.4 – Ussing chamber analysis of rectal biopsies. Ussing chamber setup arrangement for analysis of rectal biopsies.

To exclude/support a CF diagnosis and prognosis through Ussing chamber analysis of human rectal biopsies, a standard protocol was developed to study the Cl^- channel function of CFTR in the context of this native epithelium[48]. A schematic representation of ion transport mechanisms in colonic epithelial cells is presented in Figure 1.5.

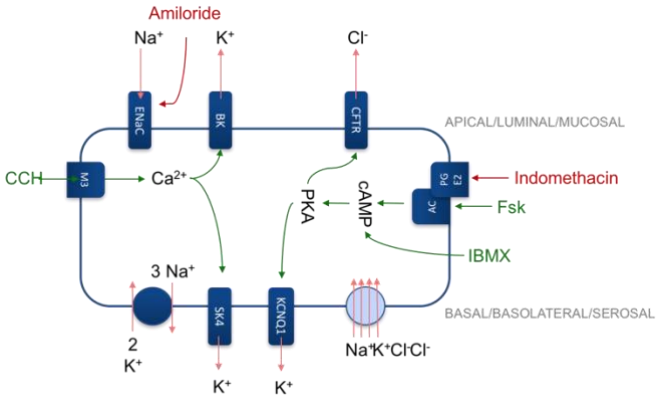

Figure 1.5 – Ion transport processes in human colonic epitelhial cells. Schematic representation of transcellular ion transport regulation in colonic epithelial cells with external stimulators (in green) and inhibitors (in red).

In this protocol, luminal Amiloride is first applied to block electrogenic Na^+ absorption through ENaC (Figure 1.5). Then, basolateral stimulation with carbachol (CCH), a cholinergic agonist, leads to calcium (Ca^{2+})-activation of potassium (K^+) channels and K^+ release, constituting the driving force for the apical Cl^- exit through CFTR, and has been show to typically induce Cl^- secretory responses (transient lumen-negative deflections in transepithelial voltage (V_{te})) in normal tissues and predominant apical K^+ secretory responses (transient lumen-positive) in CF tissues, due to lack of CFTR activity (Figure 1.6 A-C, first peak). However, due to low levels of endogenous prostaglandins that stimulate adenyl cyclase (AC) to produce cAMP, lumen-positive responses can also be observed in normal tissues[48,49]. Stimulation with CCH in the presence of Indomethacin, which abolishes the endogenous prostaglandin-dependent production of cAMP, has been shown to induce predominant apical K^+ secretory responses in all tissues due to general inhibition of CFTR activity, and thus poses as a positive control step for this CF diagnosis protocol (Figure 1.6 A-C, second peak). Then, addition of 3-isobutyl-1-methylxanthine (IBMX) and Forskolin (Fsk), agonists that increase cytosolic cAMP in a prostaglandin-independent manner, was shown to induce sustained Cl^- secretory lumen-negative responses in tissues where there is functional CFTR (Figure 1.6 A-B). Finally, a third CCH stimulation has been show to further increase the Cl^- secretion in normal tissues, in a transient form (Figure 1.6 A, third peak), to induce an inverse predominant apical K^+ secretory lumen-positive response in tissues of classic CF patients (Figure 1.6 C, third peak) and a biphased lumen-positive-then-negative response in tissues of residual function/non-classic CF patients (Figure 1.6 B, third peak).

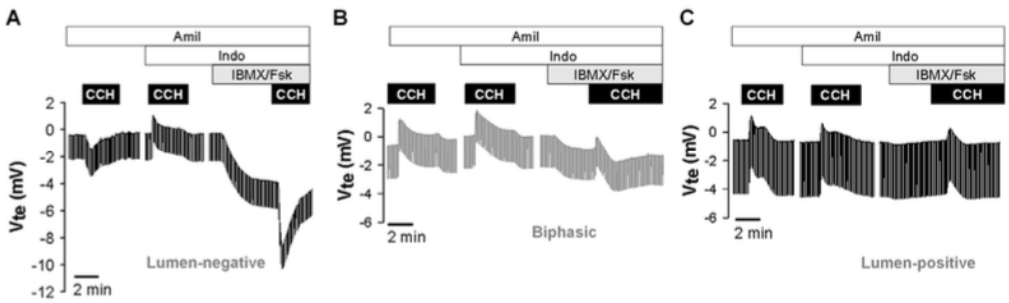

Figure 1.6 – Representation of Ussing chamber measurements in rectal biopsies using the Cystic Fibrosis diagnosis protocol. Characteristic profiles of **(A)** non-CF controls, **(B)** non-classic and **(C)** classic CF patients. V_{te} values were referred to the basolateral side of the epithelium. **Adapted from Sousa *et al.* (2012)[50].**

1.3.3. Newborn Screening

Currently implemented newborn screening (NBS) programs are especially important because early detection allows for the immediate administration of treatment before symptoms appear and improved disease outcome. For the diagnosis of CF in the NBS, the immunoreactive trypsinogen (IRT) test is performed, based on the observation that elevated blood levels of IRT are characteristic of all newborn CF patients[41,51]. However, these tests are only screening and thus they ultimately refer potential CF patients to specialized CF centers for diagnosis confirmation[52].

1.3.4. *CFTR* genotyping

Genotyping of mutations in the *CFTR* gene is usually performed to confirm a CF diagnosis. Although this works well for the set of mutations which have been established as CF-causing[40], genotyping does not always provide a clear diagnosis of CF vs. non-CF, since not all of the identified sequence variations in the *CFTR* gene have been confirmed as CF-causing variants. Also, most methods used in *CFTR* genetic testing are targeted at known mutations and so, many unidentified mutations and those that lie within the introns or regulatory regions of the gene may remain undetected unless extensive scanning methods are used[53].

In addition, different patients, even those sharing the same *CFTR* genotype, show variable CF clinical phenotype due to the contribution of genetic modifiers, environmental factors and other undefined mechanisms (Figure 1.7), making a genotype/phenotype/therapy correlation hard to establish. This is even more challenging for patients that carry orphan variants. To overcome this issue, several cellular tools have been developed to help measure individual CFTR activity, as well as to establish drug responsiveness, and ultimately to help predict the best therapy for each individual, contributing to a personalized medicine approach for all CF patients, independent of their *CFTR* mutations.

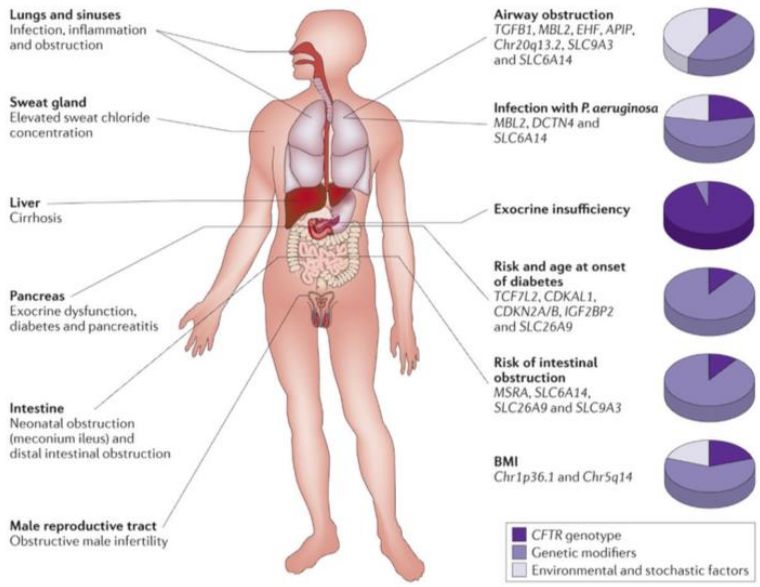

Figure 1.7 – Key features of Cystic Fibrosis and relative contribution of genetic modifiers and other factors to phenotype variability in CF. CF is a multysistemic disease and the degree of each organ system disfunction varies considerably amongst affected individuals. This is influenced by genetic factors such as the *CFTR* genotype and other modifier genes (such as *TGFB1* and *SLC26A9*), and also by non-genetic determinants like environmental and stochastic factors (e.g. smoking). The *CFTR* genotype is the primary explanation for pancreatic exocrine insufficiency in CF. BMI = body mass index. **Retrieved from Cutting (2015)[7].**

1.4. Towards personalized therapies

1.4.1. 3D-intestinal organoids

A recently developed primary intestinal culture method[54] has allowed for the generation of human intestinal organoids, by isolating the stem cell-containing crypts of rectal biopsies and culturing them in the appropriate conditions. These stem cells expand *in vitro* into closed 3D-organoids that contain crypt-like structures and these can be used in the so-called Fsk-induced swelling (FIS) assay[55], that uses Fsk as a CFTR agonist. Fsk increases intracellular levels of cAMP, leading to the activation of CFTR in the apical membrane of the organoid cells, which in turn induces secretion of electrolytes and fluids to the inside of the organoids, resulting in their 3D-swelling. This CFTR-dependent fluid secretion has been shown to provide an indirect measurement of CFTR activity, by analysis of CFTR-deficient organoids – derived from CFTR-knockout mice and CF-patients – and the usage of CFTR-specific inhibitors[55] (Figure 1.8). FIS in the organoids has been shown to correlate quantitatively to Fsk-induced currents measured in the Ussing chamber in freshly excised *ex vivo* rectal biopsies. Also, the fact that these cells can expand indefinitely *in vitro* allows for functional studies and drug response testing for individual patients in their own-derived material[55,56].

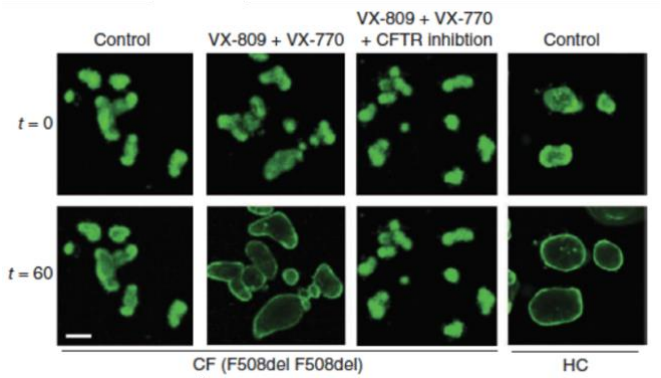

Figure 1.8 – Representative images of the CFTR-dependent FIS assay. Representative confocal fluorescence microscopy images of calcein green-labelled intestinal organoids from a CF patient carrying the F508del/F508del *CFTR* genotype in control conditions (Fsk only), after incubation with VX-809 + VX-770 (Orkambi®) and after incubation with Orkambi® and CFTR-specific inhibitors, and from a healthy control (HC) in control conditions, for t = 0 and t = 60 min of incubation with Fsk. Scale bar, 100 µm. **Adapted from Dekkers *et al.* (2013)[55].**

1.4.2. Primary human nasal/bronchial epithelial cells (HNECs/HBECs)

Primary cultures of human bronchial epithelial cells (HBECs) derived from lung explants are another currently used and clinically relevant model for CFTR function analysis and drug testing, for e.g., through Ussing chamber measurements[57]. More recently, it was shown that it is also possible to grow cells derived from patients' nasal brushings (HNECs) and that stem cell hyperplasia can be induced *in vitro*[58]. Also, these cultures have been shown to maintain the ability to differentiate into functional tissues and to recapitulate many features of the native epithelium when grown in permeable supports in appropriate air-liquid interface (ALI) conditions[58]. However, patient material is restricted and the long-term expansion of some nasal/bronchial cells is still limited, making reproducible results difficult to achieve.

1.4.3. Cystic Fibrosis Bronchial Epithelial (CFBE) 41o- cell line

Besides intestinal organoids and primary airway cells, many other model systems have been developed to study the different aspects of CF pathology. Because most mutations exist in compound heterozygosity, it is hard to establish the contribution of each allele for the observed molecular and functional defects. To overcome this issue, cellular models were designed in order to characterize the molecular effects elicited by individual mutations. The Cystic Fibrosis Bronchial Epithelial (CFBE) 41o- cell line was generated through immortalization of HBECs from a F508del homozygous CF patient[59], and with increasing passages they have lost endogenous CFTR expression. CFBEs retain some aspects of *in vivo* HBECs, such as the ability to polarize forming electrically tight cell monolayers with functional cell-cell contacts when grown under immersed culture conditions, and expressing several proteins relevant for pulmonary drug absorption[60]. Because of this, they have been engineered to express different CFTR mutants and used to characterize these mutations and their response to approved therapeutics, as well as to search for novel rescuing strategies through high-throughput approaches[61,62]. Despite this, more physiologically relevant models of the airway epithelium may be required. Particularly, CFBEs do not achieve a full epithelial phenotype when grown in ALI conditions, which are more representative of the respiratory epithelium (e.g., no cilia formation)[60].

Overall, since CFTR activity may vary among patients with different genotypes, patients that share the same genotype and even between tissues of the same patient, it is extremely important to validate different biological models to be used as diagnosis, prognosis and drug response assessment tools, aiming to improve and personalize CF care.

2. Objectives

The aim of the present MSc work was to study *CFTR* genotypes at the functional level in native tissues/primary cultures from patients with CF or suspicion of CF and to test their responsiveness to novel drugs by making use of innovative approaches in the CF field. The main focus was on patients carrying rare *CFTR* variants with the broad goal of expanding and improving CF diagnosis, prognosis and personalized therapies for all CF patients.

(1) Diagnosis

***Task:* Assessing CFTR function in native/primary tissues from patients with CF or suspicion of CF**

The first task was to assess the CFTR protein function in native tissues from patients with CF or suspicion of CF and carrying different (rare) mutations in *CFTR*. For this, Ussing chamber intestinal current measurements were performed in native rectal biopsies to assess for CFTR-mediated Cl^- secretion; intestinal 3D-organoids were generated from those biopsies and used for assessment of CFTR activity through the forskolin-induced swelling (FIS) assay using fluorescence microscopy; HNECs were also isolated and cultured from these patients and CFTR activity was evaluated using Ussing chamber measurements. With this, we aimed to establish a CF diagnosis and possible prognosis for the studied patients.

(2) Drug response assessment

***Task:* Testing approved corrective drugs for CFTR**

The second task was to test, and possibly repurpose, approved CFTR modulator drugs in the primary cultures from patients with different mutations, using the same approaches as above: Ussing chamber measurements using HNECs and FIS assay using 3D-organoids; to assess CFTR rescue after incubation with CFTR modulators, so as to identify the best therapy for each patient, in a personalized medicine approach.

(3) Validation of predictive CF biomarkers

***Task*: Establishing functional correlations between different CFTR function parameters, established CF biomarkers and clinical outcomes**

The final task was to establish good correlations between the different CFTR function parameters used in our project and more established CF-relevant parameters and clinical data obtained from the studied patients, in an attempt to further validate the former as robust biomarkers for CF diagnosis, prognosis and personalized treatment.

3. Materials and Methods

Experiments included in this thesis were performed at the labs of Professor Dr. Margarida Amaral's group (FunGP, BioISI, Faculty of Sciences, University of Lisbon, Portugal) and of Professor Dr. Karl Kunzelmann's group (Department of Physiology, University of Regensburg, Germany), over a work period of one year and two months.

3.1. Cell Culture

All cells were grown at 37 ºC in a 5% CO_2 and 95% air-humidified water saturated atmosphere. All cell culture was performed according to standard conditions.

3.1.1. Culture conditions of human intestinal organoids

Crypt isolation from human rectal biopsies and intestinal organoid culturing was carried out as previously described by the Beekman's lab, Utrecht, The Netherlands[55]. Briefly, biopsies were treated with 10 mM EDTA (Invitrogen, USA) in PBS for 90 min at 4ºC, with continuous shaking. Then, stem-cell containing intestinal crypts were disrupted from biopsies by vigorously washing them up-and-down in PBS and saving the supernatant. Supernatant was centrifuged (230 g, 5 min, 4 ºC) and pelleted crypts were resuspended in 50% (v/v) Matrigel Matrix (Corning, USA), diluted in complete culture medium consisting of 20% (v/v) $F12^{ghp}$, 2% (v/v) B27 (Invitrogen, USA), 1.25 mM N-acetylcysteine (Sigma-Aldrich, USA), 50 ng/mL mouse epidermal growth factor (Invitrogen, USA), 50% (v/v) Wnt-3a-conditioned medium (lab-made), 10% (v/v) Noggin-conditioned medium (lab-made), 20% (v/v) R-spondin-conditioned medium (lab-made), 10 mM nicotinamide (Sigma-Aldrich, USA), 500 nM TGF-β inhibitor A83-01 (Tocris Bioscience, Germany), 10 µM P38 MAPK inhibitor SB 202190 (Sigma-Aldrich, USA); and 0.2% (v/v) Primocin antibiotic (InvivoGen, USA). Crypts in matrigel were seeded at a density of 10-30 crypts per 10 µL droplet. The matrigel was polymerized for ~20 min at 37 ºC 5% CO_2. 0.1% (v/v) Gentamicin (Sigma-Aldrich, USA) was added to culture medium for the first week of culture since passage 0 is more susceptible to contamination. Medium was changed every 2-3 days. Crypts closed quickly and started to bud into intestinal organoids in 7-10 days, after which they were passaged (Figure 3.1).

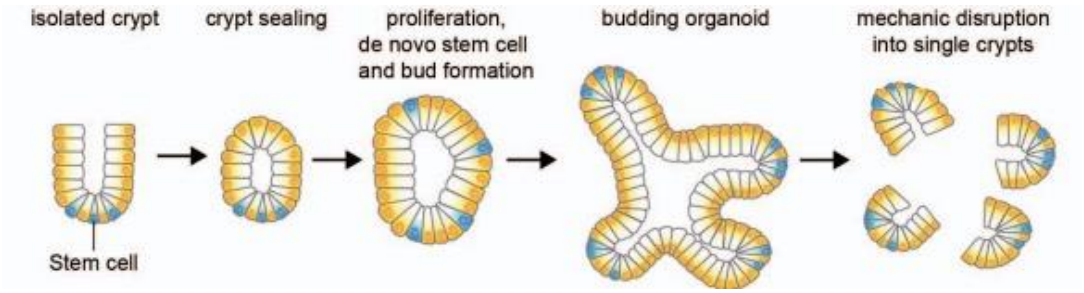

Figure 3.1 – Schematic representation of organoid generation from isolated crypts from rectal biopsies. Isolated crypts seal and start to sprout in 7-10 days after which they are passaged by mechanical disruption into single smaller organoids. **Adapted from Dekkers, van der Ent & Beekman (2013)**[63].

3.1.2. Culture conditions of primary HNECs

Bilateral nasal brushings of patients were collected in Hospital de Santa Maria (Lisbon, Portugal) or Hospital de Dona Estefânia (Lisbon, Portugal). Specimens were stored in PBS at 4 ºC.

HNECs were isolated, and cultured using dual SMAD signaling inhibition in the absence of a feeder-cell layer[58], following unpublished protocols by Jeffrey Beekman's lab, Utrecht, The Netherlands. Briefly, nasal cells were detached from the brushes by mechanical force and pelleted by centrifugation (1200 rpm, 5 min, RT). Pellet was resuspended in 4 mL of culture medium and transferred into two wells of a 6-well culture plate previously coated with PureCol (type I collagen) for 2-24 h (30 µg/mL, Advanced Biomatrix, USA). Culture medium (confidential) was refreshed every 2-3 days until 80% confluency was reached. Upon further expansion in 75 cm^2 flasks, cells were transferred for differentiation in air-liquid interface (ALI) conditions. 200.000 cells were added onto the apical side of Transwell® 6.5 mm polyester membrane inserts (Corning, USA) and the basal compartment of each well was filled with 800 µL of culture medium. The next day, medium was refreshed with Polarization medium (ALI-differentiation medium + 500 nM A83-01) (Figure 3.2). When confluent, culture medium was removed from the apical surface and basal medium was refreshed, so that cells started growing in ALI conditions. In the first week, cells were cultured in Polarization medium, in the second week, medium was changed to Maturation medium (ALI-differentiation medium + 10 µM DAPT (Sigma-Aldrich, USA)), and finally, in the third week, medium was changed to Maintenance medium (ALI-differentiation medium) and cells were cultured in this condition for 7 more days. ALI-differentiation medium consisted of Advanced DMEM/F12 supplemented with 0.5 µg/mL hydrocortisone (Sigma-Aldrich, USA), 100 nM triiodothyronine (Sigma-Aldrich, USA), 0.5 µg/mL epinephrine (Sigma-Aldrich, USA), 0.5 µg/mL human epidermal growth factor (PeproTech, UK), 100 nM TTNPB (Cayman, USA), 50 nM A83-01 and 1% (v/v) Pen/Strep. Basal medium was always refreshed every 2-3 days after a gentle apical 1X PBS-wash with a 15 min incubation at 37 ºC 5% CO_2.

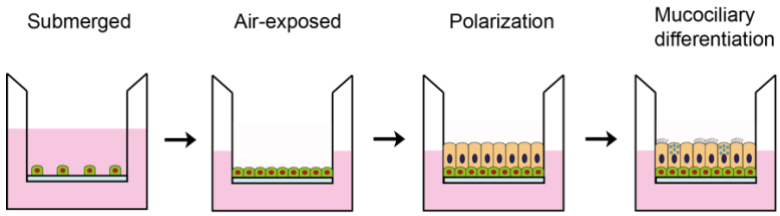

Figure 3.2 – Schematic representation of HNECs' differentiation protocol. Seeding cells in culture plate inserts with porous membranes allows for the establishment of apical and basolateral domains and cell differentiation. Cells were cultured in submerged conditions until confluent. After this, apical medium was removed and cells started growing in ALI conditions. In the first week, basal medium was added to allow for cell polarization, in the second week, medium was added for mucociliary differentiation (maturation) of the nasal epithelial cells and in the third week, cells were cultured in unsupplemented ALI-differentiation medium for maintenance purposes. **Adapted from a protocol from Jeffrey Beekman's lab**.

Transepithelial electrical resistance (TEER) measurements of HNEC-monolayers were taken using a Millicell-ERS voltohmmeter with a chopstick electrode (Millipore, USA), to check for tightness of the epithelium. After the 3 weeks required for HNECs differentiation, TEER values ranged between 200-800 Ωxcm^2. HNECs were then incubated for 48 h with CFTR correctors for assessment of rescue and function of CFTR, by Ussing chamber analysis. For that, basal medium was refreshed with Maintenance medium supplemented with 3 µM VX-809, 5 µM VX-661, both DMSO dissolved, or 0.05% DMSO (control condition).

3.1.3. Culture conditions of the human cell-line NCI-H441

The human lung adenocarcinoma cell line NCI-H441, shown to be a useful *in vitro* model of human distal lung epithelium[64], was used to test the effect of CFTR correctors in the biosynthesis of other epithelial channels. This cell line does not express CFTR[65].

NCI-H441 cells were cultured in RPMI1640 with L-Glutamine (Invitrogen, USA) supplemented with 1% (v/v) Pen/Strep, 10% (v/v) FBS and 1% (v/v) Insulin-Transferrin-Selenium (Gibco, USA). For differentiation in Millicell® 12-well culture plate inserts (Millipore, USA) with 0.45 µm pore size, the cells were cultured with 2% (v/v) Ultroser G serum substitute (Pall, USA)-supplemented medium. 200.000 cells were seeded apically per insert in 500 µL culture medium. 1 mL of medium was added to the basal compartment of each well and cells were incubated at 37 ºC 5% CO_2 for 3 days, before removal of the apical medium and culturing in ALI conditions. A gentle apical 1X PBS-wash of the cells was performed upon basolateral medium refreshing every 2-3 days. After 10-14 days of culturing cells reached TEER values of 400 $\Omega x cm^2$, after which they were analysed in the Ussing chamber. 48 h-previously to Ussing chamber experimenting, NCI-H441 cells were treated with 3 µM VX-809, 5 µM VX-661 or 0.05% DMSO in culture medium, and some were left untreated (control conditions).

3.2. Functional analyses

3.2.1. Measurement of CFTR-mediated Cl^- secretion in rectal biopsies

Patients' colon preparation was performed by applying an enema of saline solution, and superficial rectal mucosa biopsies (2.8 mm in diameter) were obtained by rectoscopy and forceps biopsy in Hospital de Dona Estefânia (Lisbon, Portugal), Hospital de Santa Maria (Lisbon, Portugal), Centro Hospitalar e Universitário de Coimbra (Coimbra, Portugal) or Motol University Hospital (Prague, Czech Republic). Mounting of tissues was performed under a stereomicroscope using dissection forceps. Once the tissues were mounted on circular disk inserts (with central convex open areas of 0.0079-0.0283 cm^2), these were fixed between the two-half cells of the micro-Ussing chambers, separating luminal from basolateral bath solutions (Figure 3.3).

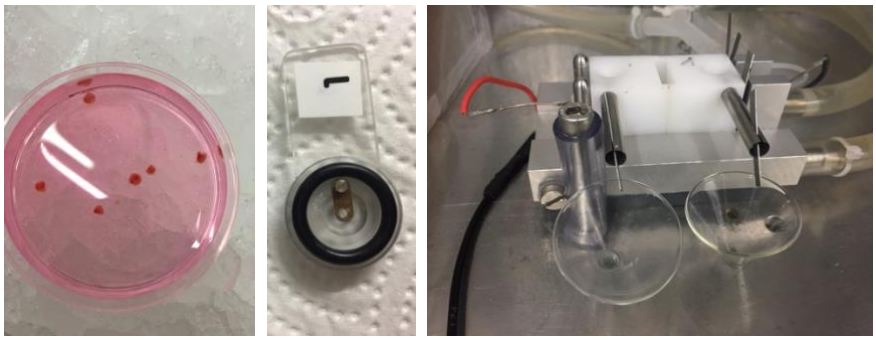

Figure 3.3 – Rectal biopsies procedure (tissue mounting). Rectal biopsy specimens from one CF patient (left); circular disk inserts used for rectal biopsy mounting (centre); micro-Ussing chambers arrangement for rectal biopsy analysis (right).

Transepithelial measurements were performed under open-circuit conditions in perfused micro-Ussing chambers as previously described[48,50]. The samples were continuously perfused with Ringer buffer (NaCl 145 mM, KH_2PO_4 0.4 mM, $K_2HPO_4 \cdot 3H_20$ 1.6 mM, D-glucose 5 mM, $MgCl_2 \cdot 6H_20$ 1 mM, Ca-Gluconate$\cdot 1H_20$ 1.3 mM, pH 7.4 (NaOH, HCl), 280 mosm/Kg) followed by experimental solutions.

V_{te} values were continuously recorded using Power Lab software (AD Instruments Inc., New Zealand) and referred to the basolateral/serosal side of the epithelium. R_{te} was determined by applying short (1 sec) intermittent current pulses (0.5 µA), measuring pulsated deviations in V_{te} and accounting for open area of the inserts. Measured values were later corrected for empty insert/system resistances. Equivalent short-circuit currents (I_{eq-sc}) were calculated according to Ohm's law ($I_{eq-sc} = V_{te} / R_{te}$).

All experimental solutions used were prepared in Ringer buffer. Amiloride (Amil, 20 µM, luminal) (Sigma-Aldrich, USA) was first applied to block electrogenic Na^+ absorption through ENaC. Next, CCH (100 µM, basolateral) (Sigma-Aldrich, USA) was added for cholinergic activation of K^+ channels and K^+ release, constituting a driving force for Cl^- exit through CFTR. Indomethacin (Indo, 10 µM, basolateral) (Sigma-Aldrich, USA) was then applied for 20 min to inhibit production of prostaglandins and abolish endogenous cAMP levels and thus CFTR-mediated Cl^- secretion. CCH was then re-applied in the presence of Indo as a control step for the protocol, due to general inhibition of CFTR activity in healthy or diseased tissues. After the CCH washout, an IBMX/Fsk solution (100 µM/2 µM, basolateral) (both from Sigma-Aldrich, USA) was added to stimulate prostaglandins-independent cAMP production and cAMP-dependent (CFTR-mediated) Cl^- secretion. CCH was finally re-added on top of IBMX/Fsk for cholinergic co-activation of CFTR.

1-5 rectal biopsies were measured per patient. The percentage of CFTR function in these tissues was calculated for the average maximal CFTR activation ($\Delta I_{eq-sc,IBMX/Fsk(Indo)} + \Delta I_{eq-sc,CCH(IBMX/Fsk(Indo))}$), normalized to the corresponding mean value determined previously for a reference non-CF control group (-217.45 µA/cm^2)[50]. A threshold of 30% of wild-type CFTR function was defined to distinguish non-CF subjects from CF patients, as proposed previously[49,50].

3.2.2. Measurement of CFTR-mediated Cl^- secretion in HNEC-monolayers

HNEC-monolayers grown on porous supports (see Section 3.1.2**)** were mounted between two round half-inserts with central open areas of 0.33 cm^2 and fixed in the middle of the two-half cells of the micro-Ussing chambers, separating apical from basal bath solutions. Transepithelial measurements were performed as described above (see Section 3.2.1). All experimental solutions used were prepared in Ringer buffer. Amil (20 µM, apical) was applied to block electrogenic Na^+ absorption by ENaC, as before. After, IBMX/Fsk (100 µM/2 µM, apical) was added to stimulate CFTR-mediated Cl^- secretion. After this, Genistein (Gen, 25 µM, apical) (Sigma-Aldrich, USA) was added to further potentiate the CFTR response. Finally, a CFTR-specific inhibitor ($CFTR_{inh}$-172, 30 µM, apical) (Cystic Fibrosis Foundation Therapeutics, USA) was applied to show the specificity of the cAMP(IBMX/Fsk)-dependent response. At least three replicates were measured per patient and per treatment. CFTR rescue by corrector compounds was assessed by comparison of $\Delta I_{eq-sc,IBMX/Fsk}$ values between control (DMSO 0.05%) and treated (VX-809 3 µM or VX-661 5 µM) nasal cells.

3.2.3. Measurement of non-CFTR epithelial channels' activity in NCI-H441-monolayers

Monolayers of NCI-H441 cells grown on permeable supports (see Section 3.1.3**)** were mounted between two round half-inserts with central open areas of 0.6 cm^2 and fixed in the middle of the two-half cells of the micro-Ussing chambers, separating luminal from basolateral bath solutions. Transepithelial measurements were performed as described above (see Section 3.2.1**)**. All experimental

solutions used were prepared in Ringer buffer. In this protocol, Amil (20 µM, apical) was added to inhibit electrogenic Na^+ absorption by ENaC, as previously. After, Amil was washed-out with Ringer buffer and IBMX/Fsk (100 µM/2 µM, basolateral) was added to activate cAMP-dependent channels such as basolateral K^+ channel KCNQ1. The specific KCNQ1 inhibitor Chromanol 293B (293B, 10 µM, basolateral) (Sigma-Aldrich, USA) was then added on top of IBMX/Fsk to check for the contribution of this channel in the previous response. 293B was washed-out with IBMX/Fsk and Amil was re-added apically to assess for alterations in ENaC activity after activation of cAMP-dependent channels. Lastly, Amil was washed-out with Ringer and the basolateral solution was changed from IBMX/Fsk to Clotrimazole (10 µM, basolateral) (Sigma-Aldrich, USA) to block Ca^{2+}-dependent K^+ channels KCNN4 (also known as SK4). Seven replicates were measured per treatment. ENaC, KCNQ1 and KCNN4 activities measured by specific inhibitor responses were compared between controls and treatments (untreated, 0.05% DMSO, 3 µM VX-809 and 5 µM VX-661) to assess for rescue of their function by CFTR corrector compounds.

3.2.4. Forskolin-induced swelling (FIS) assay

Organoids were seeded in matrigel in a pre-warmed 96-well culture plate and treated for 24 h with CFTR correctors, VX-809 (3µM, Selleckchem, USA) or VX-661 (5µM, Selleckchem, USA). The FIS assay was carried out as previously described[55]. Briefly, after calcein green incubation (3µM) (Invitrogen, USA), 0.02, 0.128, 0.8 and 5 µM Fsk (Sigma-Aldrich, USA) solutions or a combination of Fsk and VX-770 (3 µM, Selleckchem, USA) were added to the organoids. Live cell imaging was performed in a wide-field fluorescence microscope (Leica DMI 6000B, Leica Microsystems, Germany) at 37 ºC with 5% CO_2, and wide-field and fluorescence images were taken for 60 min with 10 min intervals.

To analyse the organoid swelling, Cell Profiler software (Broad Institute's Imaging Platform, USA) was used for image processing and a lab-designed script (Organoid Explorer, developed in our lab by Hugo Botelho) and Graph Pad Prism version 6 software were used to obtain and plot values for organoid surface areas. Quantification of the surface area increase of organoids, relative to t = 0 min (Normalized area, Figure 3.4), at different Fsk concentrations per treatment, was averaged from two independent wells per assay. Organoid swelling analysis was then expressed as the absolute area under the curve (AUC) calculated from the normalized surface area increase (baseline = 100%, t = 60 min), averaged from at least three independent assays. CFTR rescue was assessed by comparison of average AUC values between control (Fsk only) and treatments (Fsk + VX-809; Fsk + VX-770; Fsk + VX-809/770; Fsk + VX-661; Fsk + VX-661/770), for [Fsk] = 0.128 µM, established as standard for prediction of *in vivo* treatment efficacy[66]. AUC thresholds of 750 and 1500 have been established for the prognosis of medium and high clinical benefit potential of treatments, respectively[66].

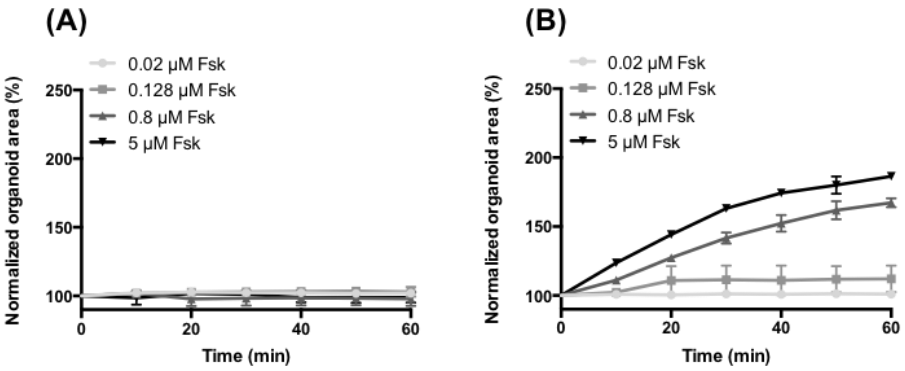

Figure 3.4 – Organoid surface area increase. Representative tracings of the surface area increase of organoids relative to t = 0 min (Normalized area) at different Fsk concentrations for **(A)** a treatment that has no effect in organoid swelling and **(B)** a treatment that leads to organoid swelling.

3.3. Statistical Analyses

Statistical differences were determined with Student's *t*-test or analysis of variance (ANOVA), as suitable. Data are expressed as mean ± standard error of mean (SEM). Pearson coefficients (*r*) were used to find correlations and partial correlations between patients' CF outcome parameters and laboratory assessed CFTR function. *P*-values of <0.05 were considered significant.

4. Results and Discussion

4.1. Patients' samples

In this project, samples were collected and analysed from CF/CF-suspicion patients at several centers, namely from patients CFL05/06 at Hospital de Dona Estefânia (Lisbon, Portugal), CFL41/44 at Hospital de Santa Maria (Lisbon, Portugal), CFL68/69 at Centro Hospitalar e Universitário de Coimbra (Coimbra, Portugal) and CFL26/27/49-66 at Motol University Hospital (Prague, Czech Republic). An overview of laboratory and clinical data and biologic material analysed from these patients is presented in Table 4.1.

4.2. Mild *CFTR* genotypes

4.2.1. D1152H/F508del

One of the patients we analysed in this project (CFL26) had the D1152H/F508del genotype. D1152H is reported as being a class IV conductance mutation and F508del as a class II processing mutation.

Diagnosis

Ussing chamber recordings of transepithelial voltage (V_{te}) measurements in rectal biopsies from patient CFL26 (Figure 4.1 A) show a transient positive V_{te} deflection followed by a small negative deflection after basal cholinergic stimulation by carbachol (CCH), evidencing both K^+ and Cl^- luminal secretions. Then, administration of CCH in the presence of Indomethacin shows a positive V_{te} deflection indicative of the detection of luminal K^+ secretion only, due to the inhibition of CFTR-mediated Cl^- secretion, validating this CF diagnosis protocol. Finally, cAMP-mediated stimulation of the tissue by IBMX/Fsk shows a significant Cl^- secretory lumen-negative response, further increased following cholinergic co-activation with CCH, in a monophasic manner.

These results all together suggested that this individual might actually not be a CF patient, or might just have a high CFTR activity. Then, the quantification of the average maximal CFTR activation ($\Delta I_{eq\text{-}sc,IBMX/Fsk(Indo)} + \Delta I_{eq\text{-}sc,CCH(IBMX/Fsk(Indo))}$) in CFL26's rectal biopsies (Figure 4.1 B), in comparison to that previously determined in WT samples from a reference non-CF control group (-217.45 $\mu A/cm^2$)[50], showed that this patient has 35.5% of WT CFTR function, which is above the threshold for the exclusion of a CF diagnosis (>30%)[49,50].

Table 4.1 – Patients' data overview: patient codes, *CFTR* genotypes, sex (M = male/F = female); age at study and at diagnosis/time of CF-suspicion (years old; NBS = newborn screening/PN = prenatal) and fecal elastase E1 values (FEE, µg/g stool), exocrine pancreatic function (PS = pancreatic sufficient/PI = pancreatic insufficient), forced expiratory volume in 1 sec in percentage predicted (FEV_1, %) and sweat [Cl^-] (mmol/L) at time of samples collection; samples analysed (rectal biopsies, intestinal organoids and/or nasal epithelial cells) and familial relationship to other patients within the study group. Clinical/laboratory data was obtained at the hospital of samples collection. NA = Not available.

Patient code	*CFTR* Genotype	Sex	Age at study	Age at diagnosis	FEE	Exocrine pancreatic function	FEV_1	Sweat [Cl^-]	Samples analysed	Familial relationship
CFL05	P205S/Y1092X	F	12	NA	NA	PS	NA	91.5	Biopsies, organoids, nasals	Twin to CFL06
CFL06	P205S/Y1092X	F	12	NA	NA	PS	NA	89.5	Biopsies, organoids, nasals	Twin to CFL05
CFL26	D1152H/F508del	F	40	23.5	NA	PS	61	51.0	Biopsies, organoids	None
CFL27	2789+5G>A/F508del	M	37	0.92	NA	PS	80	78.0	Biopsies	None
CFL41	1717-1G>A/G85E	F	29	13	NA	PI	80	90.0	Biopsies, organoids	None
CFL44	D614G/F508del	NA	NA	NA	NA	NA	NA	NA	Biopsies, organoids, nasals	None
CFL49	3849+10kbC>T/dele2,3(21kb)	F	10	0.25	479.0	PS	75	60.0	Biopsies	None
CFL50	D1152H/N1303K	M	7	0 (NBS)	497.3	PS	124	20.0	Biopsies	Sibling to CFL51
CFL51	D1152H/N1303K	M	8	3	1036.7	PS	111	33.0	Biopsies	Sibling to CFL50
CFL52	F508del/G542X	F	19	2.3	40.0	PI	57	84.7	Biopsies, organoids	None
CFL53	F508del/G542X	F	11	2.5	10.0	PI	80	78.9	Biopsies, organoids	None
CFL54	F508del/R347P	F	18	1	351.0	PS	64	84.6	Biopsies	None
CFL55	2789+5G>A/F508del	F	36	-0.33 (PN)	371.0	PS	52	91.0	Biopsies	None
CFL56	3849+10kbC>T/621+1G>T	M	13	5	NA	PS	41	81.5	Biopsies	None
CFL57	3849+10kbC>T/F508del	F	30	11.5	573.0	PS	72	43.5	Biopsies, organoids	Sibling to CFL58
CFL58	3849+10kbC>T/F508del	F	28	9.2	NA	PS	47	36.0	Biopsies, organoids	Sibling to CFL57
CFL59	F508del/S955P	M	7	0 (NBS)	500.0	PS	95	56.5	Biopsies, organoids	None
CFL60	711+5G>A/F508del	M	15	5.5	50.0	PI	102	84.3	Biopsies	None
CFL61	F508del/G542X	M	8	0 (NBS)	1.0	PI	95	82.7	Biopsies	None
CFL62	2789+5G>A/dele2,3(21kb)	F	10	5	NA	PS	93	100.5	Biopsies	None
CFL63	3272-26A>G/W57G	M	11	4	NA	PS	89	89.2	Biopsies	None
CFL64	3272-26A>G/F508del	M	8	0.75	NA	PS	88	88.3	Biopsies	None
CFL65	F508del/F508del	M	13	2	NA	PI	89	117.0	Biopsies, organoids	Sibling to CFL66
CFL66	F508del/F508del	M	16	4	NA	PI	108	113.0	Biopsies, organoids	Sibling to CFL65
CFL68	711+1G>T/F508del	M	13	0.12	NA	PI	105.0	NA	Organoids	None
CFL69	F508del/R334W	M	17	15	NA	PI	95	112.5	Organoids	None

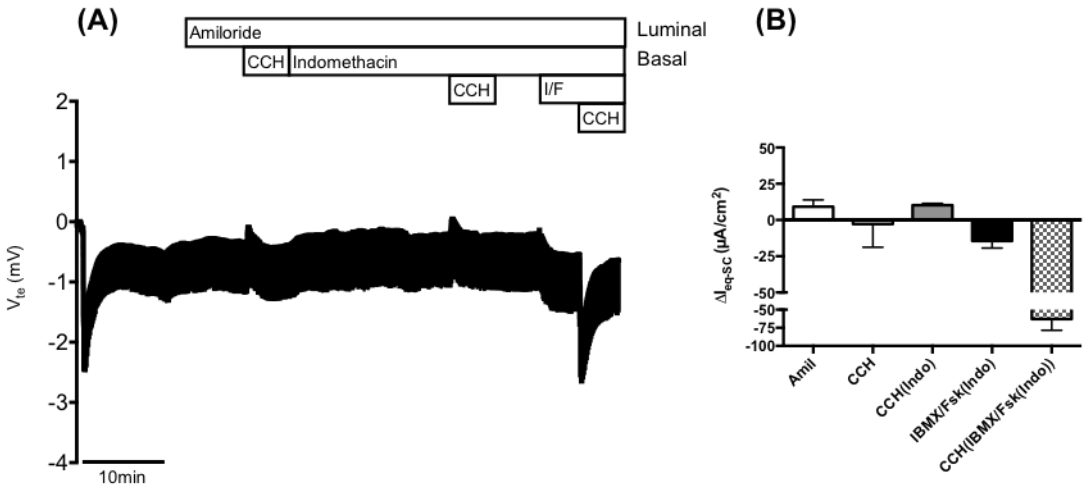

Figure 4.1 – Results from Ussing chamber measurements in rectal biopsies from patient CFL26 (D1152H/F508del genotype). (A) Representative original recording of the effects of cholinergic (CCH, 100 µM, basolateral) and cAMP-dependent (IBMX/Fsk (I/F), 100 µM/2 µM, basolateral) activation on transepithelial voltage (V_{te}) in D1152H/F508del rectal biopsies from patient CFL26. Experiments were performed in the presence of Amiloride (Amil, 20 µM, luminal) and/or Amiloride + Indomethacin (Indo, 10 µM, basolateral), as indicated in the figure. **(B)** Summary of activated equivalent short-circuit currents (ΔI_{eq-sc}) for Amil ($\Delta I_{eq-sc,Amil}$), basal CCH ($\Delta I_{eq-sc,CCH}$), CCH + Indo ($\Delta I_{eq-sc,CCH(Indo)}$), IBMX/Fsk + Indo ($\Delta I_{eq-sc,IBMX/Fsk(Indo)}$) and CCH following IBMX/Fsk application ($\Delta I_{eq-sc,CCH(IBMX/Fsk(Indo))}$); data represent the mean of measurements on three rectal biopsies ± SEM. $\Delta I_{eq-sc,IBMX/Fsk(Indo)}$ = -14.380 ± 5.014 µA/cm²; $\Delta I_{eq-sc,CCH(IBMX/Fsk(Indo))}$ = -62.860 ± 15.540 µA/cm² (35.5% of WT CFTR function).

CFTR function was also assessed in the intestinal organoids derived from this patient (Figure 4.2 A-C). Without any drug, stimulation with Fsk leads to production of intracellular cAMP, which in turn activates CFTR, if it is present and functional at the membrane of the cells, and results in the secretion of electrolytes and following fluids to the inside of the organoids, leading to their 3D-swelling. We can observe this swelling for patient CFL26's organoids with low Fsk concentrations (0.128 µM, Figure 4.2 A-C), which supports that this patient has residual to normal CFTR function. Furthermore, they even present a highly pre-swollen phenotype in basal conditions (no treatment – Figure 4.2 A, Fsk, 0 min), resembling healthy control organoids[66], which reinforces our previous conclusions.

Overall, results from the analyses of patient CFL26's samples support the exclusion of a CF diagnosis for this individual. Nevertheless, using this FIS assay, a quantification of function in relation to healthy controls cannot be correctly established, since this analysis has been shown to lead to the underestimation of wild-type CFTR function due to the greatly pre-swollen phenotype of healthy organoids that originates from a basal CFTR activity[66]. Withal, the clinical data obtained from this patient, namely of pancreatic sufficiency and borderline sweat chloride concentrations (51.0 mmol/L), also support the exclusion of CF. However, the fact that this patient presents CF-suggestive symptoms, such as mild to severe pulmonary disease, leads us to propose a diagnosis of a *CFTR*-related disorder (*CFTR*-RD), as described for other individuals also sharing the D1152H/F508del genotype[67].

The D1152H mutation found in patient CFL26 (frequency of 0.00402[40]) is a missense mutation localized in the intracytoplasmic loop connecting TMD12 and NBD2. Previous studies in transfected COS-1 cells and *Xenopus laevis* oocytes have shown that this mutation does not interfere with the proper maturation of the CFTR protein but it does so with the proper function of the channels, being only partially activated by cAMP[68]. Thus, this mutation is associated with a residual CFTR function and has been classified as class IV[69]. However, D1152H has not been consistently considered a CF-causing mutation, since discordant results have been reported on the clinical expression of individuals carrying it[67,69]. The need for this mutation to be in a complex allele to be CF-causing, as has been described before

for other mutations[2], may partially explain the variable phenotype associated to it. Nevertheless, in the CFTR2 database, this mutation is reported as a variant of varying clinical consequence[40].

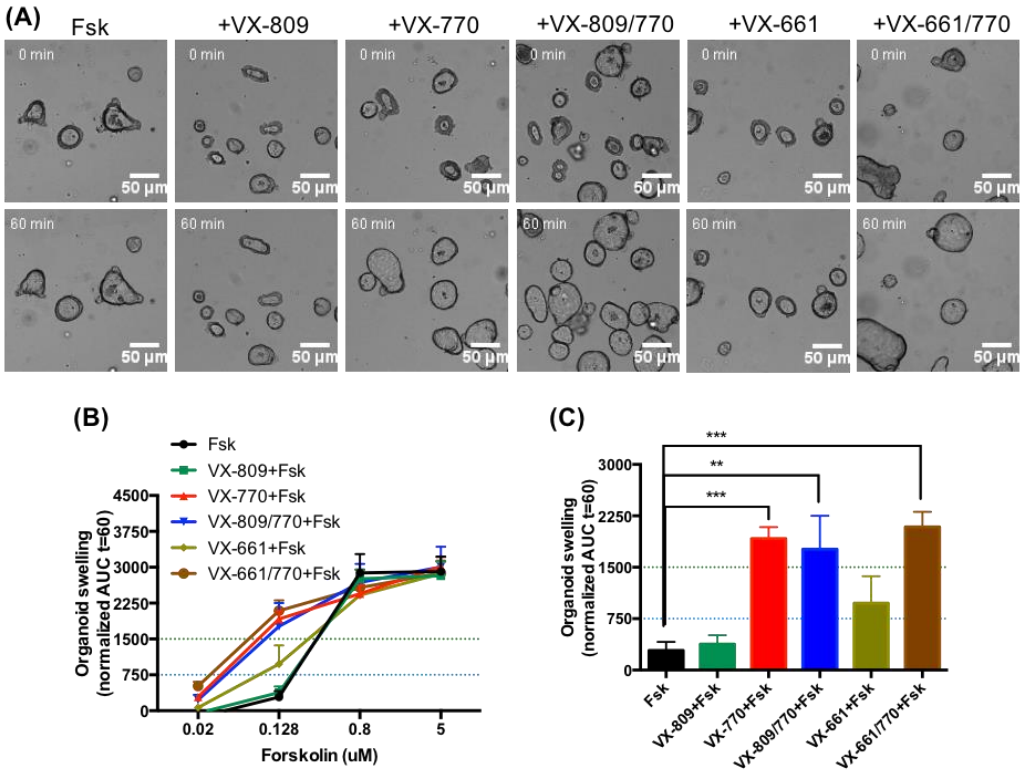

Figure 4.2 – Results from the forskolin-induced swelling (FIS) assay on intestinal organoids from patient CFL26 (D1152H/F508del genotype). (A) Representative original wide-field microscopy images of intestinal organoids from patient CFL26 (D1152H/F508del) at times 0 and 60 min of incubation with the following treatments: Forskolin (Fsk) alone at the concentration of 0.128 µM, VX-809 (3 µM) + Fsk, VX-770 (3 µM) + Fsk, VX-809/770 + Fsk, VX-661 (5 µM) + Fsk and VX-661/770 + Fsk. **(B)** Quantification of FIS in organoids for all treatments at the Fsk concentrations of 0.02, 0.128, 0.8 and 5 µM, expressed as the AUC of organoid surface area increase (baseline = 100%, t = 60 min). **(C)** Quantification of organoid swelling for all treatments at [Fsk] = 0.128 µM. The dashed blue and green lines represent the established thresholds for medium and high clinical benefit potential for treatments, respectively. **(B)** and **(C**) data represent the mean of measurements on 4-6 replicate wells per condition ± SEM. Asterisks (*) indicate degree of significant difference calculated by unpaired one-way ANOVA to control (Fsk) using Fisher's LSD test. [Experiments were performed in collaboration with Iris Silva and included with permission].

On the other *CFTR*-allele, patient CFL26 carries the mutation F508del. F508del is the most common *CFTR* mutation with a frequency of 0.69744[40]. This deletion in NBD1 has been extensively characterized as a CF-causing class II processing mutation. F508del-CFTR misfolding induces a global conformational change that produces a mutant channel that is defective in trafficking to the membrane and has gating and peripheral stability problems when there[70]. This mutation has been associated to severe (classical) CF phenotypes, such as elevated levels of sweat Cl^- and severe pulmonary and pancreatic disease. Nonetheless, phenotypic variability has also been observed even between homozygotes for this mutation, that share the most common *CFTR* genotype amongst CF patients (F508del/F508del). Recently, a role for non-coding variants in the *CFTR* gene has been proposed to explain trait variation among individuals carrying this allele[71].

Drug response

At [Fsk] = 0.128 µM, established as standard for prediction of the *in vivo* drug efficacy for CFTR modulators[66], intestinal organoid swelling for patient CFL26 with the treatments VX-770, VX-809/770

and VX-661/770 was significantly different from control conditions (Fsk only) and above the threshold for high clinical benefit potential (1500[66], Figure 4.2 B-C).

A comparison by unpaired one-way ANOVA to VX-770 using Fisher's LSD test showed that there are no statistically significant differences between combination and potentiator-only treatments (p = 0.7460 for VX-809/770 and p = 0.7157 for VX-661/770). This implies that the increase in CFTR function should be reached mainly by potentiation of D1152H-CFTR and not correction of F508del-CFTR in this patient's organoids, supporting the classification of D1152H as a class IV mutation that interferes with channel conductance.

Therapeutic efforts have mostly been directed at rescuing F508del-CFTR, and corrector/potentiator therapies (VX-809/770 or Orkambi® and VX-661/770 or Symdeco®) have been primarily developed and approved to treat this particular defect. However, unresponsiveness to treatment has also been observed in patients carrying the F508del mutation, which might be explained by each individual's genetic background being able to modify the response to drug therapy. Notwithstanding, through this personalized approach we can support that if this individual ever develops CF and/or treatment is required, CFL26 would most likely benefit from administration of VX-770 (Kalydeco®). In fact, D1152H is one of the 38 residual function mutations for which treatment with this drug has been approved[38].

4.2.2. D1152H/N1303K

Two other patients analysed in this project carried the D1152H mutation, however, *in trans* with N1303K, namely CFL50 and CFL51 (siblings). N1303K (frequency of 0.01581[40]) is a missense mutation localized in NBD2, that interferes with the proper maturation and trafficking of CFTR, being classified as a CF-causing class II mutation that leads to a severe phenotype, especially in the pancreas[40,72,73].

Diagnosis

Results from analyses of rectal biopsies from patients CFL50 (Figure 7.2 A-B in Appendix II) and CFL51 (Figure 4.3) also led to the exclusion of a CF diagnosis for both patients. The CFTR function calculated from these samples was of 29.5% and 39.7% of WT, respectively. Both siblings are pancreatic sufficient (PS) and present normal sweat chloride concentration values (< 40 mmol/L), and they present with rectal prolapses and gastroesophageal reflux as the only CF-suggestive symptoms, with no pulmonary disease. As such, these patients could also be diagnosed with *CFTR*-RD. However, the patients' age at study (7 and 8 years old) suggests that CF clinical manifestations may have later onset. Also, earlier CF suspicion (CFL50 through NBS and CFL51 at 3 years old) and prompt follow up may explain the normal respiratory function and good nutritional status of these patients. Testing of the approved CFTR modulator drugs remains to be performed for these patients' organoids, and they should be closely monitored.

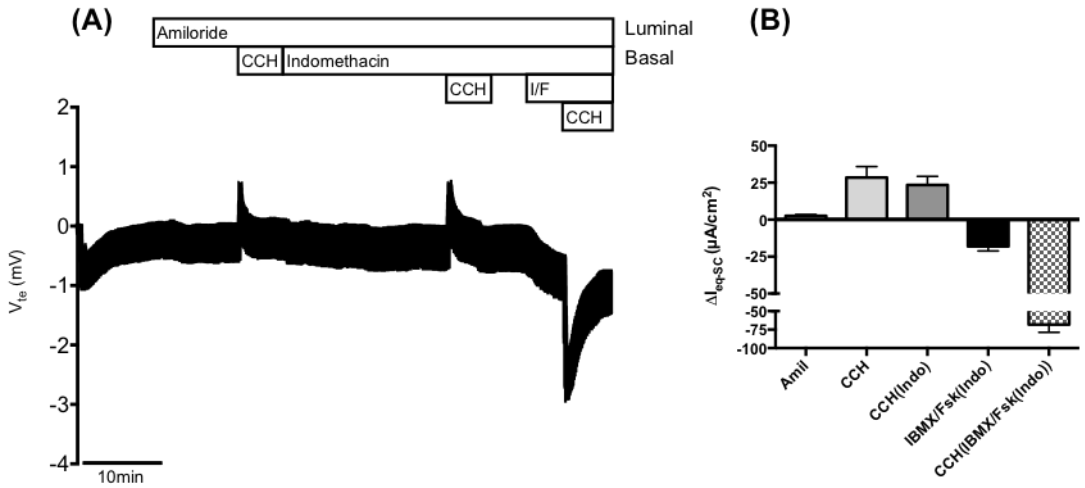

Figure 4.3 – Results from Ussing chamber measurements in rectal biopsies from patient CFL51 (D1152H/N1303K genotype). (A) Representative original recording of the effects of cholinergic (CCH, 100 µM, basolateral) and cAMP-dependent (IBMX/Fsk (I/F), 100 µM/2 µM, basolateral) activation on transepithelial voltage (V_{te}) in D1152H/N1303K rectal biopsies from patient CFL51. Experiments were performed in the presence of Amiloride (Amil, 20 µM, luminal) and/or Amiloride + Indomethacin (Indo, 10 µM, basolateral), as indicated in the figure. **(B)** Summary of activated equivalent short-circuit currents (ΔI_{eq-sc}) for Amil ($\Delta I_{eq-sc,Amil}$), basal CCH ($\Delta I_{eq-sc,CCH}$), CCH + Indo ($\Delta I_{eq-sc,CCH(Indo)}$), IBMX/Fsk + Indo ($\Delta I_{eq-sc,IBMX/Fsk(Indo)}$) and CCH following IBMX/Fsk application ($\Delta I_{eq-sc,CCH(IBMX/Fsk(Indo))}$); data represent the mean of measurements on four rectal biopsies ± SEM. $\Delta I_{eq-sc,IBMX/Fsk(Indo)}$ = -18.060 ± 3.075 µA/cm^2; $\Delta I_{eq-sc,CCH(IBMX/Fsk(Indo))}$ = -68.180 ± 10.430 µA/cm^2 (39.7% of WT CFTR function).

4.2.3. F508del/S955P

Patient CFL59 studied in this project carried a F508del/S955P genotype. S955P is a new and uncharacterized *CFTR* variant.

Diagnosis

Analysis of the Ussing chamber recordings of V_{te} measurements in rectal biopsies from patient CFL59 (Figure 4.4 A) shows a K^+ secretory response after basal cholinergic stimulation by CCH, and cAMP-mediated stimulation of the tissue by IBMX/Fsk shows a small Cl^- secretory response further increased following cholinergic co-activation, again in a monophasic manner.

Once more, these results all together suggested that this individual might actually not be a CF patient, or might just present high levels of functional CFTR. However, in this case, the currents elicited by the maximal CFTR activation are not large enough to imply normal function. In fact, only 7.5% of WT CFTR function was detected in this patient's rectal biopsies, supporting a CF diagnosis.

CFTR function was also analysed in this patient's organoids and FIS assay in control conditions and at [Fsk] = 0.128 µM evidenced some residual CFTR function (Figure 4.5 A-C). Furthermore, CFL59's unswollen organoid phenotype in basal conditions (Figure 4.5 A, Fsk, 0 min) is also supportive of a CF diagnosis.

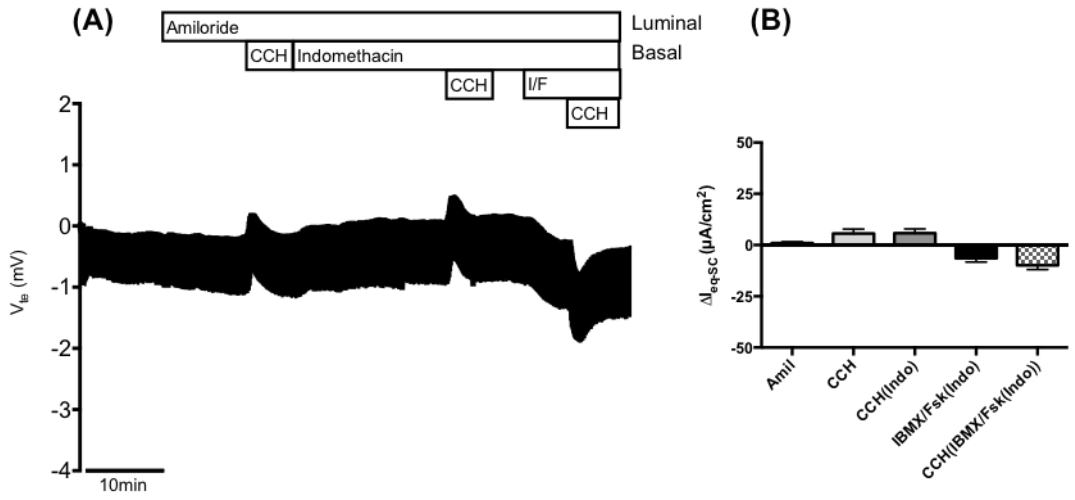

Figure 4.4 – Results from Ussing chamber measurements in rectal biopsies from patient CFL59 (F508del/S955P genotype). (A) Representative original recording of the effects of cholinergic (CCH, 100 µM, basolateral) and cAMP-dependent (IBMX/Fsk (I/F), 100 µM/2 µM, basolateral) activation on transepithelial voltage (V_{te}) in F508del/S955P rectal biopsies from patient CFL59. Experiments were performed in the presence of Amiloride (Amil, 20 µM, luminal) and/or Amiloride + Indomethacin (Indo, 10 µM, basolateral), as indicated in the figure. **(B)** Summary of activated equivalent short-circuit currents (ΔI_{eq-sc}) for Amil ($\Delta I_{eq-sc,Amil}$), basal CCH ($\Delta I_{eq-sc,CCH}$), CCH + Indo ($\Delta I_{eq-sc,CCH(Indo)}$), IBMX/Fsk + Indo ($\Delta I_{eq-sc,IBMX/Fsk(Indo)}$) and CCH following IBMX/Fsk application ($\Delta I_{eq-sc,CCH(IBMX/Fsk(Indo))}$); data represent the mean of measurements on three rectal biopsies ± SEM. $\Delta I_{eq-sc,IBMX/Fsk(Indo)}$ = -6.421 ± 1.844 µA/cm²; $\Delta I_{eq-sc,CCH(IBMX/Fsk(Indo))}$ = -9.877 ± 2.044 µA/cm² (7.5% of WT CFTR function).

In general, results from the analyses of patient CFL59's samples indicated that this patient should probably present non-classic/mild/atypical CF. Although monophasic lumen-negative Cl^- secretory responses upon cAMP and cholinergic co-activation in rectal biopsies are typically associated to healthy tissues[50], previous studies have reported a monophasic profile of response for some residual function CF tissues[49], which might be explained by a tissue's ability for quicker response (faster kinetics). On the other hand, this patient presents borderline sweat chloride levels (56.5 mmol/L), is PS and presents no pulmonary symptoms, a good nutritional status and only mild obstipation, apparently indicating no CF clinical manifestations. However, the patient's age (7 years old) and early CF suspicion (with NBS) and close follow-up might again be an explanation for the apparent lack of CF symptoms.

To our knowledge, S955P is a new, uncharacterized variant for which there are no reports of patients in common CF databases or current literature. It is localized in the intracytoplasmic loop (ICL) 4, connecting the RD to TMD7. We can propose that this mutation should lead to class IV-VI functional defects (resulting in residual functioning CFTR) since F508del is a typically severe class II mutation.

Drug response

At [Fsk] = 0.128 µM, organoid swelling for patient CFL59 with the corrector/potentiator combination treatments VX-809/770 and VX-661/770 was significantly different from control conditions and above the threshold for medium clinical benefit potential (Figure 4.5 B-C).

The fact that this patient presents S955P *in trans* with F508del, for which both combinatorial treatments have been approved, makes it difficult to infer if or how much the S955P-allele is contributing for treatment response. A closely related mutation to S955P, S945L, localized also in CFTR's ICL4, has received approval for Kalydeco® treatment[38]. However, patient CFL59 appears to be unresponsive to this potentiator-only treatment (p = 0.2960). Eventually, the S955P mutation could even lead to mild defects in CFTR processing and also be responsible for the response to combination treatments, or simply be unresponsive to all currently approved modulators. Either way, we predict that the synergistic

action of combo treatments would help to rescue CFTR function in this patient, with potential for clinical benefit (either Orkambi® or Symdeko®; no statistical significant differences detected between them by an unpaired *t*-test, $p = 0.9112$). Following studies should include the characterization of this mutation at the molecular, cellular and functional levels and its specific drug response assessment in CF-relevant cell lines, such as the CFBE cell line.

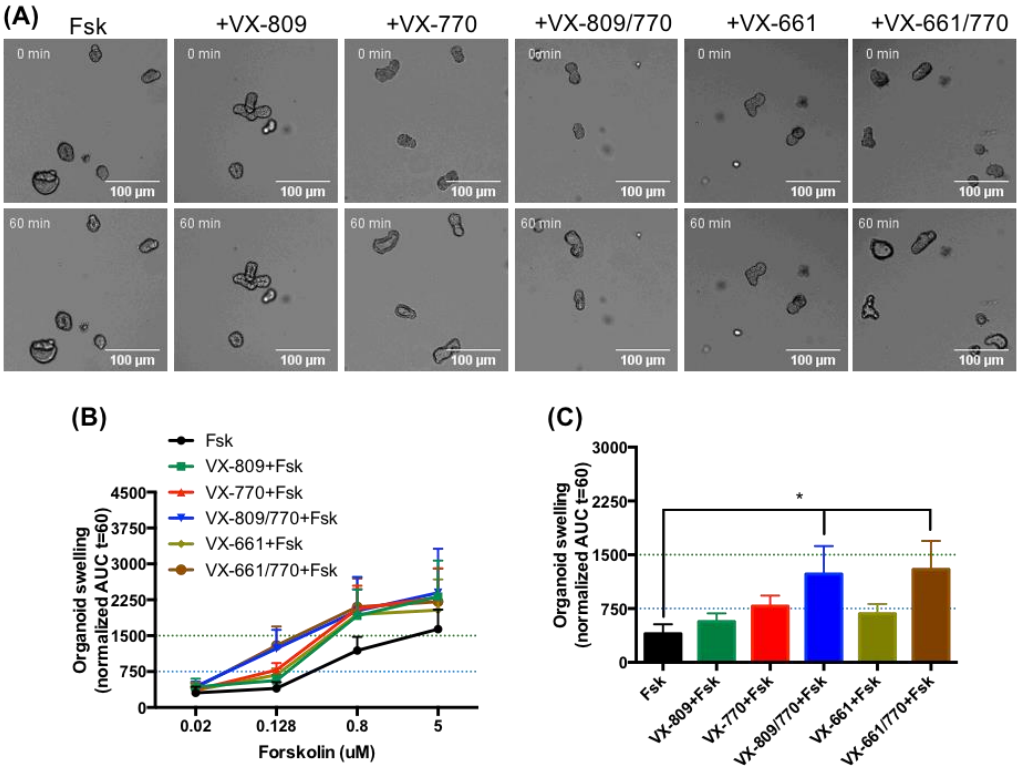

Figure 4.5 – Results from the forskolin-induced swelling (FIS) assay on intestinal organoids from patient CFL59 (F508del/S955P genotype). (A) Representative original wide-field microscopy images of intestinal organoids from patient CFL59 (F508del/S955P) at times 0 and 60 min of incubation with the following treatments: Forskolin (Fsk) alone at the concentration of 0.128 µM, VX-809 (3 µM) + Fsk, VX-770 (3 µM) + Fsk, VX-809/770 + Fsk, VX-661 (5 µM) + Fsk and VX-661/770 + Fsk. **(B)** Quantification of FIS in organoids for all treatments at the Fsk concentrations of 0.02, 0.128, 0.8 and 5 µM, expressed as the AUC of organoid surface area increase (baseline = 100%, t = 60 min). **(C)** Quantification of organoid swelling for all treatments at [Fsk] = 0.128 µM. The dashed blue and green lines represent the established thresholds for medium and high clinical benefit potential for treatments, respectively. **(B)** and **(C**) data represent the mean of measurements on 5-8 replicate wells per condition ± SEM. Asterisks (*) indicate degree of significant difference calculated by unpaired one-way ANOVA to control (Fsk) using Fisher's LSD test.

4.2.4. P205S/Y1092X

Patients CFL05 and CFL06 analysed in the present work were twin sisters sharing the P205S/Y1092X genotype. P205S is reported as being a class II mutation and Y1092X is poorly characterized but thought to interfere with protein production.

Diagnosis

Ussing chamber recordings of V_{te} measurements in P205S/Y1092X rectal biopsies from both twin patients CFL05 and CFL06 (Figure 4.6 A) show a similar profile as for patient CFL59, with a K^+ secretory response upon basal cholinergic stimulation, a small Cl^- secretory response after IBMX/Fsk

stimulation of the tissues and a further increase of this response with a monophasic profile following cholinergic co-activation.

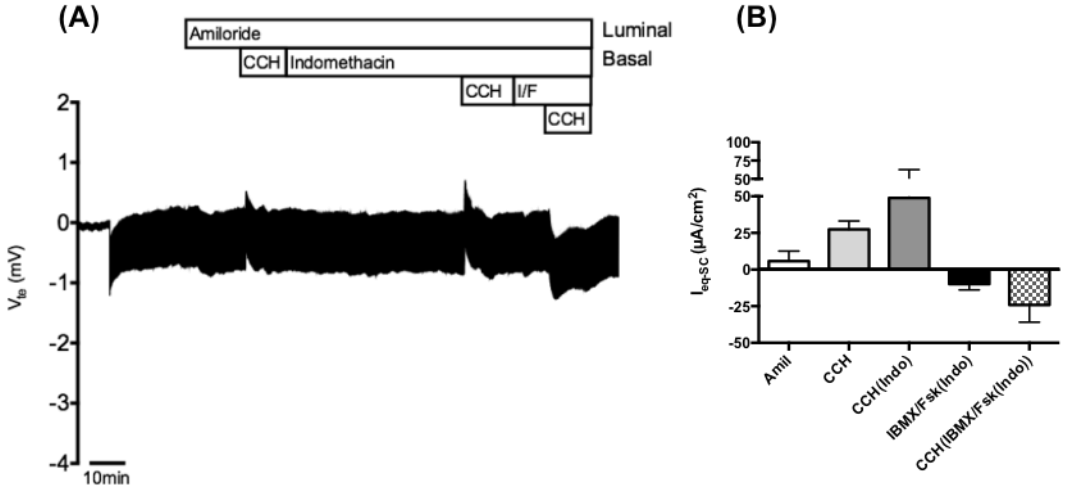

Figure 4.6 – Results from Ussing chamber measurements in rectal biopsies from patients CFL05/06 (P205S/Y1092X genotype). (A) Representative original recording of the effects of cholinergic (CCH, 100 µM, basolateral) and cAMP-dependent (IBMX/Fsk (I/F), 100 µM/2 µM, basolateral) activation on transepithelial voltage (V_{te}) in P205S/Y1092X rectal biopsies from patients CFL05 and CFL06. Experiments were performed in the presence of Amiloride (Amil, 20 µM, luminal) and/or Amiloride + Indomethacin (Indo, 10 µM, basolateral), as indicated in the figure. **(B)** Summary of activated equivalent short-circuit currents ($\Delta I_{eq\text{-}sc}$) for Amil ($\Delta I_{eq\text{-}sc,Amil}$), basal CCH ($\Delta I_{eq\text{-}sc,CCH}$), CCH + Indo ($\Delta I_{eq\text{-}sc,CCH(Indo)}$), IBMX/Fsk + Indo ($\Delta I_{eq\text{-}sc,IBMX/Fsk(Indo)}$) and CCH following IBMX/Fsk application ($\Delta I_{eq\text{-}sc,CCH(IBMX/Fsk(Indo))}$); data represent the mean of measurements on three rectal biopsies ± SEM. $\Delta I_{eq\text{-}sc,IBMX/Fsk(Indo)}$ = -9.882 ± 4.031 µA/cm²; $\Delta I_{eq\text{-}sc,CCH(IBMX/Fsk(Indo))}$ = -24.150 ± 11.720 µA/cm² (15.7% of WT CFTR function). [Experiments were performed by Nikhil Awatade and included with permission].

Again, this tracing profile suggests that these samples should come from mild CF patients. The CFTR function detected in the rectal biopsies was of 15.7% of WT (Figure 4.6 B), which supports a non-classic CF diagnosis for these patients.

However, CFTR function analyses in the intestinal organoids derived from patients CFL05 (Figure 4.7 A-C) and CFL06 (Figure 7.3 A-B, in Appendix II) suggest no residual CFTR function for both patients (no swelling in control conditions for low Fsk concentrations). Besides this, their organoids' basal unswollen phenotype is also supportive of a CF diagnosis.

Furthermore, for both CFL05 and CFL06, CFTR function was additionally analysed in their primary human nasal epithelial cells (HNECs). Analysis of the Ussing chamber recordings of V_{te} measurements in HNECs from patient CFL05 in control conditions (DMSO, Figure 4.8 A) shows a small negative V_{te} deflection after cAMP-mediated stimulation of the cells by IBMX/Fsk, which suggests CFTR residual activity. There was no apparent effect of potentiator Genistein and a positive V_{te} deflection after CFTR-specific inhibition with $CFTR_{inh}$-172 (Inh-172) was observed, confirming a CFTR-dependent response to IBMX/Fsk (Cl^- secretion). A similar pattern was observed for the analysis of the HNECs from patient CFL06 (Figure 7.4 A, in Appendix II).

Overall, results from the analyses of samples from twin siblings patients CFL05 and CFL06 support a mild CF diagnosis for both. Although at first results obtained from the FIS analyses of the organoids appeared to contradict results obtained in rectal biopsies and in HNECs, in the Ussing chamber analyses, a cocktail of 2 µM Fsk + 100 µM IBMX, another cAMP agonist, was used, leading to maximal CFTR activation, while in the FIS assay we assess swelling under a [Fsk] = 0.128 µM alone. At higher Fsk titrations, swelling of the organoids is also detected for both patients in control conditions (Figure 4.7 B

and Figure 7.3 A, in Appendix II). On the other hand, CFTR expression or biosynthesis can be differently regulated in native tissues or cultured systems, which may also be an explanation for the difference observed. Additionally, regarding clinical data, both sisters present pathologic sweat chloride values (91.5 and 89.5 mmol/L, respectively), are PS and present with recurrent respiratory infections and sinusitis, which are also supportive of a CF diagnosis, potentially mild.

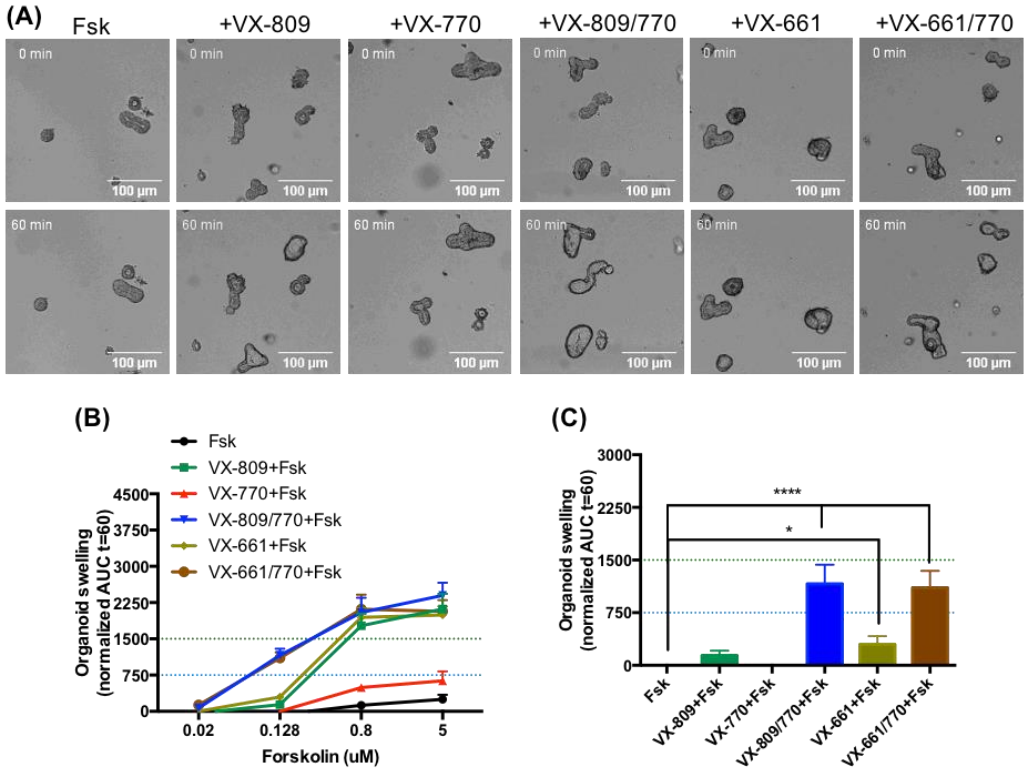

Figure 4.7 – Results from the forskolin-induced swelling (FIS) assay on intestinal organoids from patient CFL05 (P205S/Y1092X genotype). (A) Representative original wide-field microscopy images of intestinal organoids from patient CFL05 (P205S/Y1092X) at times 0 and 60 min of incubation with the following treatments: Forskolin (Fsk) alone at the concentration of 0.128 µM, VX-809 (3 µM) + Fsk, VX-770 (3 µM) + Fsk, VX-809/770 + Fsk, VX-661 (5 µM) + Fsk and VX-661/770 + Fsk. **(B)** Quantification of FIS in organoids for all treatments at the Fsk concentrations of 0.02, 0.128, 0.8 and 5 µM, expressed as the AUC of organoid surface area increase (baseline = 100%, t = 60 min). **(C)** Quantification of organoid swelling for all treatments at [Fsk] = 0.128 µM. The dashed blue and green lines represent the established thresholds for medium and high clinical benefit potential for treatments, respectively. **(B)** and **(C)** data represent the mean of measurements on 5-8 replicate wells per condition ± SEM. Asterisks (*) indicate degree of significant difference calculated by unpaired one-way ANOVA to control (Fsk) using Fisher's LSD test. [Experiments were performed in collaboration with Iris Silva and included with permission].

P205S (frequency of 0.00023[40]) is a missense mutation localized in TMD3. Previous studies have shown that this variant interferes with the correct CFTR processing, but it is associated to a mild CF phenotype, generally with pancreatic sufficiency and no gastrointestinal symptoms[74,75].

Y1092X, on the other hand, is a nonsense mutation (frequency of 0.00158[40]) localized in the ICL5[76], poorly characterized and thought to produce a truncated and non-functional CFTR[77] when the CFTR mRNA is not degraded by nonsense-mediated decay (NMD).

Drug response

For patient CFL05, at [Fsk] = 0.128 µM, there is significant organoid swelling with the combination treatments VX-809/770 and VX-661/770, above the threshold for medium clinical benefit potential (Figure 4.7 B-C). There is also a slight increase in organoid swelling with the corrector VX-661 alone,

however it is below the threshold for low clinical benefit potential. For patient CFL06, a similar pattern was observed, however with higher magnitudes of response (Figure 7.3 A-B, in Appendix II).

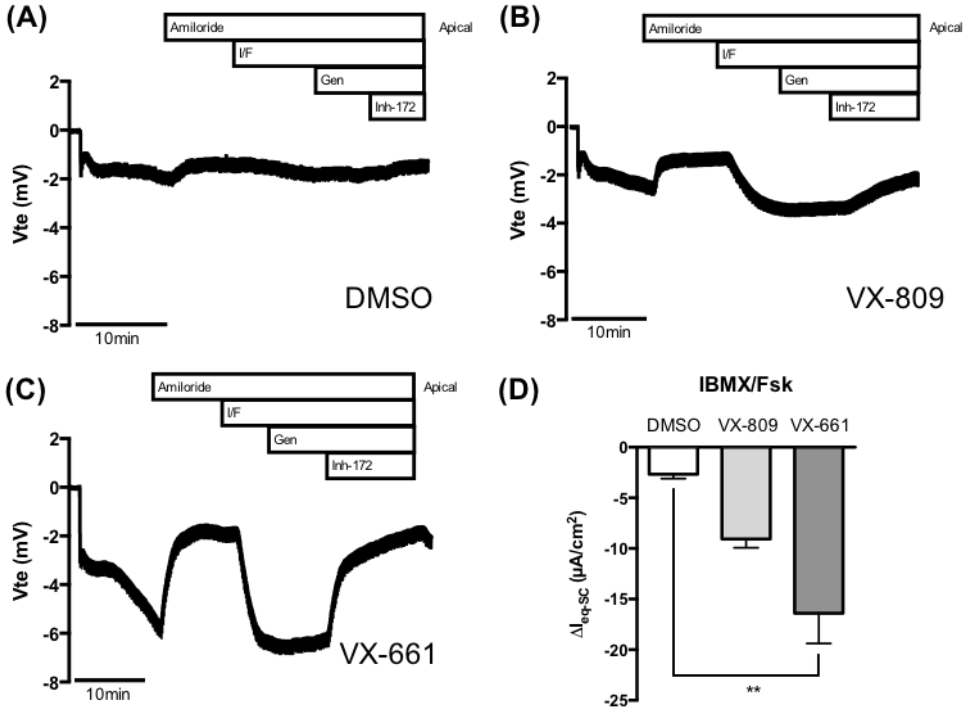

Figure 4.8 – Results from Ussing chamber measurements in human nasal epithelial cells (HNECs) from patient CFL05 (P205S/Y1092X genotype). Representative original recordings of the effects of cAMP-dependent (IBMX/Fsk (I/F), 100 µM/2 µM, apical) activation, CFTR potentiation (Genistein (Gen), 25 µM, apical) and CFTR-specific inhibition ($CFTR_{inh}$-172 (Inh-172), 30 µM, apical) on transepithelial voltage (V_{te}) in HNECs from patient CFL05 (P205S/Y1092X). Experiments were performed in the presence of Amiloride (Amil, 20 µM, apical) for **(A)** 0.05% DMSO **(B)** 3 µM VX-809 and **(C)** 5 µM VX-661 48 h-treated cells. **(D)** Summary of activated equivalent short-circuit currents ($\Delta I_{eq\text{-}sc}$) upon IBMX/Fsk addition for all conditions. Data represent the mean of measurements on 3-5 replicates per condition ± SEM. Asterisks (*) indicate degree of significant difference calculated by unpaired one-way ANOVA to control (DMSO) using Fisher's LSD test.

In patient CFL05 HNECs' analyses, basal CFTR function was further increased in cells treated with VX-809 and VX-661 (Figure 4.8 B-C). Comparison of cAMP-mediated activated currents between the control condition (DMSO) and treatments (Figure 4.8 D) suggests that treatment with corrector VX-661 leads to a significant CFTR function rescue in these cells. Increase in CFTR function was also observed with VX-809, however it was not statistically different from the control (p = 0.1404). For patient CFL06, again a similar pattern was observed. For this patient, however, there were no significant statistical differences when both treatments were compared to control, although there was a tendency observed for CFTR rescue with the two correctors VX-809 and VX-661 (Figure 7.4 D, in Appendix II).

For both patients, significant organoid swelling is observed with combination treatments, which supports that the P205S mutation might mildly interfere with normal CFTR maturation and may present defects (e.g. in conductance) when correctly transported to the PM, assuming that the Y1092X-allele leads to severely reduced CFTR mRNA levels and completely non-functional CFTR. Ussing chamber analyses of P205S/Y1092X nasal cells suggest that treatment with either corrector alone seems to have an effect in CFTR rescue in these cells, despite sometimes not significant, which again supports a CFTR processing defect for this genotype. Both environmental and stochastic factors may generally explain the differences detected between twins' samples, but, our experience with HNECs tell us that their process of re-differentiation is very arbitrary and can lead to various degrees of differentiation even between cells from the same patient, seeded and treated in equal form, leading to disparate results. Thus,

testing of a bigger sample should be performed to validate the obtained results. Also, we might be using a saturating concentration of cAMP agonists in the Ussing chamber, that does not allow us to correctly detect more subtle functional differences between untreated and treated cells, which are relevant since the nasal epithelium, in contrast to the intestinal epithelium, expresses very low levels of CFTR. Nevertheless, we predict that these patients would probably benefit most from treatment with combos Orkambi® or Symdeko®.

4.2.5. D614G/F508del

Patient CFL44 analysed in this project had the D614G/F508del genotype. The D614G mutation has been shown to lead to processing defects in CFTR.

Diagnosis

The profile of the representative Ussing chamber tracing from analysis of the rectal biopsies from patient CFL44 (Figure 4.9 A) suggests, as in previous results, that these samples should be from a mild CF patient. The percentage of normal CFTR function in these tissues was calculated at 23.8% (Figure 4.9 B), backing a non-classic CF diagnosis.

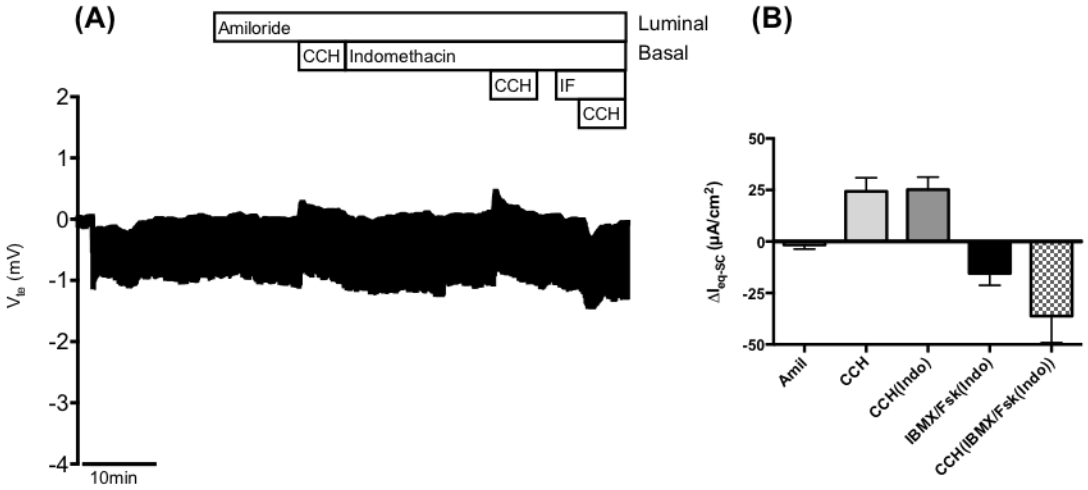

Figure 4.9 – Results from Ussing chamber measurements in rectal biopsies from patient CFL44 (D614G/F508del genotype). (A) Representative original recording of the effects of cholinergic (CCH, 100 µM, basolateral) and cAMP-dependent (IBMX/Fsk (I/F), 100 µM/2 µM, basolateral) activation on transepithelial voltage (V_{te}) in D614G/F508del rectal biopsies from patient CFL44. Experiments were performed in the presence of Amiloride (Amil, 20 µM, luminal) and/or Amiloride + Indomethacin (Indo, 10 µM, basolateral), as indicated in the figure. **(B)** Summary of activated equivalent short-circuit currents (ΔI_{eq-sc}) for Amil ($\Delta I_{eq-sc,Amil}$), basal CCH ($\Delta I_{eq-sc,CCH}$), CCH + Indo ($\Delta I_{eq-sc,CCH(Indo)}$), IBMX/Fsk + Indo ($\Delta I_{eq-sc,IBMX/Fsk(Indo)}$) and CCH following IBMX/Fsk application ($\Delta I_{eq-sc,CCH(IBMX/Fsk(Indo))}$); data represent the mean of measurements on three rectal biopsies ± SEM. $\Delta I_{eq-sc,IBMX/Fsk(Indo)}$ = -15.550 ± 5.743 µA/cm^2; $\Delta I_{eq-sc,CCH(IBMX/Fsk(Indo))}$ = -36.200 ± 12.900 µA/cm^2 (23.8% of WT CFTR function). [Experiments were performed in collaboration with Iris Silva and included with permission].

Analysis of CFTR function was also performed in patient CFL44's intestinal organoids and indicated some residual function at [Fsk] = 0.128 µM (Figure 4.10 A-C). Moreover, CFL44's predominantly unswollen organoid phenotype in basal conditions (Figure 4.10 A, Fsk, 0 min) also reinforces the CF diagnosis.

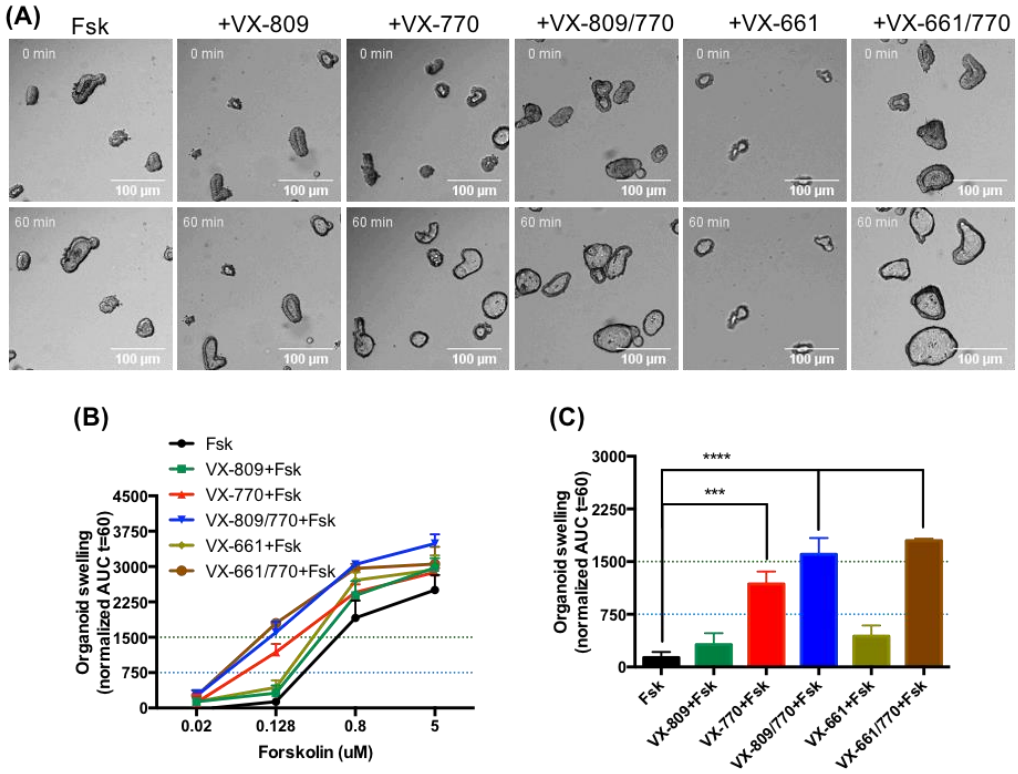

Figure 4.10 – Results from the forskolin-induced swelling (FIS) assay on intestinal organoids from patient CFL44 (D614G/F508del genotype). (A) Representative original wide-field microscopy images of intestinal organoids from patient CFL44 (D614G/F508del) at times 0 and 60 min of incubation with the following treatments: Forskolin (Fsk) alone at the concentration of 0.128 µM, VX-809 (3 µM) + Fsk, VX-770 (3 µM) + Fsk, VX-809/770 + Fsk, VX-661 (5 µM) + Fsk and VX-661/770 + Fsk. **(B)** Quantification of FIS in organoids for all treatments at the Fsk concentrations of 0.02, 0.128, 0.8 and 5 µM, expressed as the AUC of organoid surface area increase (baseline = 100%, t = 60 min). **(C)** Quantification of organoid swelling for all treatments at [Fsk] = 0.128 µM. The dashed blue and green lines represent the established thresholds for medium and high clinical benefit potential for treatments, respectively. **(B)** and **(C**) data represent the mean of measurements on 5-8 replicate wells per condition ± SEM. Asterisks (*) indicate degree of significant difference calculated by unpaired one-way ANOVA to control (Fsk) using Fisher's LSD test. [Experiments were performed in collaboration with Iris Silva and included with permission].

In addition, CFTR function was analysed in patient CFL44's nasal cells. As before, Ussing chamber recordings of V_{te} measurements in control conditions (DMSO) show a negative V_{te} deflection after cAMP-mediated stimulation of the cells with IBMX/Fsk, and an increase in V_{te} after inhibition with $CFTR_{inh}$-172 (Inh-172), in agreement with residual CFTR function in these cells (Figure 4.11 A).

In general, although clinical data is not available from this patient, all together, our results suggest that patient CFL44 presents a milder form of CF.

D614G (frequency of 0.00012[40]) is a missense mutation localized in the RD. Previous studies in transfected COS-1 cells have shown that D614G mutants present an abnormal CFTR maturation pattern[78]. However, this mutation has been associated with atypical late-onset CF, suggesting residual CFTR activity, with phenotypic discordance among closely related subjects (siblings) sharing the D614G/F508del genotype[79]. In the CFTR2 database, D614G is reported as having varying clinical consequences, as discussed previously for D1152H.

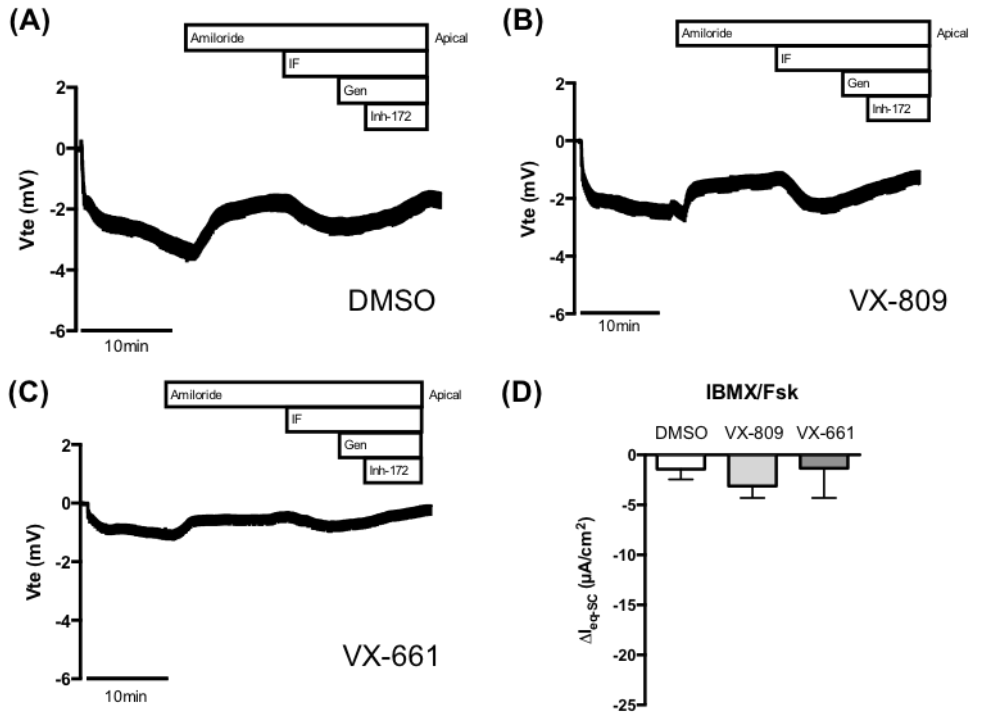

Figure 4.11 – Results from Ussing chamber measurements in human nasal epithelial cells (HNECs) from patient CFL44 (D614G/F508del genotype). Representative original recordings of the effects of cAMP-dependent (IBMX/Fsk (I/F), 100 µM/2 µM, apical) activation, CFTR potentiation (Genistein (Gen), 25 µM, apical) and CFTR-specific inhibition ($CFTR_{inh}$-172 (Inh-172), 30 µM, apical) on transepithelial voltage (V_{te}) in HNECs from patient CFL44 (D614G/F508del). Experiments were performed in the presence of Amiloride (Amil, 20 µM, apical) for **(A)** 0.05% DMSO **(B)** 3 µM VX-809 and **(C)** 5 µM VX-661 48 h-treated cells. **(D)** Summary of activated equivalent short-circuit currents ($\Delta I_{eq\text{-}sc}$) upon IBMX/Fsk addition for all conditions. Data represent the mean of measurements on 3-5 replicates per condition ± SEM. No statistically significant differences were detected by unpaired one-way ANOVA to control (DMSO) using Fisher's LSD test.

Drug response

Analysis of CFTR function rescue through FIS assay showed a significant increase in swelling of the organoids from patient CFL44 with the combination treatments VX-809/770 and VX-661/770 at [Fsk] = 0.128 µM, above the threshold for high clinical benefit potential of treatments, and with the potentiator-only treatment VX-770, with medium clinical benefit potential (Figure 4.10 B-C).

As for the HNECs analysis, there were no significant differences detected in the CFTR-dependent Cl^- secretion response after IBMX/Fsk stimulation, between control and treated cells (Figure 4.11 A-D).

Overall, CFTR rescue in organoids from patient CFL44 is observed for all treatments with potentiator VX-770. A higher and statistically significant difference to VX-770 alone was obtained for combo treatment VX-661/770 (p = 0.0411) but not for VX-809/770 (p = 0.1267), which suggests that CFTR function rescue is mainly obtained by CFTR potentiation and that there is a synergistic action of corrector VX-661 and VX-770 which further increases rescue in this patient's organoids. This supports a residual function character for the D614G mutant and that, in this patient particularly, this mutation appears to not lead to a severe defect in CFTR maturation, unlike previously reported[78]. Western blot analyses of these samples will help understand if this D614G-CFTR mutant presents indeed a maturation defect and its severity. As for the nasal cells analyses, results appeared to indicate that treatment with either corrector alone seems to not have any effect in CFTR rescue in these cells, which supports the previously drawn conclusions from the FIS analysis of the organoids. Globally, our results support that

although this patient might benefit from a CFTR potentiation treatment alone (Kalydeco®), the combination treatments Orkambi® or, most likely, Symdeco® may to lead to better clinical outcomes.

4.2.6. 3849+10kbC>T/F508del

Another two patients analysed in this study were CFL57 and CFL58, siblings sharing the 3849+10kbC>T/F508del genotype. 3849+10kbC>T is a class V splicing mutation.

Diagnosis

Analysis of the Ussing chamber recordings of V_{te} measurements in rectal biopsies from patient CFL57 (Figure 4.12 A) shows, after cAMP-mediated stimulation of the tissue by IBMX/Fsk, a barely detectable negative V_{te} deflection which is then followed by a biphased positive-then-negative transient response upon cholinergic co-activation, most characteristic of CF patients with residual CFTR function (mild CF). Quantification of CFTR function for this patient's rectal tissues was of 4.2% of WT samples, supporting a CF diagnosis (Figure 4.12 B). A slightly similar profile is observed for patient CFL58 (Figure 7.5 A-B in Appendix II). The percentage of CFTR function in CFL58's rectal biopsies was estimated at 1.8% of WT, also supporting a CF diagnosis for this patient.

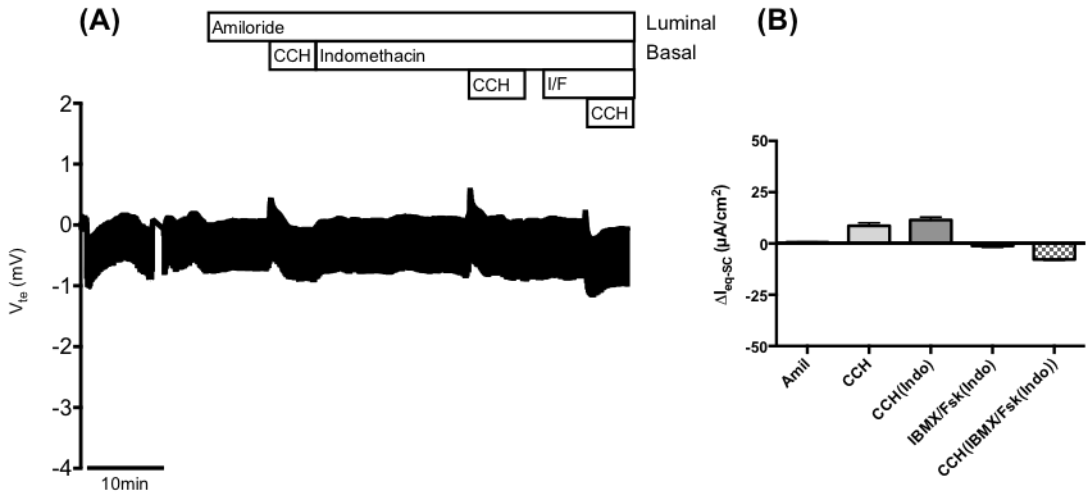

Figure 4.12 – Results from Ussing chamber measurements in rectal biopsies from patient CFL57 (3849+10kbC>T/F508del genotype). (A) Representative original recording of the effects of cholinergic (CCH, 100 µM, basolateral) and cAMP-dependent (IBMX/Fsk (I/F), 100 µM/2 µM, basolateral) activation on transepithelial voltage (V_{te}) in 3849+10kbC>T/F508del rectal biopsies from patient CFL57. Experiments were performed in the presence of Amiloride (Amil, 20 µM, luminal) and/or Amiloride + Indomethacin (Indo, 10 µM, basolateral), as indicated in the figure. **(B)** Summary of activated equivalent short-circuit currents ($\Delta I_{eq\text{-}sc}$) for Amil ($\Delta I_{eq\text{-}sc,Amil}$), basal CCH ($\Delta I_{eq\text{-}sc,CCH}$), CCH + Indo ($\Delta I_{eq\text{-}sc,CCH(Indo)}$), IBMX/Fsk + Indo ($\Delta I_{eq\text{-}sc,IBMX/Fsk(Indo)}$) and CCH following IBMX/Fsk application ($\Delta I_{eq\text{-}sc,CCH(IBMX/Fsk(Indo))}$); data represent the mean of measurements on three rectal biopsies ± SEM. $\Delta I_{eq\text{-}sc,IBMX/Fsk(Indo)}$ = -1.236 ± 0.638 µA/cm^2; $\Delta I_{eq\text{-}sc,CCH(IBMX/Fsk(Indo))}$ = -7.796 ± 0.370 µA/cm^2 (4.2% of WT CFTR function).

Analysis of patient CFL57's intestinal organoids indicates residual CFTR function in control conditions (Figure 4.13 A-C), and a lower function appears to be detected for sibling patient CFL58 (Figure 7.6 A-B in Appendix II). Once more, the basal organoid phenotype also suggests CF disease for both patients.

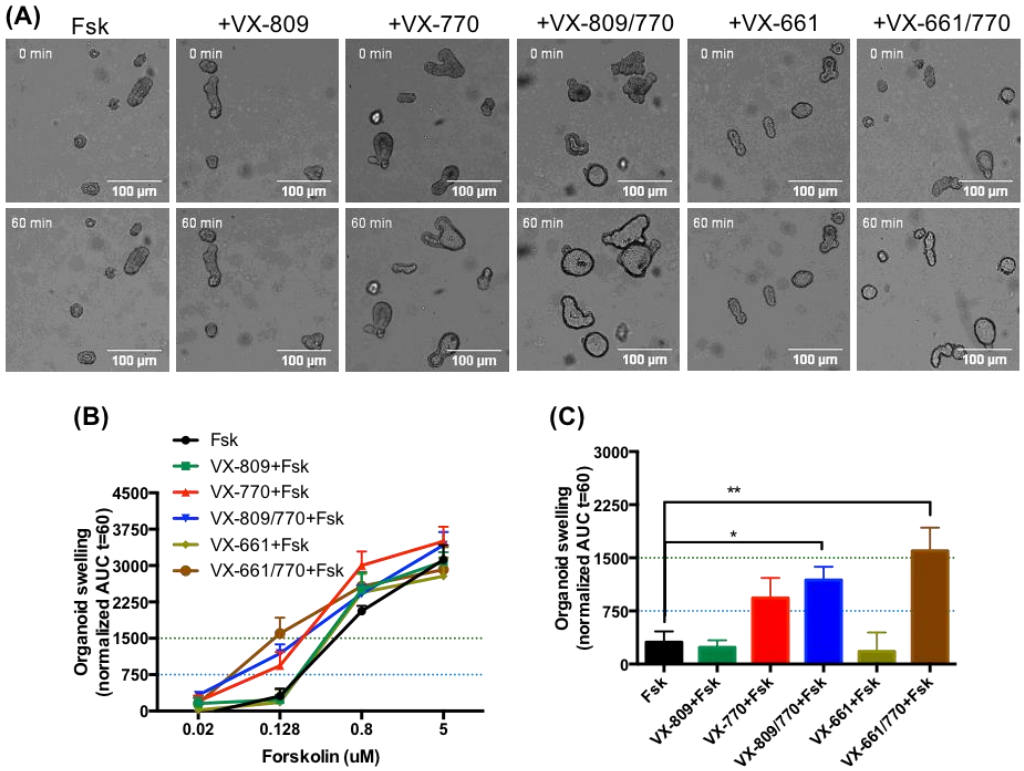

Figure 4.13 – Results from the forskolin-induced swelling (FIS) assay on intestinal organoids from patient CFL57 (3849+10kbC>T/F508del genotype). (A) Representative original wide-field microscopy images of intestinal organoids from patient CFL57 (3849+10kbC>T/F508del) at times 0 and 60 min of incubation with the following treatments: Forskolin (Fsk) alone at the concentration of 0.128 µM, VX-809 (3 µM) + Fsk, VX-770 (3 µM) + Fsk, VX-809/770 + Fsk, VX-661 (5 µM) + Fsk and VX-661/770 + Fsk. **(B)** Quantification of FIS in organoids for all treatments at the Fsk concentrations of 0.02, 0.128, 0.8 and 5 µM, expressed as the AUC of organoid surface area increase (baseline = 100%, t = 60 min). **(C)** Quantification of organoid swelling for all treatments at [Fsk] = 0.128 µM. The dashed blue and green lines represent the established thresholds for medium and high clinical benefit potential for treatments, respectively. **(B)** and **(C)** data represent the mean of measurements on 4-6 replicate wells per condition ± SEM. Asterisks (*) indicate degree of significant difference calculated by unpaired one-way ANOVA to control (Fsk) using Fisher's LSD test.

Results from the analyses of patients CFL57 and CFL58's samples support a diagnosis of mild CF for both patients, being that for patient CFL57 we can clearly observe a biphasic profile of response to cholinergic co-activation in rectal biopsies. Poorer gastrointestinal tract conditions of CFL58 could explain the not so clear tracings obtained for this patient, and FIS results do appear to evidence higher residual function for CFL57 than for CFL58. Furthermore, regarding the clinical data obtained from these sibling patients, both present normal sweat chloride values, are PS, and present with mild (CFL57) to severe (CFL58) pulmonary disease. Sibling CFL58 also presents gastroesophageal reflux and has indeed a poorer nutritional status.

The 3849+10kbC>T mutation (frequency of 0.00815[40]) is a class V splicing mutation that creates a partially active splice site in intron 19 of the *CFTR* gene, which can lead to the insertion of a new 84-bp pseudoexon that harbours an in-frame stop codon, between exons 19 and 20[80]. This CF-causing mutation has been shown to produce normal and aberrantly spliced CFTR transcripts and lower levels of normal mRNA have been correlated with histopathologic changes observed in different organs[81]. In general, this mutation has in fact been associated to milder disease forms with normal sweat [Cl^-] levels, pancreatic sufficiency and varying severity of pulmonary and gastrointestinal disease[80,81].

Drug response

FIS analysis in patient CFL57's intestinal organoids shows, at [Fsk] = 0.128 μM, significant increase in organoid swelling (hence, CFTR rescue) with the combo treatments VX-809/770 and VX-661/770 (no significant difference between them), when compared to control, with predicted medium and high clinical benefit potentials, respectively (Figure 4.13 B-C). A tendency for rescue although not statistically significant is also observed for VX-770 (p = 0.0827). FIS analyses of patient CFL58's organoids also show a similar pattern of results, with the combinations VX-809/770 and VX-661/770 having an effect above the threshold for medium clinical benefit potential. In this case, although the VX-770 treatment was also responsible for a significant effect in CFTR rescue, it was with predicted low clinical benefit potential (Figure 7.6 A-B in Appendix II).

VX-770 alone (Kalydeco®) has been approved for the treatment of patients carrying the 3849+10kbC>T mutation[38]. The differences in results obtained between these siblings can be explained by different ratios of normal/aberrant transcripts being expressed by both patients and even by different levels of total *CFTR* expression between the siblings. This could also account for the differences observed in responses to combination treatments which are also rescuing F508del-CFTR, for which they have been primarily designed. A quantification of the levels of normal transcripts being produced by these alleles would help to better understand the difference in functional results obtained for the siblings' samples. Still, we predict that either combo treatments, Orkambi® or Symdeco®, could potentially lead to better clinical outcomes for both patients CFL57 and CFL58.

4.2.7. 3849+10kbC>T/other

Two more patients analysed in this project carried the 3849+10kbC>T mutation, although *in trans* with other non-F508del mutations, namely, CFL49 (3849+10kbC>T/dele2,3(21kb)) and CFL56 (3849+10kbC>T/621+1G>T). dele2,3(21kb) (frequency of 0.00294[40]) is a large genomic deletion of 21.080 bp spanning introns 1-3 of the *CFTR* gene that results in the loss of exons 2 and 3 in the CFTR mRNA, producing a premature termination signal within exon 4[82]. It is classified as a CF-causing class VII (no mRNA) pharmacologically unrescuable mutation, associated to a severe phenotype[1].

The 621+1G>T mutation (frequency of 0.00931[40]) has been shown to activate an alternative splice site within exon 4 or the complete skipping of exon 4 and to result in aberrant splicing of the CFTR mRNA in nasal epithelial cells, leading to almost absence of correctly spliced transcripts[52,83]. This mutation has been classified as severe with regards to pancreatic and pulmonary phenotypes and sweat chloride concentrations, but 621+1G>T-*CFTR* homozygous patients have also presented milder forms of CF[84].

Diagnosis

Results from analyses of rectal biopsies from patients CFL49 (Figure 4.14 A-B) and CFL56 (Figure 7.7 A-B in Appendix II) support the diagnosis of mild CF for both patients. The CFTR function calculated in relation to WT samples was of 7.9% and 6.6%, respectively. Regarding clinical data, patient CFL49 presents a borderline abnormal sweat chloride concentration (60.0 mmol/L), is PS and has bronchiectasis. Patient CFL56 presents a more severe form of disease, with higher abnormal levels of sweat chloride (81.5 mmol/L), PS although presenting a poor nutritional status, bronchiectasis in the left lung and has suffered surgical removal of the right lung. These data are also in agreement with an

atypical CF diagnosis for both patients. CFL56's more severe phenotype may again be related to different levels of normal CFTR being transcribed amongst patients and each patients' tissues, so the quantification of normal transcripts being produced by these specific alleles would help better explain the obtained results and observed phenotypes. Also, these patients' response to therapy should next be analysed using their own-derived intestinal organoids.

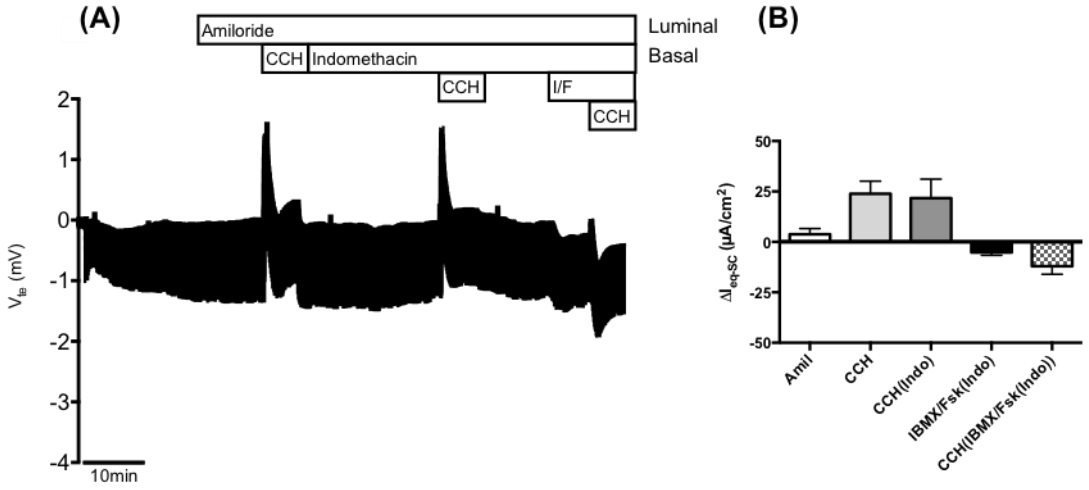

Figure 4.14 – Results from Ussing chamber measurements in rectal biopsies from patient CFL49 (3849+10kbC>T/dele2,3(21kb) genotype). (A) Representative original recording of the effects of cholinergic (CCH, 100 µM, basolateral) and cAMP-dependent (IBMX/Fsk (I/F), 100 µM/2 µM, basolateral) activation on transepithelial voltage (V_{te}) in 3849+10kbC>T/dele2,3(21kb) rectal biopsies from patient CFL49. Experiments were performed in the presence of Amiloride (Amil, 20 µM, luminal) and/or Amiloride + Indomethacin (Indo, 10 µM, basolateral), as indicated in the figure. **(B)** Summary of activated equivalent short-circuit currents (ΔI_{eq-sc}) for Amil ($\Delta I_{eq-sc,Amil}$), basal CCH ($\Delta I_{eq-sc,CCH}$), CCH + Indo ($\Delta I_{eq-sc,CCH(Indo)}$), IBMX/Fsk + Indo ($\Delta I_{eq-sc,IBMX/Fsk(Indo)}$) and CCH following IBMX/Fsk application ($\Delta I_{eq-sc,CCH(IBMX/Fsk(Indo))}$); data represent the mean of measurements on four rectal biopsies ± SEM. $\Delta I_{eq-sc,IBMX/Fsk(Indo)}$ = -5.167 ± 1.476 µA/cm^2; $\Delta I_{eq-sc,CCH(IBMX/Fsk(Indo))}$ = -12.020 ± 3.996 µA/cm^2 (7.9% of WT CFTR function).

4.2.8. F508del/R347P

Other patients with potentially mild *CFTR* genotypes were also analysed in this project.

Patient CFL54 carries a F508del/R347P genotype. R347P (frequency of 0.00375[40]) is a missense CF-causing mutation localized in TMD6 that has been shown to allow for normal CFTR processing but to present reduced conductance of the channel[85]. Thus, this mutation was classified as class IV and it has been associated to milder phenotypes. However, in a study with 19 patients carrying this mutation, it has also been shown to lead to severe CF, including two homozygotes for R347P-*CFTR* that showed PI, pathologic sweat chloride values, early onset of pulmonary symptoms and growth retardation[86]. When tested in transfected FRT cells, this variant has shown low[61] to no[87] residual function.

Diagnosis

Analysis of rectal biopsies from patient CFL54 (Figure 4.15 A-B) supports a diagnosis of mild CF, with the detection of 4.6% of normal CFTR function in these tissues. This patient (18 years old) presents abnormal sweat chloride values (84.6 mmol/L), severe pulmonary disease with obstruction of peripheral airways but is PS. These results are in agreement with a CF diagnosis, mild but potentially evolving to more severe. The intestinal organoids and nasal cells from this patient should be analysed in the future

for assessment of a personalized therapy response. Kalydeco® has been approved for the treatment of patients carrying the closely related mutation R347H[38], that also leads to conductance defects in CFTR, which suggests it could eventually also be a potential treatment for patient CFL54.

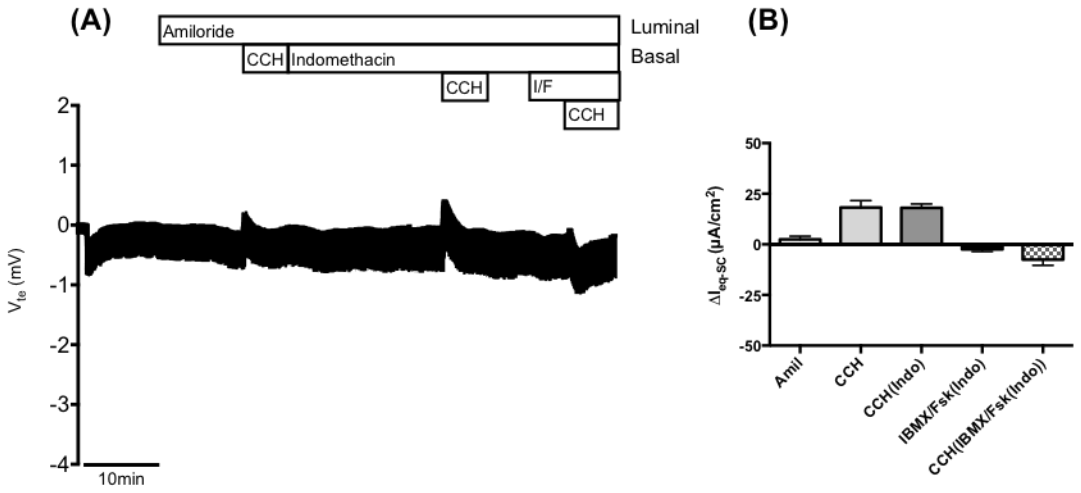

Figure 4.15 – Results from Ussing chamber measurements in rectal biopsies from patient CFL54 (F508del/R347P genotype). (A) Representative original recording of the effects of cholinergic (CCH, 100 µM, basolateral) and cAMP-dependent (IBMX/Fsk (I/F), 100 µM/2 µM, basolateral) activation on transepithelial voltage (V_{te}) in F508del/R347P rectal biopsies from patient CFL54. Experiments were performed in the presence of Amiloride (Amil, 20 µM, luminal) and/or Amiloride + Indomethacin (Indo, 10 µM, basolateral), as indicated in the figure. **(B)** Summary of activated equivalent short-circuit currents (ΔI_{eq-sc}) for Amil ($\Delta I_{eq-sc,Amil}$), basal CCH ($\Delta I_{eq-sc,CCH}$), CCH + Indo ($\Delta I_{eq-sc,CCH(Indo)}$), IBMX/Fsk + Indo ($\Delta I_{eq-sc,IBMX/Fsk(Indo)}$) and CCH following IBMX/Fsk application ($\Delta I_{eq-sc,CCH(IBMX/Fsk(Indo))}$); data represent the mean of measurements on four rectal biopsies ± SEM. $\Delta I_{eq-sc,IBMX/Fsk(Indo)}$ = -2.473 ± 1.051 µA/cm^2; $\Delta I_{eq-sc,CCH(IBMX/Fsk(Indo))}$ = -7.509 ± 2.846 µA/cm^2 (4.6% of WT CFTR function).

4.2.9. F508del/R334W

Patient CFL69 carries a F508del/R334W genotype. R334W (frequency of 0.00302[40]) is a CF-causing mutation, also localized in TMD6 and classified as class IV due to normal protein processing but severely reduced channel conductance observed in transfected FRT cells[61,85]. Patients carrying this variant have presented variable phenotypic traits regarding pancreatic sufficiency and respiratory disease, and sweat chloride values are generally pathologic[88].

Drug response

Although proper Ussing chamber recordings from analyses of rectal biopsies from patient CFL69 were not obtained, intestinal organoid cultures were still produced from these biopsies. Results from FIS analyses in organoids from patient CFL69 (Figure 4.16 A-B) suggest a low residual CFTR function, likely associated to the R334W allele, and rescue is observed with combination treatments VX-809/770 and VX-661/770, although with low potential for clinical benefit. F508del-CFTR is potentially being responsible for therapy response and unresponsiveness to potentiator-only treatment suggests that the R334W-CFTR conductance defect is insensitive to VX-770. Overall, we do not predict a significant clinical benefit for patient CFL69 from treatment with any of the CFTR-corrective drugs tested.

Regarding clinical data, patient CFL69 (17 years old) presents elevated sweat chloride levels (112.5 mmol/L), mild pulmonary disease characterized by chronic coughs and asthma, and has recently been

diagnosed with PI. Ultimately, the FIS assay results and clinical data from the patient support the diagnosis of CF, potentially freshly evolved to a more severe form. However, a clearer diagnostic recommendation from our analyses would request a new assessment of CFL69's rectal biopsies.

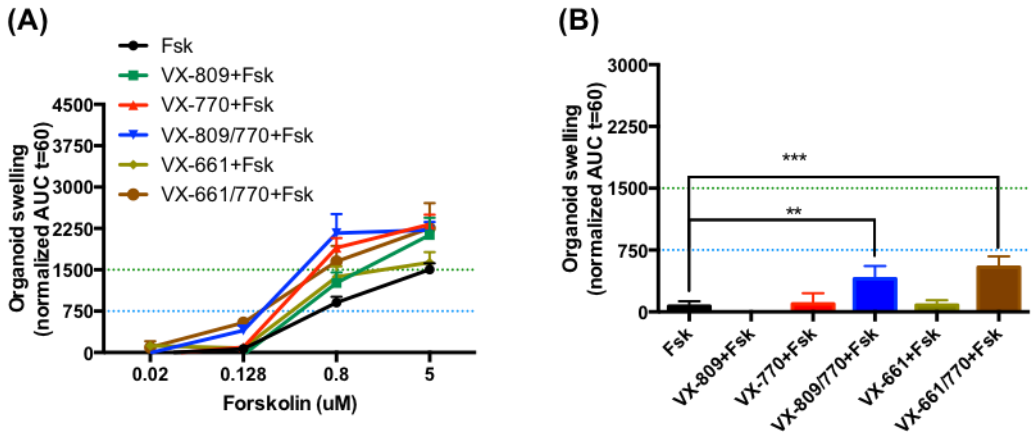

Figure 4.16 – Results from the forskolin-induced swelling (FIS) assay on intestinal organoids from patient CFL69 (F508del/R334W genotype). (A) Quantification of FIS in organoids for all treatments tested (Forskolin (Fsk) alone, VX-809 (3 µM) + Fsk, VX-770 (3 µM) + Fsk, VX-809/770 + Fsk, VX-661 (5 µM) + Fsk and VX-661/770 + Fsk) at the Fsk concentrations of 0.02, 0.128, 0.8 and 5 µM, expressed as the AUC of organoid surface area increase (baseline = 100%, t = 60 min). **(B)** Quantification of organoid swelling for all treatments at [Fsk] = 0.128 µM. The dashed blue and green lines represent the established thresholds for medium and high clinical benefit potential for treatments, respectively. Data represent the mean of measurements on 5-8 replicate wells per condition ± SEM. Asterisks (*) indicate degree of significant difference calculated by unpaired one-way ANOVA to control (Fsk) using Fisher's LSD test.

4.2.10. 2789+5G>A/other

Patients CFL55 and CFL27 both carry a F508del/2789+5G>A genotype and patient CFL62 carries a 2789+5G>A/dele2,3(21kb) genotype. 2789+5G>A (frequency of 0.00723[40]), a CF-causing splicing mutation, was shown to disrupt the splice donor site of exon 14b, leading to its skipping and resulting in a frameshift of the CFTR mRNA and early termination of the protein[89]. However, this allele was also shown to generate a small amount of normal CFTR mRNA in nasal epithelial cells, which should lead to a milder respiratory phenotype for patients that carry it. It has been associated to PS and abnormal sweat chloride concentrations and classified as class V[89].

Diagnosis

Rectal biopsies analyses for patients CFL55 and CFL27 (Figure 7.8 A-B and Figure 7.9 A-B in Appendix II) support a mild CF diagnosis for both patients, with 5.5% and 1.5% of normal CFTR function detected, respectively. They are both PS, present abnormal levels of sweat chloride (91.0 and 78.0 mmol/L, respectively) and mild to severe pulmonary disease. Regarding patient CFL62, also a mild CF diagnosis is proposed (Figure 4.17 A-B; 2.0% of normal CFTR function). This patient also presents abnormal sweat chloride levels (100.5 mmol/L), is PS and shows mild respiratory symptoms. Residual function in these patients is probably associated to the 2789+5G>A-*CFTR* allele. Their rectal biopsy-derived organoids and HNECs should next be analysed for assessment of their individual drug response, particularly since Kalydeco® has been approved for the treatment of patients carrying the 2789+5G>A mutation in *CFTR*[38].

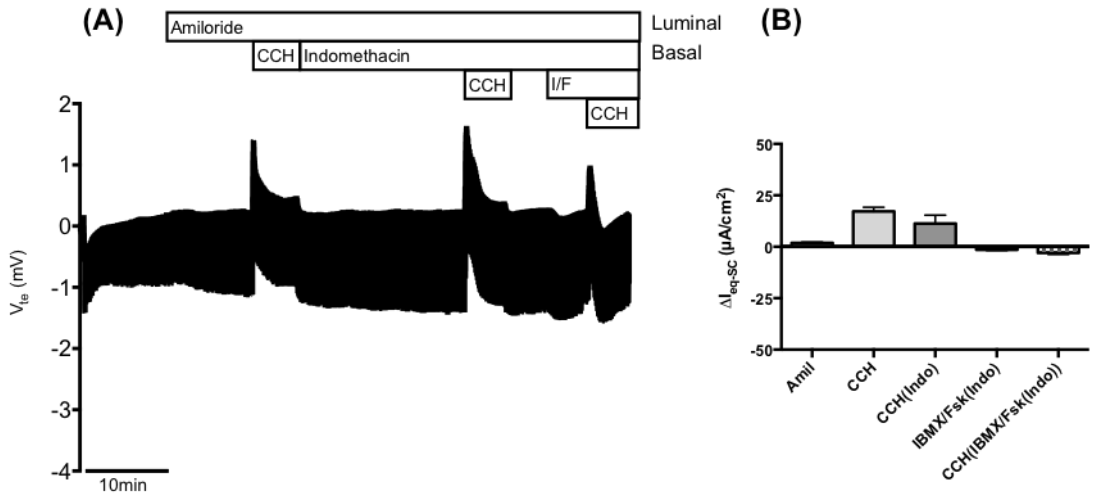

Figure 4.17 – Results from Ussing chamber measurements in rectal biopsies from patient CFL62 (2789+5G>A/dele2,3(21kb) genotype). Representative original recording of the effects of cholinergic (CCH, 100 µM, basolateral) and cAMP-dependent (IBMX/Fsk (I/F), 100 µM/2 µM, basolateral) activation on transepithelial voltage (V_{te}) in 2789+5G>A/dele2,3(21kb) rectal biopsies from patient CFL62. Experiments were performed in the presence of Amiloride (Amil, 20 µM, luminal) and/or Amiloride + Indomethacin (Indo, 10 µM, basolateral), as indicated in the figure. **(B)** Summary of activated equivalent short-circuit currents (ΔI_{eq-sc}) for Amil ($\Delta I_{eq-sc,Amil}$), basal CCH ($\Delta I_{eq-sc,CCH}$), CCH + Indo ($\Delta I_{eq-sc,CCH(Indo)}$), IBMX/Fsk + Indo ($\Delta I_{eq-sc,IBMX/Fsk(Indo)}$) and CCH following IBMX/Fsk application ($\Delta I_{eq-sc,CCH(IBMX/Fsk(Indo))}$); data represent the mean of measurements on four rectal biopsies ± SEM. $\Delta I_{eq-sc,IBMX/Fsk(Indo)}$ = -1.451 ± 0.305 µA/cm^2; $\Delta I_{eq-sc,CCH(IBMX/Fsk(Indo))}$ = -2.952 ± 0.758 µA/cm^2 (2.0% of WT CFTR function).

4.2.11. 3272-26A>G/other

Finally, patients CFL63 and CFL64 both carry the 3272-26A>G mutation in *CFTR*, although *in trans* with W57G (CFL63) or F508del (CFL64). The 3272-26A>G mutation (frequency of 0.00331[40]) has been shown to create a new splice acceptor site in intron 17a that leads to alternative splicing including 25 nucleotides from intron 17a, causing a frameshift and premature termination of the CFTR protein. Both aberrant and normal splicing products are generated by this allele and it was thus classified as class V[90]. Patients carrying this mutation present typically abnormal levels of sweat chloride, are PS and have mild to moderate pulmonary disease, with extensive nasal polyposis being a common trait[90].

W57G (frequency of 0.00007[40]) is a missense CF-causing mutation localized in the amino-terminal (*N*-term) cytoplasmic tail of CFTR. This mutation has been shown to interfere with the correct processing and maturation of the CFTR protein[91], being classified as class II. W57G has also been associated to abnormal sweat chloride levels and pancreatic insufficiency[40].

Diagnosis

Analysis of rectal biopsies from patients CFL63 (Figure 4.18 A-B) and CFL64 (Figure 7.10 in Appendix II) (8.9 and 5.5% of normal CFTR function, respectively) was supportive of a mild CF diagnosis for these patients, probably associated to the 3272-26A>G-allele. This diagnosis was also supported by clinical data: CFL63 presents abnormal sweat chloride values (89.2 mmol/L), PS and mild pulmonary disease; CFL64's profile is similar, with a sweat chloride concentration of 88.3 mmol/L, PS and no pulmonary symptoms. The age of diagnosis for CFL64 (9 months old vs. CFL63 at 4 years old) and prompt follow up might explain the normal respiratory phenotype of this patient. Furthermore, although a higher residual CFTR function was detected in rectal biopsies for patient CFL63, CFL64's better pulmonary outcome may also be related to higher levels of normal CFTR expression in his airway

epithelia. Next, organoids and nasal cells from these patients should be analysed for individual treatment response, especially since Kalydeco® has been approved for the treatment of patients carrying the 3272-26A>G variant[38].

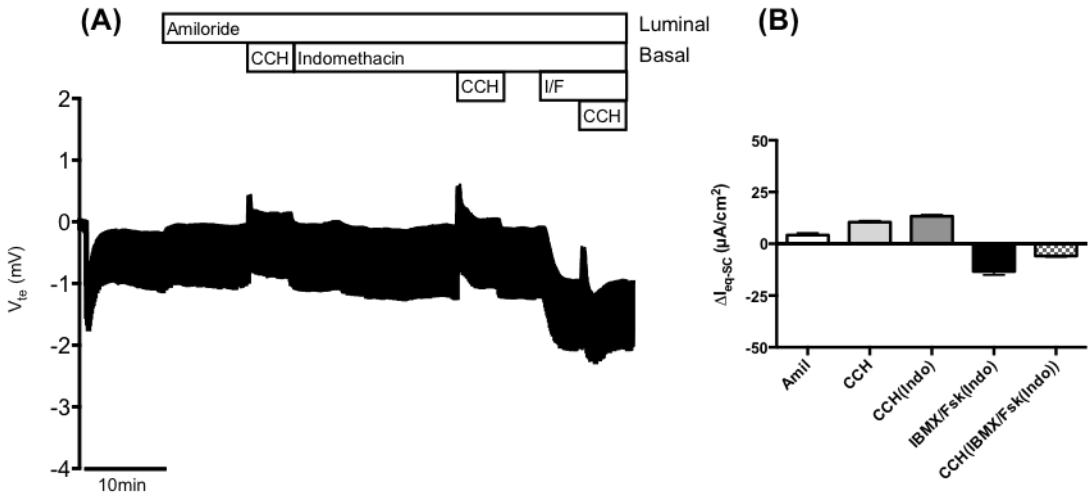

Figure 4.18 – Results from Ussing chamber measurements in rectal biopsies from patient CFL63 (3272-26A>G/W57G genotype). (A) Representative original recording of the effects of cholinergic (CCH, 100 µM, basolateral) and cAMP-dependent (IBMX/Fsk (I/F), 100 µM/2 µM, basolateral) activation on transepithelial voltage (V_{te}) in 3272-26A>G/W57G rectal biopsies from patient CFL63. Experiments were performed in the presence of Amiloride (Amil, 20 µM, luminal) and/or Amiloride + Indomethacin (Indo, 10 µM, basolateral), as indicated in the figure. **(B)** Summary of activated equivalent short-circuit currents ($\Delta I_{eq\text{-}sc}$) for Amil ($\Delta I_{eq\text{-}sc,Amil}$), basal CCH ($\Delta I_{eq\text{-}sc,CCH}$), CCH + Indo ($\Delta I_{eq\text{-}sc,CCH(Indo)}$), IBMX/Fsk + Indo ($\Delta I_{eq\text{-}sc,IBMX/Fsk(Indo)}$) and CCH following IBMX/Fsk application ($\Delta I_{eq\text{-}sc,CCH(IBMX/Fsk(Indo))}$); data represent the mean of measurements on four rectal biopsies ± SEM. $\Delta I_{eq\text{-}sc,IBMX/Fsk(Indo)}$ = -13.410 ± 1.631 µA/cm^2; $\Delta I_{eq\text{-}sc,CCH(IBMX/Fsk(Indo))}$ = -5.851 ± 0.425 µA/cm^2 (8.9% of WT CFTR function).

4.3. Severe *CFTR* genotypes

4.3.1. 1717-1G>A/G85E

Patient CFL41 analysed in this project carried a 1717-1G>A/G85E genotype. 1717-1G>A is reported as a class VII mutation and G85E as a class II processing mutation.

Diagnosis

Analysis of the Ussing chamber recordings of V_{te} measurements in rectal biopsies from patient CFL41 (Figure 4.19 A) shows a positive V_{te} deflection (K^+ secretory response) after cholinergic stimulation by CCH, and cAMP-mediated stimulation of the tissue by IBMX/Fsk shows a barely detectable and dubious negative V_{te} deflection (Cl^- secretory response) followed by a monophasic lumen-positive deflection upon cholinergic co-activation.

This latter monophasic profile of response supports that these samples should come from a CF patient carrying a severe *CFTR* genotype and likely presenting classical CF symptoms, since a K^+ secretory response in these conditions of maximal CFTR activation is characteristic of a lack of CFTR activity. In fact, the percentage of normal CFTR function for this patient's rectal tissues was calculated at 0%, supporting the diagnosis of severe CF (Figure 4.19 B).

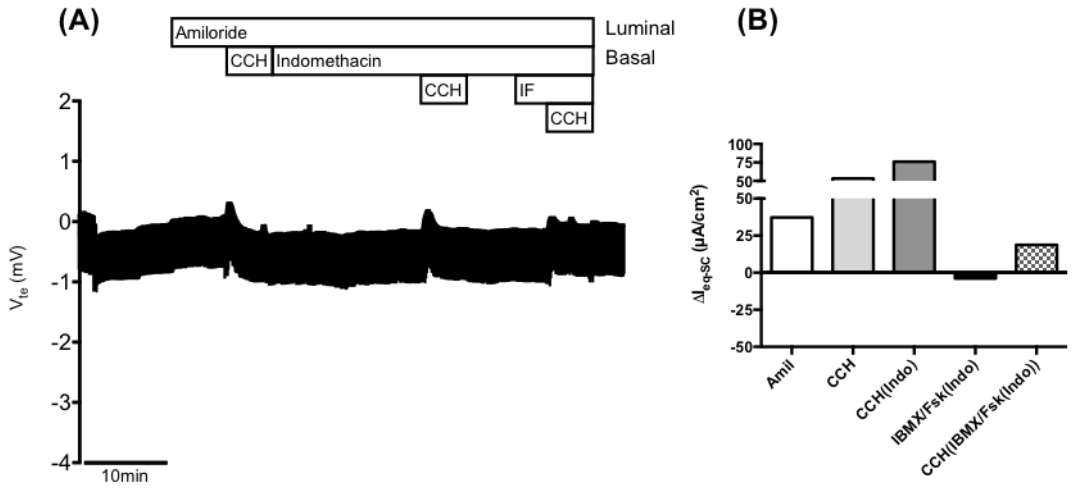

Figure 4.19 – Results from Ussing chamber measurements in a rectal biopsy from patient CFL41 (1717-1G>A/G85E genotype). (A) Representative original recording of the effects of cholinergic (CCH, 100 µM, basolateral) and cAMP-dependent (IBMX/Fsk (I/F), 100 µM/2 µM, basolateral) activation on transepithelial voltage (V_{te}) in 1717-1G>A/G85E rectal biopsies from patient CFL41. Experiments were performed in the presence of Amiloride (Amil, 20 µM, luminal) and/or Amiloride + Indomethacin (Indo, 10 µM, basolateral), as indicated in the figure. **(B)** Summary of activated equivalent short-circuit currents ($\Delta I_{eq\text{-}sc}$) for Amil ($\Delta I_{eq\text{-}sc,Amil}$), basal CCH ($\Delta I_{eq\text{-}sc,CCH}$), CCH + Indo ($\Delta I_{eq\text{-}sc,CCH(Indo)}$), IBMX/Fsk + Indo ($\Delta I_{eq\text{-}sc,IBMX/Fsk(Indo)}$) and CCH following IBMX/Fsk application ($\Delta I_{eq\text{-}sc,CCH(IBMX/Fsk(Indo))}$); data represent the measurements on one rectal biopsy. $\Delta I_{eq\text{-}sc,IBMX/Fsk(Indo)}$ = -3.899 µA/cm^2; $\Delta I_{eq\text{-}sc,CCH(IBMX/Fsk(Indo))}$ = 18.767 µA/cm^2 (0% of WT CFTR function). [Experiments were performed by Iris Silva and included with permission].

CFTR function was also assessed through FIS analyses of patient CFL41's intestinal organoids, suggesting no residual function for this patient in control conditions, at [Fsk] = 0.128 µM (Figure 4.20 A-B).

Overall, analyses of patient CFL41's samples concluded in a severe CF diagnosis. In relation to clinical data, CFL41 presents pathologic sweat chloride values (90.0 mmol/L), PI and moderate pulmonary disease, which are also in agreement with a potentially severe CF diagnosis.

One of the mutations that patient CFL41 (29 years old) carries, the 1717-1G>A mutation (frequency of 0.00856[40]), has been shown to disrupt the 3' splice acceptor site of intron 10 leading to exon 11 skipping, and to result in the complete absence of correctly spliced transcripts from this *CFTR* allele in nasal epithelial cells[83], being classified as a class VII mutation[1]. Homozygous patients for this mutation have been reported to show early PI, pathologic sweat chloride values and generally early onset of respiratory symptoms, although without severe lung involvement progression[92].

The other *CFTR* mutation carried by CFL41, G85E (frequency of 0.00434[40]), is a missense mutation localized in TMD1 that has been shown to lead to a defect in CFTR maturation, being classified as class II[87,93]. Despite the variability observed in the clinical presentation of patients with G85E-CFTR, this mutation generally leads to a severe phenotype with PI, abnormal sweat chloride levels and high prevalence of respiratory complications[93].

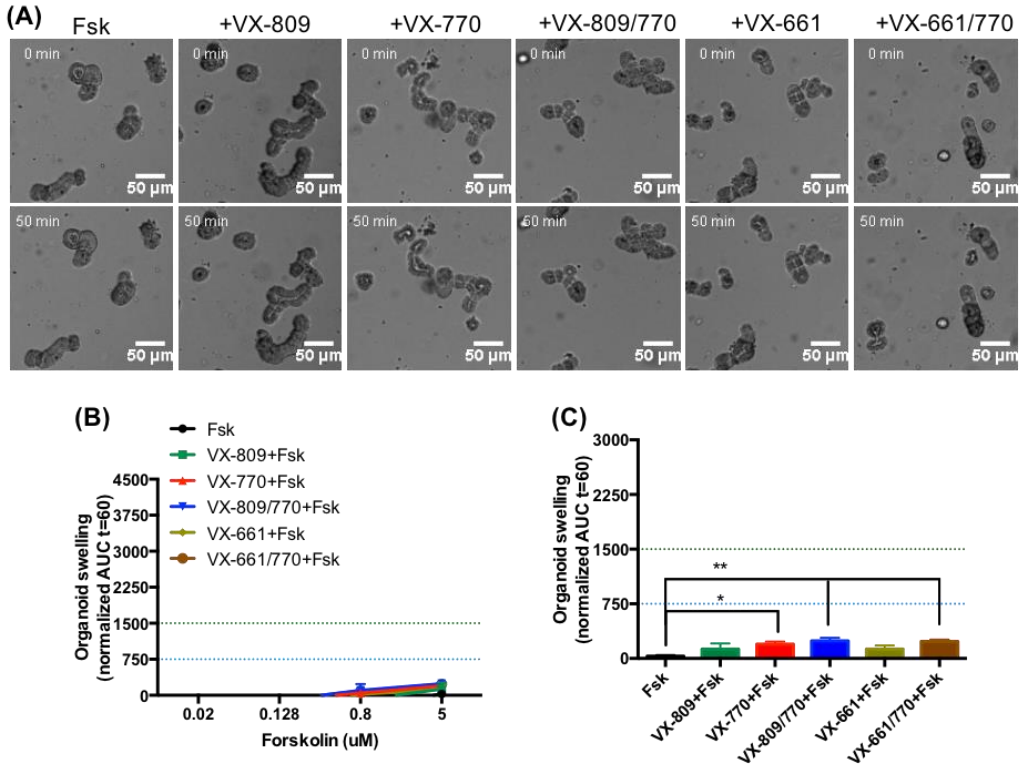

Figure 4.20 – Results from the forskolin-induced swelling (FIS) assay on intestinal organoids from patient CFL41 (1717-1G>A/G85E genotype). (A) Representative original wide-field microscopy images of intestinal organoids from patient CFL41 (1717-1G>A/G85E) at times 0 and 60 min of incubation with the following treatments: Forskolin (Fsk) alone at the concentration of 0.128 µM, VX-809 (3 µM) + Fsk, VX-770 (3 µM) + Fsk, VX-809/770 + Fsk, VX-661 (5 µM) + Fsk and VX-661/770 + Fsk. **(B)** Quantification of FIS in organoids for all treatments at the Fsk concentrations of 0.02, 0.128, 0.8 and 5 µM, expressed as the AUC of organoid surface area increase (baseline = 100%, t = 60 min). **(C)** Quantification of organoid swelling for all treatments at [Fsk] = 5 µM. The dashed blue and green lines represent the established thresholds for medium and high clinical benefit potential for treatments, respectively. **(B)** and **(C)** data represent the mean of measurements on 4-8 replicate wells per condition ± SEM. Asterisks (*) indicate degree of significant difference calculated by unpaired one-way ANOVA to control (Fsk) using Fisher's LSD test. [Experiments were performed in collaboration with Iris Silva and included with permission].

Drug response

At [Fsk] = 0.128 µM, there appears to be no swelling of the organoids from patient CFL41 for any of the tested conditions (Figure 4.20 A-B) and therefore, we predict that this patient will not get any clinical benefit from treatment with any of the approved CFTR therapeutics.

The FIS assay results suggest very low to no normal CFTR expression in this patient's organoids, and unresponsiveness of mutations 1717-1G>A and G85E to the corrector and potentiator modulators tested. For [Fsk] = 5 µM, however, in the presence of the potentiator VX-770 and combinations VX-809/770 and VX-661/770, there appears to be some swelling of these organoids, significantly different from control conditions, with low clinical benefit potential (Figure 4.20 C). This appears to suggest that these treatments might have an effect in CFTR rescue for this patient, however this is highly unlikely in physiologic conditions. A comparison by unpaired one-way ANOVA to VX-770 using Fisher's LSD test showed that there are no statistical differences between the potentiator-only treatment and combos VX-809/770 (p = 0.4207) and VX-661/770 (p = 0.5046). This supports that there might actually be very low levels of CFTR at the membrane of this patient's cells that are heavily potentiated at more saturating and possibly non-physiological concentrations of the activator cAMP. This CFTR could eventually come from a small level of normal transcripts being transcribed from the 1717-1G>A-allele in the

organoids, or from G85E-CFTR that escaped ER-degradation and that may present gating defects when at the membrane, as shown for F508del. However, these results should be further analysed, and an immunostaining of CFTR in these organoids and/or Western-blot assays would allow for the detection of fully-maturated membrane CFTR, if it exists. Also, mRNA studies should be performed to understand if, contrarily to what has been reported in nasal cells[83], the 1717-1G>A-allele can lead to the expression of any normal CFTR transcripts in these intestinal organoids.

4.3.2. F508del/F508del

Two patients analysed in this study were F508del-CFTR homozygous, namely CFL66 and CFL65 (siblings). F508del/F508del is the most common CF genotype[2].

Diagnosis

The profile of the representative Ussing chamber tracing from the analysis of rectal biopsies from patient CFL66 suggests, once more, that these samples are from a CF patient carrying a severe *CFTR* genotype and that may present classical disease symptoms, since there is a clear positive K^+ secretory response to cAMP and cholinergic co-activation of the tissues, while these also show no basal CFTR function (Figure 4.21 A). The percentage of normal CFTR function for this patient is of 0%, backing this diagnosis (Figure 4.21 B). A similar profile is observed for patient CFL65 (Figure 7.11 A-B in Appendix III). This patient also has 0% of WT CFTR function, supporting likewise a classic CF diagnosis.

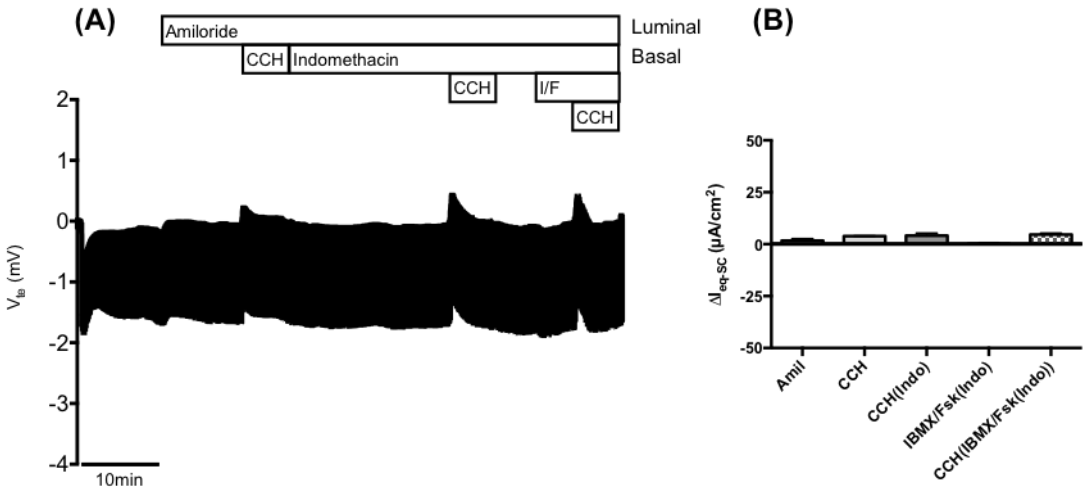

Figure 4.21 – Results from Ussing chamber measurements in rectal biopsies from patient CFL66 (F508del/F508del genotype). (A) Representative original recording of the effects of cholinergic (CCH, 100 µM, basolateral) and cAMP-dependent (IBMX/Fsk (I/F), 100 µM/2 µM, basolateral) activation on transepithelial voltage (V_{te}) in F508del/F508del rectal biopsies from patient CFL66. Experiments were performed in the presence of Amiloride (Amil, 20 µM, luminal) and/or Amiloride + Indomethacin (Indo, 10 µM, basolateral), as indicated in the figure. **(B)** Summary of activated equivalent short-circuit currents (ΔI_{eq-sc}) for Amil ($\Delta I_{eq-sc,Amil}$), basal CCH ($\Delta I_{eq-sc,CCH}$), CCH + Indo ($\Delta I_{eq-sc,CCH(Indo)}$), IBMX/Fsk + Indo ($\Delta I_{eq-sc,IBMX/Fsk(Indo)}$) and CCH following IBMX/Fsk application ($\Delta I_{eq-sc,CCH(IBMX/Fsk(Indo))}$); data represent the mean of measurements on three rectal biopsies ± SEM. $\Delta I_{eq-sc,IBMX/Fsk(Indo)}$ = 0.242 ± 0.475 µA/cm^2; $\Delta I_{eq-sc,CCH(IBMX/Fsk(Indo))}$ = 4.629 ± 0.671 µA/cm^2 (0% of WT CFTR function).

CFTR function was also assessed in the intestinal organoids from patient CFL66 and FIS results showed no residual function in control conditions and for [Fsk] = 0.128 µM (Figure 4.22 A-B).

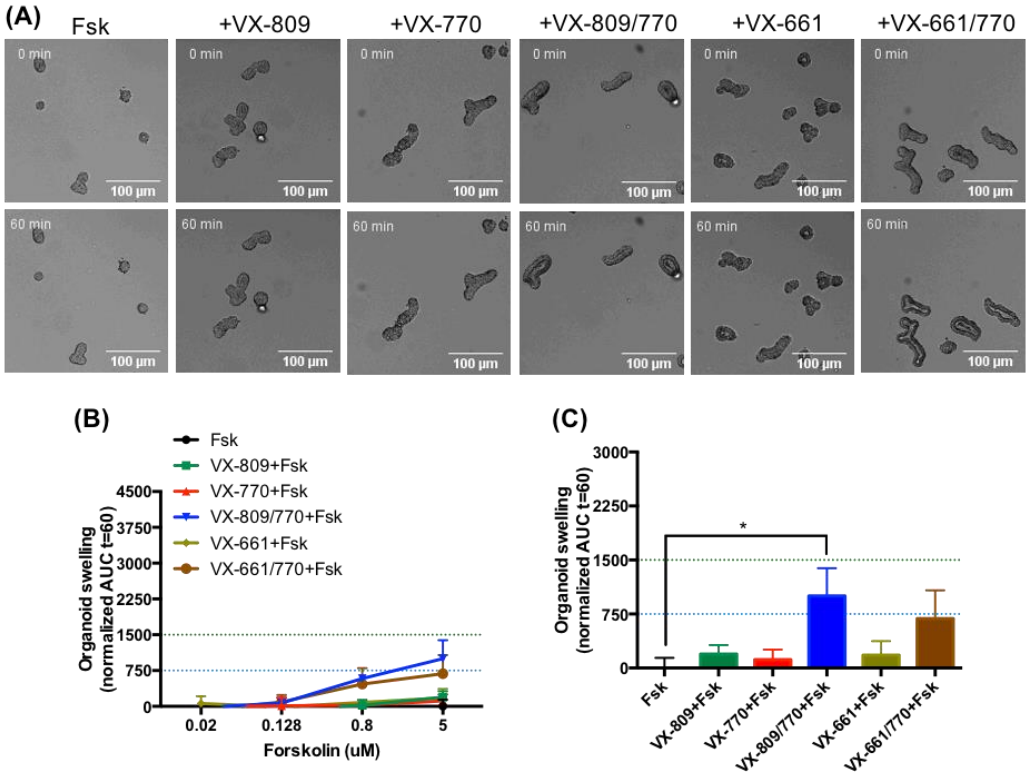

Figure 4.22 – Results from the forskolin-induced swelling (FIS) assay on intestinal organoids from patient CFL66 (F508del/F508del genotype). (A) Representative original wide-field microscopy images of intestinal organoids from patient CFL66 (F508del/F508del) at times 0 and 60 min of incubation with the following treatments: Forskolin (Fsk) alone at the concentration of 0.128 µM, VX-809 (3 µM) + Fsk, VX-770 (3 µM) + Fsk, VX-809/770 + Fsk, VX-661 (5 µM) + Fsk and VX-661/770 + Fsk. **(B)** Quantification of FIS in organoids for all treatments at the Fsk concentrations of 0.02, 0.128, 0.8 and 5 µM, expressed as the AUC of organoid surface area increase (baseline = 100%, t = 60 min). **(C)** Quantification of organoid swelling for all treatments at [Fsk] = 5 µM. The dashed blue and green lines represent the established thresholds for medium and high clinical benefit potential for treatments, respectively. **(B)** and **(C**) data represent the mean of measurements on 4-8 replicate wells per condition ± SEM. Asterisks (*) indicate degree of significant difference calculated by unpaired one-way ANOVA to control (Fsk) using Fisher's LSD test.

In general, analyses of rectal biopsies from patient CFL65 (13 years old) and all samples from patient CFL66 (16 years old) support their diagnosis as classical CF patients. Regarding clinical data, both patients are PI and have elevated levels of sweat chloride (>110 mmol/L), but present relatively mild respiratory symptoms. These clinical data are also in agreement with a CF diagnosis, potentially severe.

As previously mentioned, F508del, the most common mutation in CF patients, has been extensively characterized as a class II processing mutant with class III/VI defects when correctly transported to the membrane, that is tipically associated to classical (severe) CF phenotypes characterized by elevated levels of sweat chloride and severe pulmonary and pancreatic disease[70].

Drug response

Results from the FIS analysis of patient CFL66's intestinal organoids at [Fsk] = 0.128 µM, showed no swelling of organoids significantly different from control for any of the tested treatments, even for VX-809/770 (Orkambi®) or VX-661/770 (Symdeco®), which have been designed and approved for this genotype particularly (Figure 4.22 A-B). Thus, we predict that this patient will not have a significant clinical benefit from administration of any of these treatments.

Nevertheless, again at [Fsk] = 5 µM, in the presence of the combo treatment VX-809/770 there is swelling of these organoids, significantly different from control, with medium clinical benefit potential (Figure 4.22 C). This again implies that treatment with VX-809/770 might lead to CFTR rescue in this patient's cells, however, for the same reasons mentioned before for patient CFL41 (1717-1G>A/G85E), this is highly unlikely. The unresponsiveness of patient CFL66 to combo treatments designed primarily for F508del-homozygous patients may propose the presence of non-coding variants, modifier genes or tissue-specific factors that control the modulators efficacy and modify this patient's response to therapy. Intestinal organoids from patient CFL65 should also be analysed for a personalized response to the approved treatments for the F508del/F508del genotype, and these results would be particularly interesting since these patients are closely-related (siblings).

4.3.3. F508del/G542X

Three patients analysed in this project had a F508del/G542X genotype, namely CFL52, CFL53 and CFL61. G542X is reported as being a class I protein production mutation.

Diagnosis

The profile of the representative Ussing chamber tracing from analysis of patient CFL52's rectal biopsies (Figure 4.23 A) suggests, as before, that these samples should be from a severe CF patient, with a CFTR function in relation to healthy controls calculated at 0% (Figure 4.23 B). The same profile and conclusions can be drawn for patients CFL53 and CFL61, for whom CFTR function was also determined at 0% of WT (Figure 7.12 A-B and Figure 7.13 A-B in Appendix III, respectively).

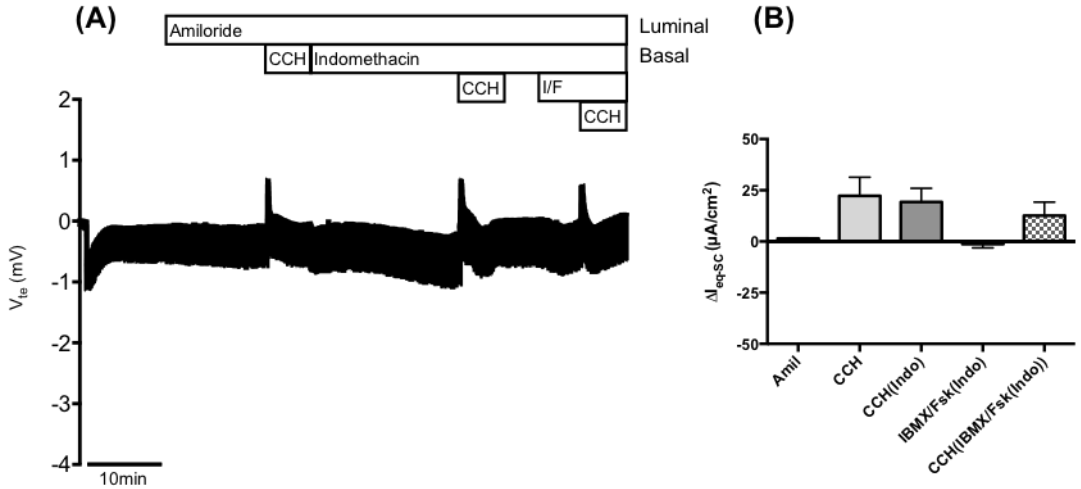

Figure 4.23 – Results from Ussing chamber measurements in rectal biopsies from patient CFL52 (F508del/G542X genotype). (A) Representative original recording of the effects of cholinergic (CCH, 100 µM, basolateral) and cAMP-dependent (IBMX/Fsk (I/F), 100 µM/2 µM, basolateral) activation on transepithelial voltage (V_{te}) in F508del/G542X rectal biopsies from patient CFL52. Experiments were performed in the presence of Amiloride (Amil, 20 µM, luminal) and/or Amiloride + Indomethacin (Indo, 10 µM, basolateral), as indicated in the figure. **(B)** Summary of activated equivalent short-circuit currents (ΔI_{eq-sc}) for Amil ($\Delta I_{eq-sc,Amil}$), basal CCH ($\Delta I_{eq-sc,CCH}$), CCH + Indo ($\Delta I_{eq-sc,CCH(Indo)}$), IBMX/Fsk + Indo ($\Delta I_{eq-sc,IBMX/Fsk(Indo)}$) and CCH following IBMX/Fsk application ($\Delta I_{eq-sc,CCH(IBMX/Fsk(Indo))}$); data represent the mean of measurements on three rectal biopsies ± SEM. $\Delta I_{eq-sc,IBMX/Fsk(Indo)}$ = -1.298 ± 1.828 µA/cm^2; $\Delta I_{eq-sc,CCH(IBMX/Fsk(Indo))}$ = 12.640 ± 6.607 µA/cm^2 (0% of WT CFTR function).

CFTR function was also analysed for patients CFL52 and CFL53's intestinal organoids and FIS results showed no residual function for patient CFL52 in control conditions and at [Fsk] = 0.128 µM (Figure 4.24 A-B), and some unexpected residual CFTR function for patient CFL53 (Figure 7.14 A in Appendix III).

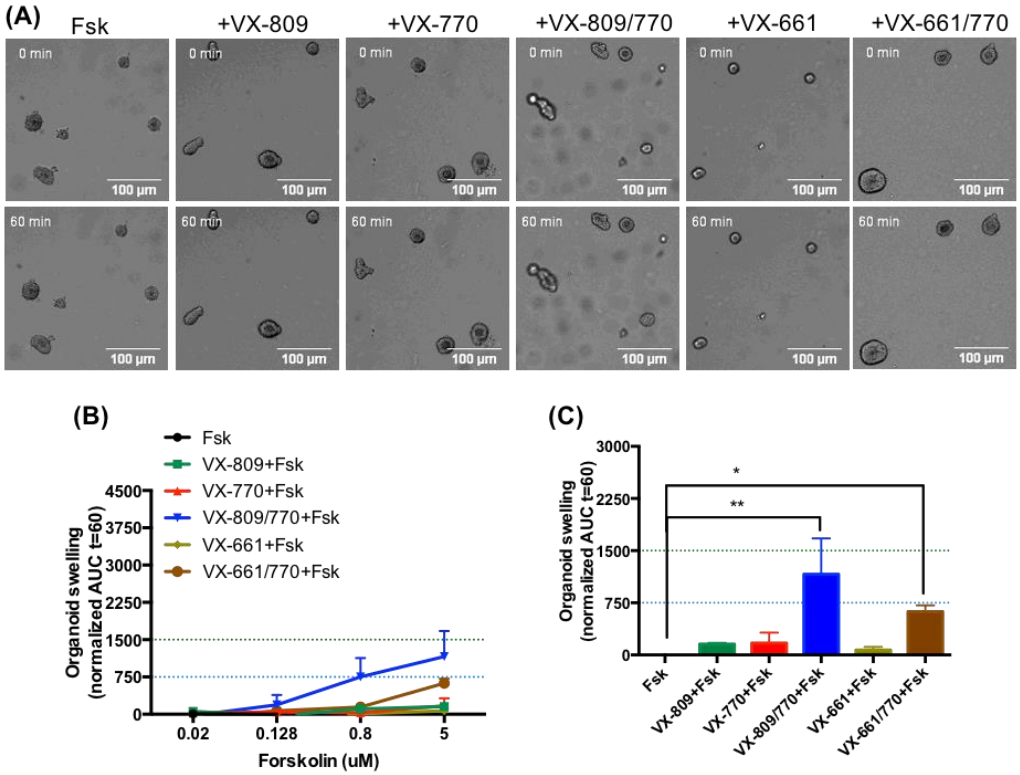

Figure 4.24 – Results from the forskolin-induced swelling (FIS) assay on intestinal organoids from patient CFL52 (F508del/G542X genotype). (A) Representative original wide-field microscopy images of intestinal organoids from patient CFL52 (F508del/G542X) at times 0 and 60 min of incubation with the following treatments: Forskolin (Fsk) alone at the concentration of 0.128 µM, VX-809 (3 µM) + Fsk, VX-770 (3 µM) + Fsk, VX-809/770 + Fsk, VX-661 (5 µM) + Fsk and VX-661/770 + Fsk. **(B)** Quantification of FIS in organoids for all treatments at the Fsk concentrations of 0.02, 0.128, 0.8 and 5 µM, expressed as the AUC of organoid surface area increase (baseline = 100%, t = 60 min). **(C)** Quantification of organoid swelling for all treatments at [Fsk] = 5 µM. The dashed blue and green lines represent the established thresholds for medium and high clinical benefit potential for treatments, respectively. **(B)** and **(C)** data represent the mean of measurements on 4-8 replicate wells per condition ± SEM. Asterisks (*) indicate degree of significant difference calculated by unpaired one-way ANOVA to control (Fsk) using Fisher's LSD test.

Overall, analyses of samples from patients CFL52, CFL53 and CFL61 support a diagnosis of severe CF for all. However, FIS analysis of CFL53's intestinal organoids suggests an unanticipated residual CFTR function in these cells that is not in agreement to that detected in the native rectal biopsies. These results should be further analysed and a determination of the levels of mature membrane CFTR being expressed, in addition to an mRNA analysis, should be performed for these patients' samples to understand if this observation is more than just a FIS experiment artefact and if it may be a result of the CFTR expression/biosynthesis/regulation being differently controlled in native tissues and cultured systems. Regarding clinical data, CFL52 and CFL53 both present with abnormal sweat chloride levels (84.7 and 78.9 mmol/L, respectively), PI and severe pulmonary disease. CFL61 presents differently only mild respiratory symptoms (sweat chloride of 82.7 mmol/L). These data are also supportive of a severe CF diagnosis for all three patients.

The G542X mutation (frequency of 0.02542[40]) is a class I nonsense mutation localized in NBD1 that has been demonstrated to severely reduce the levels of CFTR mRNA in nasal epithelial cells[94], and

that should result in markedly decreased or undetectable CFTR protein from this allele, contributing to a severe CF phenotype. Severe pancreatic and pulmonary disease and abnormal sweat chloride levels have been reported for a homozygous patient for the G542X-*CFTR* allele[95].

Drug response

FIS analysis of CFTR function rescue in intestinal organoids from patient CFL52 shows, at [Fsk] = 0.128 µM, no swelling of organoids significantly different from control for any of the tested treatments (Figure 4.24 A-B). This leads us to we predict that this patient will not have a significant clinical benefit from treatment with any of these therapeutics. Yet, for [Fsk] = 5 µM, the VX-809/770 and VX-661/770 combo treatments show swelling significantly different from control, with medium and low clinical benefit potential, respectively (Figure 4.24 C). This is thought to be potentially associated with a slight rescue of F508del-CFTR, evidenced at saturating concentrations of cAMP. Similar results were observed for patient CFL53's FIS analysis in the presence of CFTR-modulating drugs (Figure 7.14 A-B in Appendix III). However, analysis of this patient's organoids show no significant rescue for any of the tested conditions, not even at higher Fsk concentrations, despite a tendency being observed for treatment VX-809/770 (p = 0.0618). Ultimately, we also do not predict that this patient would benefit from the administration of any of the currently approved modulator treatments for CF. Nevertheless, this remains to be tested for patient CFL61.

4.3.4. 711+1G>T/F508del

Other patients with likely severe *CFTR* genotypes were also analysed in the scope of this project.

Patient CFL68 carries a 711+1G>T/F508del genotype. 711+1G>T (frequency of 0.00193[40]) is a CF-causing mutation that was shown to change the splice donor site at the 3' end of exon 5, apparently causing its skipping in the mutant transcript and abolishing production of any normal transcripts[96]. This mutation has been associated to a classic (severe) CF phenotype, with PI[96].

Drug response

Although proper Ussing chamber recordings from analyses of rectal biopsies from patient CFL68 were not obtained, organoid cultures were still produced from these biopsies. FIS results from analyses of patient CFL68's organoids propose no residual function in all control conditions. Significant CFTR rescue was detected with treatment VX-809/770 at [Fsk] = 0.128 µM but with very low potential for clinical benefit (Figure 4.25 A), so it is highly unlikely that this patient would benefit from this therapy. At [Fsk] = 5 µM, rescue is observed for the combination treatments VX-809/770 and VX-661/770 (Figure 4.25 B). This rescue should probably be associated to the patient's F508del-CFTR, however, the quantification of normal transcripts being produced from the 711+1G>T-*CFTR* allele in this patient's organoids (if any) would be informative to conclusively determine its contribution to treatment response.

In regards to clinical data, patient CFL68 (13 years old) is PI and presents moderate pulmonary disease; we have no information for sweat chloride levels. Altogether, the organoid analysis results and clinical data support a diagnosis of CF, very likely severe, however, a better assessment of this would be helped by a new Ussing chamber analysis of this patient's rectal biopsies.

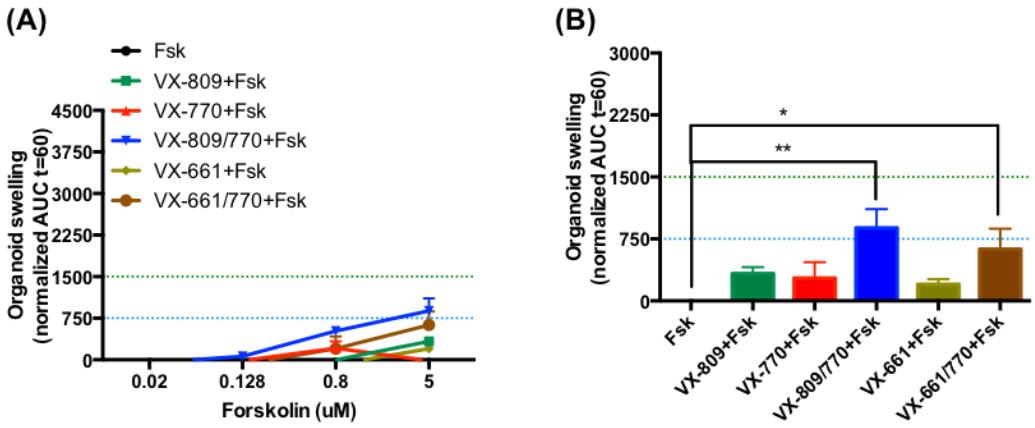

Figure 4.25 – Results from the forskolin-induced swelling (FIS) assay on intestinal organoids from patient CFL68 (711+1G>T/F508del genotype). (A) Quantification of FIS in organoids for all treatments tested (Forskolin (Fsk) alone, VX-809 (3 µM) + Fsk, VX-770 (3 µM) + Fsk, VX-809/770 + Fsk, VX-661 (5 µM) + Fsk and VX-661/770 + Fsk) at the Fsk concentrations of 0.02, 0.128, 0.8 and 5 µM, expressed as the AUC of organoid surface area increase (baseline = 100%, t = 60 min). **(B)** Quantification of organoid swelling for all treatments at [Fsk] = 5 µM; The dashed blue and green lines represent the established thresholds for medium and high clinical benefit potential for treatments, respectively. Data represent the mean of measurements on 5-8 replicate wells per condition ± SEM. Asterisks (*) indicate degree of significant difference calculated by unpaired one-way ANOVA to control (Fsk) using Fisher's LSD test.

4.3.5. 711+5G>A/F508del

Finally, patient CFL60, carrying a 711+5G>A/F508del genotype, was also analysed. 711+5G>A (frequency of 0.00042[40]) is a closely related mutation to 711+1G>T, that affects the same splicing consensus and also results in exon 5 skipping. However, 711+5G>A-*CFTR* is thought to produce about 7.4% of wt transcripts, through studies in HEK293T cells (unpublished results from our lab).

Diagnosis

A diagnosis of severe CF was proposed from the analysis of patient CFL60's rectal biopsies (Figure 4.26 A-B; 0% normal CFTR function). This patient (15 years old) presents mild pulmonary symptoms but gastrointestinal tract and liver disease, abnormal sweat chloride values (84.3 mmol/L) and PI, which are also in agreement with a classic CF diagnosis. Previously, it has been reported that 5% of normal CFTR transcripts is enough to ameliorate the severity of CF disease, in nasal epithelial cells[97]. Thus, the quantification of normal transcripts in this patient's cells would be very informative to better understand the observed phenotype. Also, the intestinal organoids and nasal cells from this patient should be analysed next for the assessment of a personalized therapy response. Kalydeco® has been approved for the treatment of patients carrying the closely related splicing mutation 711+3A>G[38], which suggests it could eventually also be a potential treatment for patient CFL60.

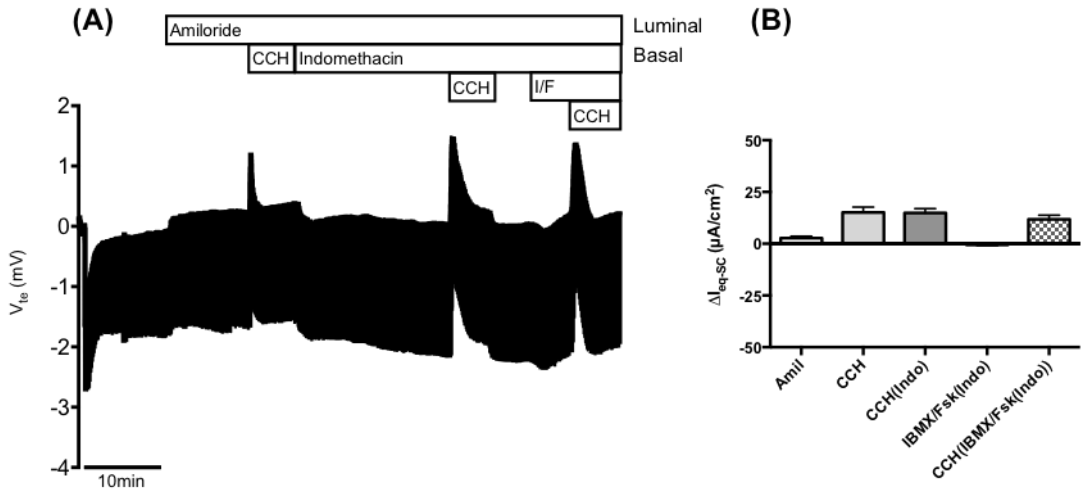

Figure 4.26 – Results from Ussing chamber measurements in rectal biopsies from patient CFL60 (711+5G>A/F508del genotype). (A) Representative original recording of the effects of cholinergic (CCH, 100 µM, basolateral) and cAMP-dependent (IBMX/Fsk (I/F), 100 µM/2 µM, basolateral) activation on transepithelial voltage (V_{te}) in 711+5G>A/F508del rectal biopsies from patient CFL60. Experiments were performed in the presence of Amiloride (Amil, 20 µM, luminal) and/or Amiloride + Indomethacin (Indo, 10 µM, basolateral), as indicated in the figure. **(B)** Summary of activated equivalent short-circuit currents (ΔI_{eq-sc}) for Amil ($\Delta I_{eq-sc,Amil}$), basal CCH ($\Delta I_{eq-sc,CCH}$), CCH + Indo ($\Delta I_{eq-sc,CCH(Indo)}$), IBMX/Fsk + Indo ($\Delta I_{eq-sc,IBMX/Fsk(Indo)}$) and CCH following IBMX/Fsk application ($\Delta I_{eq-sc,CCH(IBMX/Fsk(Indo))}$); data represent the mean of measurements on four rectal biopsies ± SEM. $\Delta I_{eq-sc,IBMX/Fsk(Indo)}$ = -0.537 ± 0.345 µA/cm²; $\Delta I_{eq-sc,CCH(IBMX/Fsk(Indo))}$ = 11.790 ± 2.005 µA/cm² (0% of WT CFTR function).

In general, values obtained for CFTR-mediated Cl^- secretion (i.e., CFTR function) from rectal biopsies analyses (average maximal CFTR activation = $\Delta I_{eq-sc,IBMX/Fsk(Indo)} + \Delta I_{eq-sc,CCH(IBMX/Fsk(Indo))}$) and normalized to a previously determined mean value for healthy controls (-217.45 µA/cm²)[50], are lower compared to previously described[50]. It has been proposed before that 30% of WT should be the threshold of CFTR function necessary to surpass to avoid any form of CF disease, and that 10% is required for a better CF prognosis[50]. However, here we obtained values <10% for 11 out of the 14 patients classified as mild/atypical CF, and all patients diagnosed with classical CF generated negative values considered as 0% of normal function. These differences suggest the need for normalization to an internal healthy control reference group, in order to obtain more accurate values and allow for comparison of analyses between laboratories.

In addition, intra- and intervariability is also present among samples from the same patient and between patients analysed in the same system by the same experimenter. This could be due to technical aspects, such as gastrointestinal tract conditions, biopsy collection and mounting and Ussing chamber system preparation, or uncontrollable factors such as the patient's diet, which influences for e.g. the expression level and function of apical K^+ channels in the gastrointestinal tract. Therefore, a within-sample correction could also be proposed. The fact that, for all subjects, healthy or diseased, a cholinergic stimulation of the tissue by CCH in the presence of Indomethacin should always lead to lumen-positive K^+ secretory responses, due to the abolishment of endogenous levels of cAMP and hence CFTR-mediated transport, makes it a good point of control for the experiment. We propose that correcting the tissue's response to CCH after CFTR activation with IBMX/Fsk (third peak + IBMX/Fsk-activated current) for the response to CCH in conditions of CFTR inactivation (with Indomethacin, second peak) would be a more faithful way to measure the residual CFTR function in native rectal biopsies and should produce less variable results between replicates. The legitimacy and accuracy of this correction should be analysed.

4.4. Summary of results from analyses of patient materials

All results from the analyses of patients' samples are summarized in Table 4.2 and Table 4.3, below, and an overview of information on *CFTR* mutations carried by the CF patients under study, based on the above discussed literature, is reported in Table 7.1 in Appendix IV.

Table 4.2 – Summary of rectal biopsy and intestinal organoid analyses results for all patients studied: *CFTR* genotypes, patient codes, final CF diagnosis, CFTR function (% of wild-type (WT)) measured in biopsies and CFTR rescue observed in organoids for all patients analysed, for [Fsk] = 0.128 µM. Asterisks (*) indicate the degree of statistical significance of detected difference to control. ns = not significant. NA = not available.

***CFTR* Genotype**	**Patient code**	**CF Diagnosis**	**CFTR Function (% of WT) (Biopsies)**	**CFTR Rescue (Organoids)**				
				VX 770	**VX809**	**VX 809/ 770**	**VX 661**	**VX 661/ 770**
D1152H/F508del	CFL26	Non-CF	35.5	***	ns	**	ns	***
D1152H/N1303K	CFL50	Non-CF	29.5	NA				
D1152H/N1303K	CFL51	Non-CF	39.7	NA				
F508del/S955P	CFL59	CF (mild)	7.5	ns	ns	*	ns	*
P205S/Y1092X	CFL05	CF (mild)	15.7	ns	ns	****	*	****
P205S/Y1092X	CFL06	CF (mild)		ns	ns	***	*	****
D614G/F508del	CFL44	CF (mild)	23.8	***	ns	****	ns	****
3849+10kbC>T/F508del	CFL57	CF (mild)	4.2	ns	ns	*	ns	**
3849+10kbC>T/F508del	CFL58	CF (mild)	1.8	**	ns	***	ns	****
3849+10kbC>T/dele2,3(21kb)	CFL49	CF (mild)	7.9	NA				
3849+10kbC>T/621+1G>T	CFL56	CF (mild)	6.6	NA				
F508del/R334W	CFL69	Inconclusive	NA	ns	ns	**	ns	***
F508del/R347P	CFL54	CF (mild)	4.6	NA				
2789+5G>A/F508del	CFL55	CF (mild)	5.5	NA				
2789+5G>A/F508del	CFL27	CF (mild)	1.5	NA				
2789+5G>A/dele2,3(21kb)	CFL62	CF (mild)	2.0	NA				
3272-26A>G/W57G	CFL63	CF (mild)	8.9	NA				
3272-26A>G/F508del	CFL64	CF (mild)	5.5	NA				
1717-1G>A/G85E	CFL41	CF (severe)	0 (-6.8)	ns	ns	ns	ns	ns
F508del/F508del	CFL66	CF (severe)	0 (-2.2)	ns	ns	ns	ns	ns
F508del/F508del	CFL65	CF (severe)	0 (-2.4)	NA				
F508del/G542X	CFL52	CF (severe)	0 (-5.1)	ns	ns	ns	ns	ns
F508del/G542X	CFL53	CF (severe)	0 (-7.1)	ns	ns	ns	ns	ns
F508del/G542X	CFL61	CF (severe)	0 (-3.0)	NA				
711+1G>T/F508del	CFL68	CF (severe)	NA	ns	ns	*	ns	ns
711+5G>A/F508del	CFL60	CF (severe)	0 (-5.2)	NA				

Table 4.3 – Summary of human nasal epithelial cells (HNECs) analyses results for all patients studied: *CFTR* genotypes, patient codes and CFTR rescue observed in HNECs for all patients analysed. Asterisks (*) indicate the degree of statistical significance of detected difference to control. ns = not significant.

***CFTR* Genotype**	**Patient code**	**CFTR Rescue (HNECs)**	
		VX-809	**VX-661**
P205S/Y1092X	CFL05	ns	**
P205S/Y1092X	CFL06	ns	ns
D614G/F508del	CFL44	ns	ns

4.5. Functional correlations between different CFTR function parameters, established CF biomarkers and clinical data

4.5.1. Correlations among different CFTR function parameters

Correlation analyses were performed between different CFTR function parameters used in this project, namely the intestinal current measurements (ICM) used as a readout for CFTR function in rectal biopsies (the cAMP-mediated activated current = $\Delta I_{eq\text{-}sc}$(I/F), the cholinergic co-activated current = $\Delta I_{eq\text{-}sc}$(CCH(I/F)) and the sum of these two currents, corresponding to the maximal CFTR activation = $\Delta I_{eq\text{-}sc}$(max)) and the patient-matched intestinal organoid swelling readouts at the different Fsk concentrations tested in the FIS assay (0.02, 0.128, 0.8 and 5 µM), in control conditions (no treatments). The intestinal organoid FIS assay is a fairly recent approach for CFTR function analysis that is currently used for the prediction of an individualized treatment response to CFTR-modulator drugs, but not as a diagnostic and prognostic aid for CF, contrarily to the ICM.

For these correlation analyses, the patients' data summarized in Table 7.2 in Appendix V was used. These analyses showed that significant correlations (p<0.05) were found only for $\Delta I_{eq\text{-}sc}$(CCH(I/F)) vs. FIS 0.8 and vs. FIS 5, the former being the most significant and strongest one (Table 4.4).

Table 4.4 – Correlation analyses between cAMP- and cholinergic-mediated activated equivalent short circuit currents in rectal biopsies and forskolin-induced organoid swelling. Correlation analyses were established between parameters 1 and 2. Parameter 1 makes reference to activated equivalent short circuit currents in rectal biopsies upon addition of IBMX/Fsk ($\Delta I_{eq\text{-}sc}$(I/F)), CCH in the presence of IBMX/Fsk ($\Delta I_{eq\text{-}sc}$(CCH(I/F))) and the sum of these two currents, corresponding to the maximal CFTR activation ($\Delta I_{eq\text{-}sc}$(max)) (µA/cm^2). Parameter 2 relates to organoid swelling at the different Fsk concentrations tested in the FIS assay (0.02, 0.128, 0.8 and 5 µM) in control conditions (no treatments). Pearson correlation coefficients (r), respective p-values and sample sizes (n) are denoted. Significant p-values (<0.05) are highlighted in bold.

Parameter 1	Parameter 2	Pearson *r*	*p*-value	n
$\Delta I_{eq\text{-}sc}$(I/F)	FIS 0.02	0.200	0.5500	11
	FIS 0.128	-0.090	0.7900	11
	FIS 0.8	-0.500	0.1100	11
	FIS 5	-0.460	0.1500	11
$\Delta I_{eq\text{-}sc}$(CCH(I/F))	FIS 0.02	0.220	0.5100	11
	FIS 0.128	-0.310	0.3600	11
	FIS 0.8	-0.740	**0.0093**	11
	FIS 5	-0.670	**0.0240**	11
$\Delta I_{eq\text{-}sc}$(max)	FIS 0.02	0.130	0.720	11
	FIS 0.128	-0.048	0.890	11
	FIS 0.8	-0.490	0.150	11
	FIS 5	-0.500	0.140	11

These results imply that only the cAMP and cholinergic co-activated current measured *ex vivo* in rectal biopsies ($\Delta I_{eq\text{-}sc}$(CCH(I/F))) correlates well with basal CFTR function analysed *in vitro* through FIS of donor-matched intestinal organoids, and best for [Fsk] = 0.8 µM. In Figure 4.27 it is possible to see a graphical representation of this correlation ($\Delta I_{eq\text{-}sc}$(CCH(I/F)) vs. FIS 0.8: r = -0.74, p = 0.0093, n = 11), that shows a negative trend: patients with higher levels of *ex vivo* CFTR-mediated Cl^- secretion (larger negative currents) and hence more CFTR function, tend to show higher *in vitro* organoid swelling.

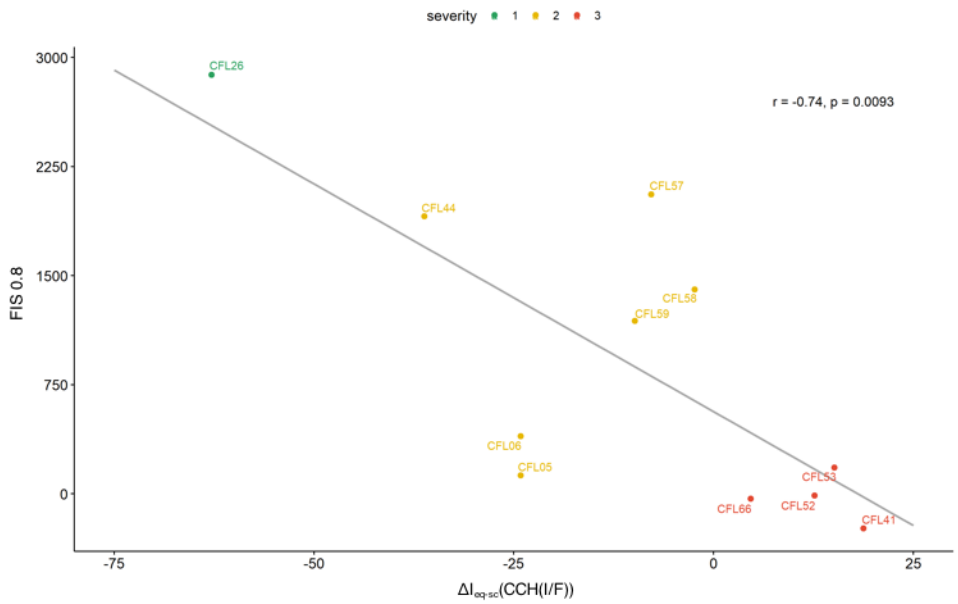

Figure 4.27 – Correlation analysis between CCH-induced equivalent short circuit currents following IBMX/Fsk stimulation of rectal biopsies and organoid swelling for [Fsk]=0.8 µM. Plot of $\Delta I_{eq\text{-}sc}$(CCH(I/F)) (µA/cm^2) determined *ex vivo* in Ussing chamber analyses of rectal biopsies versus patient-matched organoid swelling measurements in the FIS assay for [Fsk] = 0.8 µM. A degree of *CFTR* genotype severity was determined from previously proposed CF diagnosis from rectal biopsies analyses as (1) potentially non-CF (green) (2) mild CF or inconclusive (yellow) and (3) severe CF (red). Pearson r=-0.74, p=0.0093, n = 11. Grey line represents the linear regression of data.

Previous results also reported that the best correlations between *ex vivo* Fsk-induced ICM and the paired CFTR function assessed in intestinal organoids were established for FIS with [Fsk] = 0.8 µM (r = 0.5109, p = 0.0055, n = 25-30)[66].

Overall, these results suggest that analysis of CFTR function through FIS of organoids from patients with CF or a suspicion of CF (particularly at [Fsk] = 0.8 µM) may be added to the current approaches as a diagnostic or prognostic biomarker for CF. In turn, this adds value to the intestinal organoid technology, since these organoids also allow for an "unlimited" and reproducible drug response testing for individual patients in their own-derived material, and for pre-clinical selection of responders.

4.5.1. Correlations between different CFTR function parameters, established CF biomarkers and clinical data

Correlation analyses were also performed between the abovementioned CFTR function parameters used in this project (ICM and FIS readouts) and other more established CF-characteristic biomarkers and clinical data that are indicative of the disease severity, namely the sweat chloride concentrations, the fecal elastase E1 (FEE) values and the values of forced expiratory volume in 1 sec in percentage predicted (FEV_1%), which are a measure of lung function.

Again, patient data summarized in Table 7.2 in Appendix V was used. These analyses showed that significant correlations were found for the sweat [Cl^-] biomarker with all *ex vivo* ICM used for a readout of CFTR function (Table 4.5). However, the most significant and strongest correlation was between sweat [Cl^-] values and patient-matched $\Delta I_{eq\text{-}sc}$(CCH(I/F)) (r = 0.61, p = 0.00200, n = 23), although they were also closely correlated with $\Delta I_{eq\text{-}sc}$(max) (r = 0.60, p = 0.00250, n = 23). FEE values also correlated with all currents assessed and again more significantly and strongly with $\Delta I_{eq\text{-}sc}$(CCH(I/F)) (r = -0.89, p = 0.00027, n = 11). On the other hand, the hallmark clinical parameter in CF, FEV_1%, did not

significantly correlate to any of the ICM in rectal biopsies. Nonetheless, it should be mentioned that in previous correlations found between FEV_1% and CFTR-mediated Cl^- secretion detected in rectal biopsies[50], the number of patients analysed was much higher (n = 95), thus allowing for age stratification, which is essential for any correlation involving FEV_1%, since in CF it significantly decreases with age.

Table 4.5 – Correlation analyses between cAMP- and cholinergic-mediated activated equivalent short circuit currents in rectal biopsies and forskolin-induced organoid swelling with CF outcome parameters. Correlation analyses were established between parameters 1 and 2 and parameters 1 and 3. Parameter 1 makes reference to CF outcome parameters: sweat [Cl^-] (mmol/L), fecal elastasee E1 values (FEE, µg/g stool) and forced expiratory volumes in 1 sec in percentage predicted (FEV_1%). Parameter 2 relates to activated equivalent short circuit currents in rectal biopsies upon addition of IBMX/Fsk (ΔI_{eq-sc}(I/F)), CCH in the presence of IBMX/Fsk (ΔI_{eq-sc}(CCH(I/F))) and the sum of these two currents, corresponding to the maximal CFTR activation (ΔI_{eq-sc}(max)) (µA/cm^2). Parameter 3 relates to organoid swelling at the different Fsk concentrations tested in the FIS assay (0.02, 0.128, 0.8 and 5 µM) in control conditions (no treatments). Pearson correlation coefficients (*r*), respective *p*-values and sample sizes (n) are denoted. Significant *p*-values (<0.05) are highlighted in bold.

Clinical data	**Equivalent short circuit currents**				**Organoid swelling**			
Parameter 1	**Parameter 2**	**Pearson *r***	***p*-value**	**n**	**Parameter 3**	**Pearson *r***	***p*-value**	**n**
Sweat [Cl^-]	ΔI_{eq-sc}(I/F)	0.49	**0.01800**	23	FIS 0.02	-0.25	0.460	11
	ΔI_{eq-sc}(CCH(I/F))	0.61	**0.00200**	23	FIS 0.128	-0.62	**0.041**	11
	ΔI_{eq-sc}(max)	0.60	**0.00250**	23	FIS 0.8	-0.72	**0.012**	11
					FIS 5	-0.69	**0.018**	11
FEE	ΔI_{eq-sc}(I/F)	-0.79	**0.00350**	11	FIS 0.02	-0.028	0.970	4
	ΔI_{eq-sc}(CCH(I/F))	-0.89	**0.00027**	11	FIS 0.128	0.85	0.150	4
	ΔI_{eq-sc}(max)	-0.74	**0.01500**	11	FIS 0.8	0.95	**0.046**	4
					FIS 5	0.94	0.063	4
FEV_1%	ΔI_{eq-sc}(I/F)	-0.26	0.26000	21	FIS 0.02	-0.066	0.860	10
	ΔI_{eq-sc}(CCH(I/F))	-0.19	0.40000	21	FIS 0.128	-0.300	0.390	10
	ΔI_{eq-sc}(max)	-0.21	0.36000	21	FIS 0.8	-0.510	0.130	10
					FIS 5	-0.460	0.180	10

In general, these results suggest that it is the cAMP and cholinergic co-activated current measured *ex vivo* in rectal biopsies (ΔI_{eq-sc}(CCH(I/F))) that correlates best with more established CF-relevant biomarkers, namely the chloride concentrations in the patient's sweat and the FEE values. In Figure 4.28 A-B there are graphical representations of these best correlations, that show that patients with the higher levels of CFTR-mediated Cl^- secretion (more CFTR function) tend to have generally lower sweat chloride levels (Figure 4.28 A) and higher FEE values (Figure 4.28 B), which are both indicative of a better prognosis.

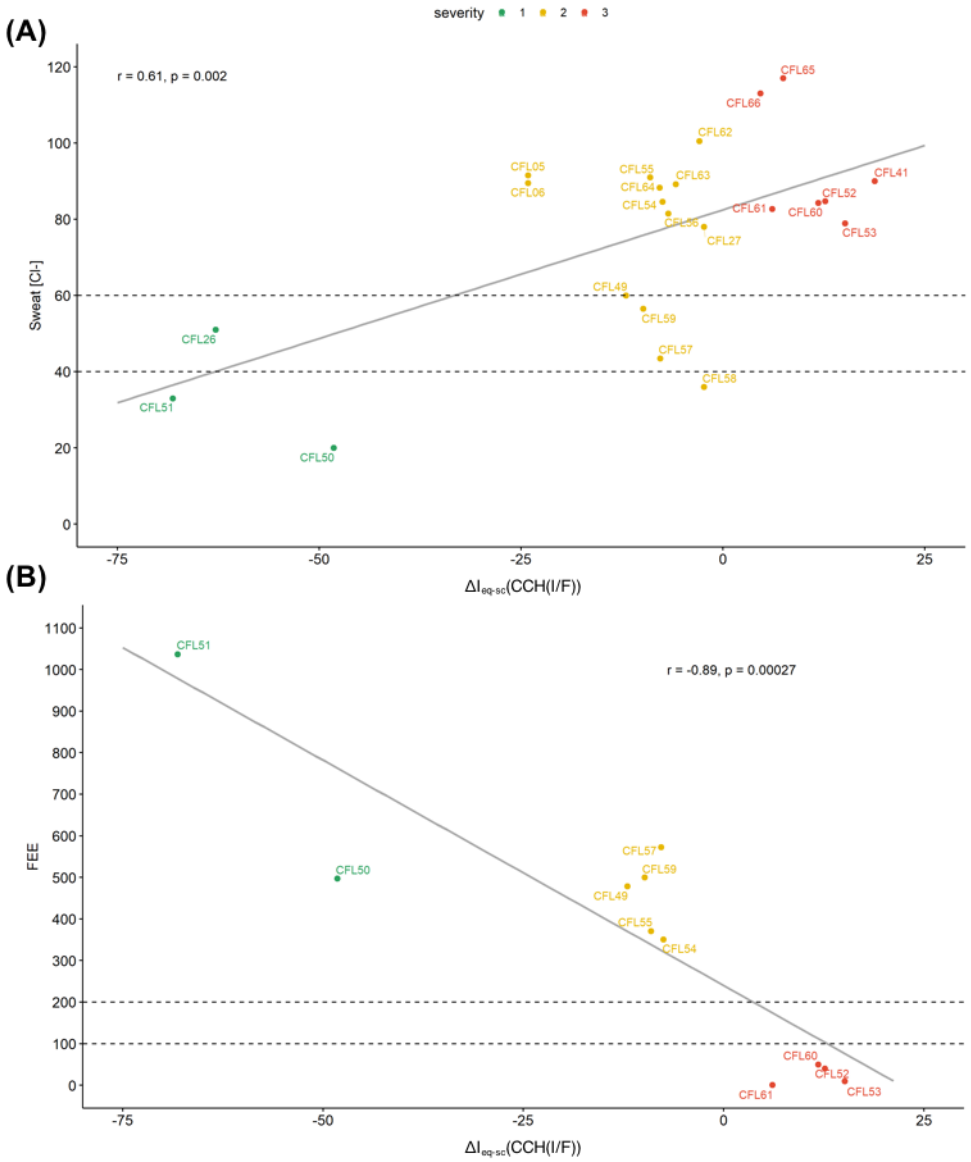

Figure 4.28 – Correlation analyses between CCH-induced equivalent short circuit currents following IBMX/Fsk stimulation of rectal biopsies and established CF biomarkers. Plot of $\Delta I_{eq\text{-}sc}$(CCH(I/F)) (µA/cm^2) determined in *ex vivo* Ussing chamber analyses of rectal biopsies versus patient-matched **(A)** sweat [Cl^-] measurements (mmol/L) (Pearson r=0.61, p=0.002, n = 23) and **(B)** fecal elastase E1 (FEE) measurements (µg/g stool) (Pearson r=-0.89, p=0.00027, n = 11). A degree of *CFTR* genotype severity was determined from previously proposed CF diagnosis from rectal biopsies analyses as (1) potentially non-CF (green) (2) mild CF or inconclusive (yellow) and (3) severe CF (red). Grey lines represent the linear regressions of the data. Dashed black lines represent the thresholds of **(A)** sweat [Cl^-] used to diagnose unlikeliness of CF (<40 mmol/L), intermediate possibility of CF (40-60 mmol/L) and high probability of CF (>60 mmol/L) and **(B)** FEE values used to diagnose normal exocrine pancreatic function (>200 µg/g stool), mild to moderate pancreatic insufficiency (100-200 µg/g stool) and exocrine pancreatic insufficiency (<100 µg/g stool).

Furthermore, the same analyses showed that the sweat [Cl^-] values significantly correlated with patient-matched organoid swelling for [Fsk] = 0.128, 0.8 and 5 µM, and this was stronger for [Fsk] = 0.8 µM (r = -0.72, p = 0.012, n = 11) (Table 4.5). On the other hand, FEE values only correlated significantly with the organoid swelling for [Fsk] = 0.8 µM (r = 0.95, p = 0.046, n = 4), although they also almost did for [Fsk] = 5 µM (r = 0.94, p = 0.063, n = 4). In agreement with the previous results, FEV_1% values did not significantly correlate to the organoid swelling for any of the Fsk concentrations used in the FIS assay, again, probably due to the fact that age sratification was not possible with the low number of patients analysed herein.

Overall, these results indicate that the *in vitro* organoid swelling in basal conditions of CFTR activation (no treatments) at the Fsk concentration of 0.8 µM evidences a stronger correlation with CF-relevant biomarkers, namely the sweat [Cl^-] and the FEE values. In Figure 4.29, the graphical representations of the strongest correlations obtained with the FIS readouts show that patients with the higher levels of organoid swelling (more CFTR function) generally present with lower levels of chloride measured in their sweat (Figure 4.29 A) and higher FEE values (Figure 4.29 B), which, once more, support a better prognosis for those patients.

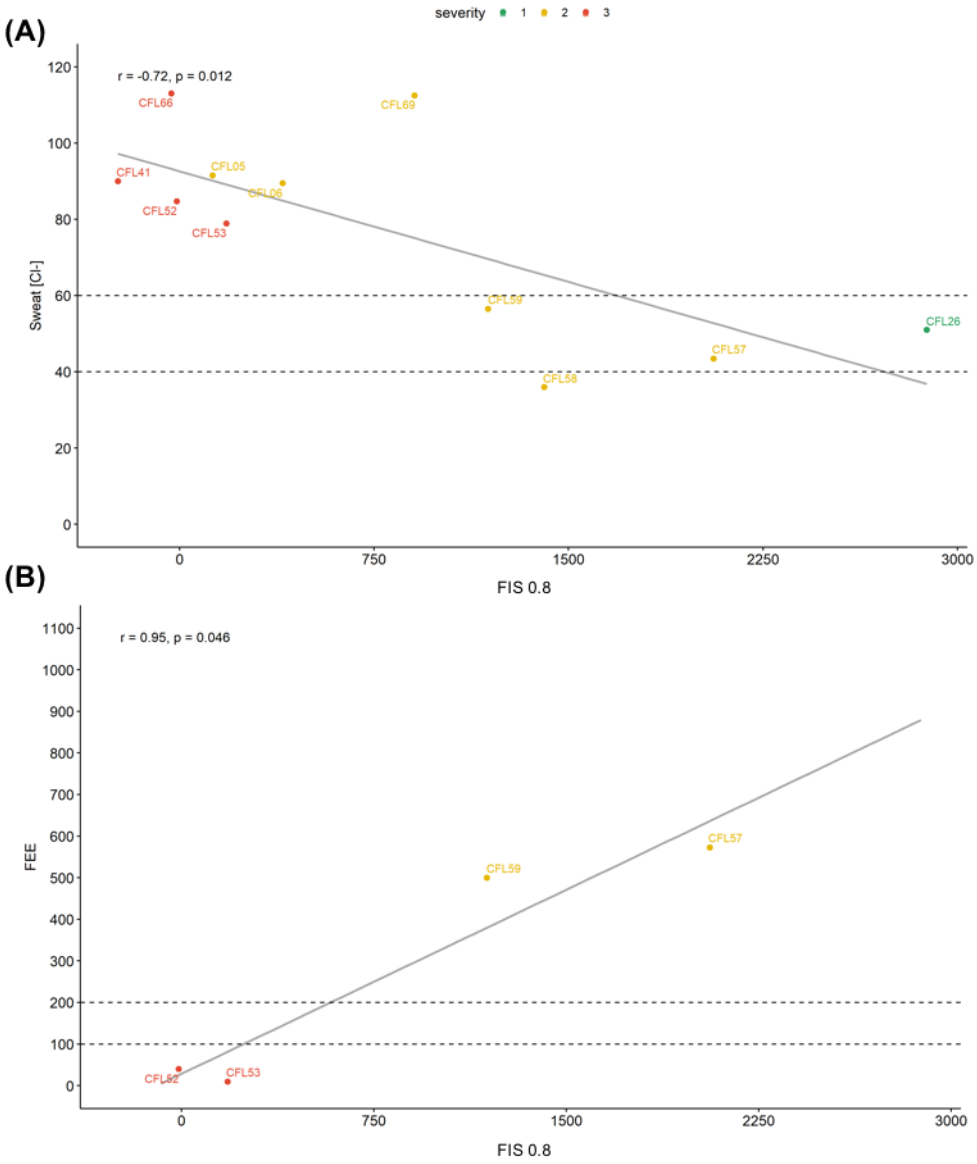

Figure 4.29 – Correlation analyses between organoid swelling for [Fsk]=0.8 µM and established CF biomarkers. Plot of organoid swelling measurements in the FIS assay for [Fsk] = 0.8 µM versus patient-matched **(A)** sweat [Cl^-] measurements (mmol/L) (Pearson r=-0.72, p=0.012, n = 11) and **(B)** fecal elastase E1 (FEE) measurements (µg/g stool) (Pearson r=0.95, p=0.046, n = 4). A degree of *CFTR* genotype severity was determined from previously proposed CF diagnosis from rectal biopsies analyses as (1) potentially non-CF (green) (2) mild CF or inconclusive (yellow) and (3) severe CF (red). Grey lines represent the linear regression of data. Dashed black lines represent the thresholds of **(A)** sweat [Cl^-] used to diagnose unlikeliness of CF (<40 mmol/L), intermediate possibility of CF (40-60 mmol/L) and high probability of CF (>60 mmol/L) and **(B)** FEE values used to diagnose normal exocrine pancreatic function (>200 µg/g stool), mild to moderate pancreatic insufficiency (100-200 µg/g stool) and exocrine pancreatic insufficiency (<100 µg/g stool).

Again, results shown here led to similar strongest correlations to those previously established as best by our own and other groups: $\Delta I_{eq\text{-}sc}$(CCH(I/F)) vs. sweat [Cl^-]: r = 0.677, p = 4.73 x 10^{-14}, n = 95[50]; $\Delta I_{eq\text{-}sc}$(CCH(I/F)) vs. FEE: r = -0.770, p = 1.10 x 10^{-16}, n = 95[50]; organoid swelling at [Fsk] = 0.8 µM vs. sweat [Cl^-]: r = -0.7011, p = <0.0001, n = 27-35[66].

Globally, these results reinforce the value of the CFTR function parameters used (*ex vivo* ICM in rectal biopsies and *in vitro* FIS of intestinal organoids) as predictive tools for CF diagnosis and prognosis, since they show good correlations with disease severity, particularly for $\Delta I_{eq\text{-}sc}$(CCH(I/F)) and FIS for [Fsk] = 0.8 µM. Also, this may propose the use of $\Delta I_{eq\text{-}sc}$(CCH(I/F)), instead of $\Delta I_{eq\text{-}sc}$(max), as a better determinant of the residual CFTR function in the *ex vivo* analysis of rectal biopsies.

Noteworthy to mention is that while CFTR function is the primary explanation for exocrine pancreatic sufficiency in CF, many other genetic, environmental and stochastic factors are involved in determining the progression of the airways disease[7,98]. This could explain why no correlation was established for lung function parameter FEV_1% and our parameters of CFTR function. Nevertheless, although weak, significant correlations between the herein assessed parameters and lung function have been established previously: $\Delta I_{eq\text{-}sc}$(CCH(I/F)) vs. FEV_1% (unstratified by age group): r = -0.240, p = 0.035, n = 95[50]; $\Delta I_{eq\text{-}sc}$(CCH(I/F)) vs. FEV_1% (stratified by age group): r = -0.301, p = 0.008, n = 95[50]. This might imply, as previously proposed, the need to study a bigger sample and/or carry out age stratification to establish significant correlations with clinical pulmonary function readouts.

4.6. Effect of CFTR correctors in the biosynthesis of other epithelial channels

We observed that for some human nasal epithelial cells, a 48 h-incubation period with CFTR correctors VX-809 or VX-661 led to an apparent enhancement of the Amiloride-sensitive Na^+ transport (e.g. in Figure 7.15 in Appendix VI). This suggested that these compounds might not specifically correct the CFTR biogenesis but instead act on CFTR rescue through unspecific folding-promoting hydrophobic interactions, and may therefore also have an effect in increasing the biosynthesis of other transmembrane proteins, such as K^+ and Na^+ channels. In this case, treatment using CFTR correctors could increase the epithelial Na^+ channel (ENaC) expression and counterproductively result in increased Na^+ hyperabsorption, one of the hallmarks of CF.

However, through analysis of the Ussing chamber recordings (Figure 7.16 A-D in Appendix VI) and respective quantification of responses to activators and inhibitors in NCI-H441 cells (Figure 4.30 A-F), which do not express CFTR, there appears to be no significant differences between baseline current values (Figure 4.30 A) or activated equivalent short-circuit currents upon cAMP-mediated activation by IBMX/Fsk (Figure 4.30 C), under specific ENaC inhibition by Amiloride (Figure 4.30 B), specific KCNQ1 inhibition by 293B (Figure 4.30 D) or KCNN4 inhibition by Clotrimazole (Figure 4.30 F), between untreated and DMSO, VX-809 or VX-661-treated cells. This implies that these compounds do not affect the activity of those channels, suggesting that they may not affect their biosynthesis.

However, the fact that a positive V_{te} deflection was never obtained upon inhibition of basolateral K^+ channels KCNQ1 and KCNN4 (Figure 7.16 in Appendix VI), suggested that these channels may actually not be present in NCI-H441 cells. By PCR, we confirmed that these cells do not express CFTR (as previously reported[65]) nor KCNQ1, and that they express high levels of ENaC and lower levels of KCNN4. Therefore, a possible explanation for the apparent unresponsiveness of KCNN4 channels is that, since they are Ca^{2+}-activated[99] and in our protocol we did not include an external stimulus for Ca^{2+} production, these channels might not have been activated, which would explain the lack of Clotrimazole effect.

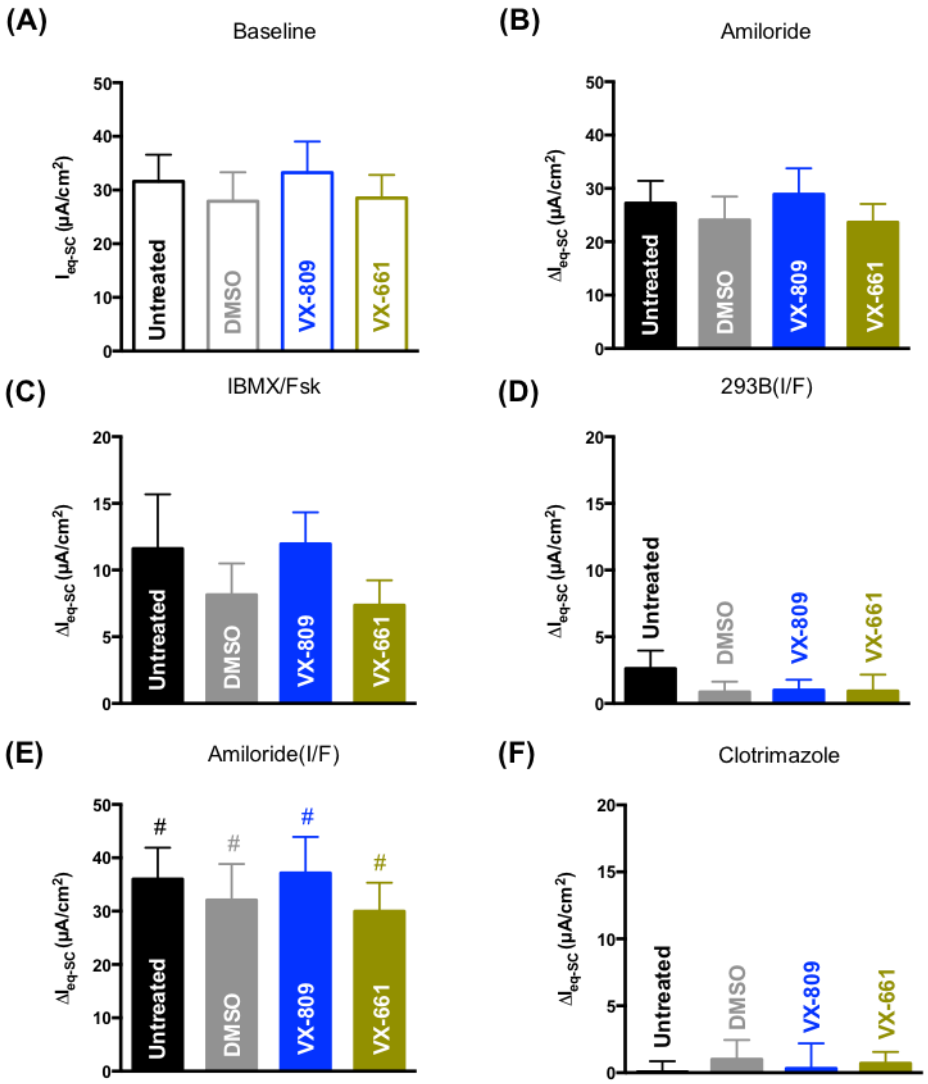

Figure 4.30 – Quantification of Ussing chamber measurements in NCI-H441 cells. Summary of **(A)** basal currents and activated equivalent short-circuit currents ($\Delta I_{eq\text{-}sc}$, $\mu A/cm^2$) after **(B)** ENaC inhibition (Amil (A), 20 µM, apical), **(C)** cAMP-dependent activation (IBMX/Fsk (I/F), 100 µM/2 µM, basolateral), **(D)** KCNQ1 channels inhibition (293B, 10 µM, basolateral) and **(E)** ENaC inhibition upon c-AMP activation, and **(F)** KCNN4 channels inhibition (Clotrimazole (C), 10 µM, basolateral) on transepithelial voltage in NCI-H441 cells either untreated or treated with 0.05% DMSO, 3 µM VX-809 or 5 µM VX-661 for 48 h. Data represent the mean of measurements on seven replicates per condition ± SEM. Asterisks (*) indicate degree of significant difference calculated by unpaired one-way ANOVA to control (Untreated) using Fisher's LSD test. Cardinals (#) indicate degree of significant difference calculated by paired *t*-test between matching treatments in **(B)** and **(E)**. Negative currents (in **(A), (C)**, **(D)** and **(F)**) were made positive to allow for easier visual comparison of generated current magnitudes.

In addition, significant differences were detected between Amiloride responses in the absence (Figure 4.30 B) or after IBMX/Fsk addition (Figure 4.30 E), indicating a cAMP-dependent stimulation of ENaC. The lack of basolateral KCNQ1 K^+ secretory channels in NCI-H441 cells, which are cAMP activated, abolishes the proposal that these could be the indirect stimulators of ENaC, through inducing electronegativity inside the polarized cells and creating the driving force for Na^+ hyperabsorption. Therefore, other cAMP-dependent channels present in these cells are probably responsible for eliciting this driving force or by directly regulating ENaC, as has been described for CFTR[4].

Overall, we cannot clearly conclude from this analysis that correctors VX-809 and VX-661 are CFTR-selective, as has been previously reported for VX-809[100], although they seem to not interfere with ENaC function. A new analysis should be performed in more CF-relevant model systems and this should be complemented with a Western blot analysis to directly assess for effects in the channels' biogenesis.

5. Conclusions and Future Perspectives

In this project, the 26 patients under study shared a total of 20 different *CFTR* mutations. Using innovative approaches in the CF field, we were able to support a diagnosis for 25/26 patients, with 3/25 being potentially non-CF, 14/25 being CF (mild) and 8/25 being CF (severe). We were also able to functionally characterize several *CFTR* genotypes in native tissues and primary cultures from these patients and to support previously reported data on individual mutations in other model systems. Furthermore, for 7 patients carrying the D1152H, S955P, P205S, Y1092X, D614G, 3849+10kbC>T and F508del mutations, we managed to predict a significant clinical benefit from treatment with current CF-approved drugs (Kalydeco®, Orkambi® or Symdeco®), allowing for the repurposing of these therapeutics for these patients, some of which carry mutations outside of the approved drug label (e.g. S955P).

Particularly for patients carrying rare variants, we expect to make a significant impact on their clinical course and general quality of life improvement once they start treatment with these drugs, since costly therapeutic efforts are not directed at developing new compounds to rescue their mutants. Also, for patients carrying mutations for which current modulators have been approved, we were able to identify those that actually do not respond to any of these treatments. This way, we also prevent patients from being exposed to clinical trials with drugs from which they would not get any benefit, or that such high-priced therapies are "wasted" in non-responders.

Finally, we were also able to establish strong correlations between the ICM and intestinal organoid FIS readouts of CFTR function, namely best for the cAMP and cholinergic co-activated current measured *ex vivo* in rectal biopsies and the *in vitro* organoid swelling for [Fsk] = 0.8 µM, and more established CF-relevant parameters, namely the sweat chloride and fecal elastase E1 values, overall further validating the first as predictive biomarkers for CF diagnosis and prognosis. However, we were not able to establish correlations with clinical pulmonary function readouts (FEV_1%).

The fact that, in CF, only a portion of the disease phenotypic variability can be explained by the functional defect caused by the different *CFTR* mutations – which is accentuated by the variability detected amongst patients carrying the same genotype –, emphasizes the role of the genetic background and environmental factors not only in disease outcome but also in the response to drugs. This highlights the value of personalized medicine approaches to help determine the best therapy for each patient independently of their *CFTR* mutations, allowing for the expansion of novel therapies to all CF patients. For this end, the intestinal organoid FIS assay appears to be a very successful approach. Not only do we intend to expand this analysis to all patients who are under study in our lab, but also to establish a biobank of these organoid cultures to allow for future testing of the efficacy of novel drugs in the patients' own-derived material, particularly for patients that appear to be nonresponsive, or show limited response, to any of the currently approved modulator therapeutics for CF.

However, patient follow-up studies, namely after they are in treatment with these drugs, are necessary to assess the *in vivo* treatment efficacy and to help establish better predictions of clinical benefit. Other biological models adopting the organoid technology concept have been proposed, such as 3D-nasoshperoids derived from nasal biopsies[101], which could potentially eliminate the problem of short-lived expansion and unreproducibility of results obtained in 2D-human nasal epithelial cell-monolayers. This model would also be more representative of the hallmark airways disease and could allow for this tissue's specific assessment of the potential effects of CFTR modulators.

Characterization of rare mutations at the molecular, cellular and functional levels also remains highly relevant for disease prognosis. Homozygosity would be the best way of analysing a specific mutation's effect, however, patients homozygous for a *CFTR* mutation other than F508del are very rare. For higher physiological relevance, this characterization should be performed in epithelial models

relevant for CF, such as the previously mentioned bronchial epithelial cell line CFBE41o-, that lacks endogenous CFTR and that can be transfected with different *CFTR* mutants. In our lab, these approaches are currently in development for mutations found in patients under study here, such as the newly identified S955P mutation.

Finally, for completely unresponsive or unrescuable mutations, mutation agnostic therapies (i.e., independent of mutation class) have been proposed and are in early stages of development. These include gene and cell-based therapies and activation of alternative Cl^- channels to bypass CFTR[1]. In addition, genome-wide techniques are also being explored to identify candidate genes that modify disease outcomes in CF. This will not only help to better understand the components that mediate CF variability, but will also suggest new targets for therapy[98].

6. References

1. De Boeck, K. & Amaral, M. D. Progress in therapies for cystic fibrosis. *Lancet Respir. Med.* **4,** 662–674 (2016).
2. Bell, S. C., De Boeck, K. & Amaral, M. D. New pharmacological approaches for cystic fibrosis: Promises, progress, pitfalls. *Pharmacol. Ther.* **145,** 19–34 (2015).
3. Proesmans, M., Vermeulen, F. & De Boeck, K. What's new in cystic fibrosis? From treating symptoms to correction of the basic defect. *Eur. J. Pediatr.* **167,** 839–849 (2008).
4. Reddy, M. M., Light, M. J. & Quinton, P. M. Activation of the epithelial Na+ channel (ENaC) requires CFTR Cl- channel function. *Nature* **402,** 301–304 (1999).
5. Xue, R. *et al.* Expression of Cystic Fibrosis Transmembrane Conductance Regulator in Ganglia of Human Gastrointestinal Tract. *Sci. Rep.* **6,** 1–8 (2016).
6. Rose, V. De, Molloy, K., Gohy, S., Pilette, C. & Greene, C. M. Airway Epithelium Dysfunction in Cystic Fibrosis and COPD. *Mediators Inflamm.* **2018,** (2018).
7. Cutting, G. R. Cystic fibrosis genetics: from molecular understanding to clinical application. *Nat Rev Genet* **16,** 45–56 (2015).
8. Collins, F. S. Cystic fibrosis: molecular biology and therapeutic implications. *Science* **256,** 774–779 (1992).
9. Borowitz, D. CFTR, bicarbonate, and the pathophysiology of cystic fibrosis. *Pediatr. Pulmonol.* **50,** S24–S30 (2015).
10. Pezzulo, A. A. *et al.* Reduced airway surface pH impairs bacterial killing in the porcine cystic fibrosis lung. *Nature* **487,** 109–113 (2012).
11. Tang, X. X. *et al.* Acidic pH increases airway surface liquid viscosity in cystic fibrosis. *J. Clin. Invest.* **126,** 879–891 (2016).
12. Elborn, J. S. Cystic fibrosis. *Lancet* **388,** 2519–2531 (2016).
13. Kunzelmann, K. & Mall, M. Electrolyte Transport in the Mammalian Colon: Mechanisms and Implications for Disease. *Physiol. Rev.* **82,** 245–289 (2002).
14. Wallis, C. Atypical cystic fibrosis–diagnostic and management dilemmas. *J. R. Soc. Med.* **96 Suppl 4,** 2–10 (2003).
15. Quinton, P. M. *et al.* Cystic Fibrosis : Lessons from the Sweat Gland. *Physiology* **22,** 212–225 (2007).
16. Andersen, D. H. Cystic Fibrosis of the pancreas and its relation to celiac disease. *Prog. Pediatr.* 344–399 (1938).
17. Elborn, J., Britton, J. & Shale, D. Cystic fibrosis: current survival and population estimates to the year 2000. *Thorax* **46,** 881–885 (1991).
18. Farrell, P. M. P. *et al.* Evidence on improved outcomes with early diagnosis of Cystic Fibrosis through neonatal screening: enough is enough! *J. Pediatr.* **147,** S30–S36 (2005).
19. Sawicki, G. S., Sellers, D. E. & Robinson, W. M. High treatment burden in adults with cystic fibrosis: Challenges to disease self-management. *J. Cyst. Fibros.* **8,** 91–96 (2009).
20. Horvais, V. *et al.* Cost of home and hospital care for patients with cystic fibrosis followed up in two reference medical centers in France. *Int. J. Technol. Assess. Health Care* **22,** 525–531 (2006).
21. Riordan, J. *et al.* Identification of the cystic fibrosis gene: cloning and characterization of complementary DNA. *Science* **245,** 1066–1073 (1989).
22. United States National Institutes of Health (NIH) Genetics Home Reference for the CFTR gene. Available at: https://ghr.nlm.nih.gov/gene/CFTR#. (Accessed: 6th July 2018)
23. Tsui, L.-C. & Dorfman, R. The Cystic Fibrosis Gene: A Molecular Genetic Perspective. *Cold Spring Harb. Perspect. Med.* **3,** (2013).
24. Cant, N., Pollock, N. & Ford, R. C. CFTR structure and cystic fibrosis. *Int. J. Biochem. Cell Biol.* **52,** 15–25 (2014).
25. Mccarthy, V. A. & Harris, A. The CFTR Gene and Regulation of Its Expression. *Pediatr. Pulmonol.* 1–8 (2005).
26. Farinha, C. M. & Canato, S. From the endoplasmic reticulum to the plasma membrane: mechanisms of CFTR folding and trafficking. *Cell. Mol. Life Sci.* **74,** 39–55 (2017).
27. Csanady, L., Vergani, P. & Gadsby, D. C. Strict coupling between CFTR's catalytic cycle and gating of its Cl- ion pore revealed by distributions of open channel burst durations. *Proc. Natl. Acad. Sci.* **107,** 1241–1246 (2010).
28. Liu, F., Zhang, Z., Csanády, L., Gadsby, D. C. & Chen, J. Molecular Structure of the Human CFTR Ion Channel. *Cell* **169,** 85–92 (2017).
29. Cystic Fibrosis Mutation Database (CFTR1) statistics. Available at: http://www.genet.sickkids.on.ca/cftr/StatisticsPage.html. (Accessed: 6th July 2018)

30. Clinical and Functional TRanslation of CFTR (CFTR2) database variant list history. Available at: https://www.cftr2.org/mutations_history. (Accessed: 14th July 2018)
31. Veit, G. *et al.* From CFTR biology toward combinatorial pharmacotherapy: expanded classification of cystic fibrosis mutations. *Mol. Biol. Cell* **27,** 424–433 (2016).
32. Welsh, M. J. & Smith, A. E. Molecular mechanisms of CFTR chloride channel dysfunction in cystic fibrosis. *Cell* **73,** 1251–1254 (1993).
33. Amaral, M. D. Novel personalized therapies for cystic fibrosis: Treating the basic defect in all patients. *J. Intern. Med.* **277,** 155–166 (2015).
34. Ooi, C. Y. Cystic Fibrosis in the Genomic Era: CFTR Genotyping as a Diagnostic Test. *J. Pulm. Respir. Med.* **4,** 4–7 (2014).
35. Ramsey, B. *et al.* A CFTR Potentiator in Patients with Cystic Fibrosis and the G551D Mutation. *N Eng J Med* **365,** 1663–1672 (2011).
36. Wainwright, C. *et al.* Lumacaftor–Ivacaftor in Patients with Cystic Fibrosis Homozygous for Phe508del CFTR C.E. *N Eng J Med* **373,** 220–231 (2015).
37. Taylor-Cousar, J. L. *et al.* Tezacaftor–Ivacaftor in Patients with Cystic Fibrosis Homozygous for Phe508del. *N. Engl. J. Med.* **377,** 2013–2023 (2017).
38. Vertex Pharmaceuticals Inc. online information on approved CFTR modulators. Available at: https://www.vrtx.com/pipeline-medicines/our-approved-medicines. (Accessed: 15th July 2018)
39. European Medicines Agency (EMA) reports on authorized marketing human medicines in Europe. Available at: http://www.ema.europa.eu/ema/index.jsp?curl=pages/medicines/landing/epar_search.jsp&mid=WC0b01ac058001d124. (Accessed: 19th July 2018)
40. Clinical and Functional TRanslation of CFTR (CFTR2) database. Available at: https://www.cftr2.org/welcome. (Accessed: 15th July 2018)
41. Farrell, P. M. P. *et al.* Guidelines for Diagnosis of Cystic Fibrosis in Newborns through Older Adults: Cystic Fibrosis Foundation Consensus Report. *J Pediatr.* **153,** S4–S14 (2008).
42. Farrell, P. M. *et al.* Diagnosis of Cystic Fibrosis: Consensus Guidelines from the Cystic Fibrosis Foundation. *J. Pediatr.* **181,** S4–S15 (2017).
43. Accurso, F. J. *et al.* Sweat Chloride as A Biomarker of CFTR Activity: Proof of Concept and Ivacaftor Clinical Trial Data. *J. Cyst. Fibros.* **13,** 139–147 (2014).
44. Ratjen, F. & Döring, G. Cystic Fibrosis. *Lancet* **361,** 681–689 (2003).
45. Rowe, S. M. Nasal Potential Difference Measurements to Assess CFTR Ion Channel Activity. *Methods Mol Biol.* **741,** 69–86 (2011).
46. Beekman, J. M. *et al.* CFTR functional measurements in human models for diagnosis, prognosis and personalized therapy. Report on the pre-conference meeting to the 11th ECFS Basic Science Conference, Malta, 26-29 March 2014. *J. Cyst. Fibros.* **13,** 363–372 (2014).
47. Guglani, L., Stabel, D. & Weiner, D. J. False-Positive and False-Negative Sweat Tests: Systematic Review of the Evidence. *Pediatr. Allergy. Immunol. Pulmonol.* **28,** 198–211 (2015).
48. Mall, M., Hirtz, S., Gonska, T. & Kunzelmann, K. Assessment of CFTR function in rectal biopsies for the diagnosis of cystic fibrosis. **3,** 165–169 (2004).
49. Hirtz, S. *et al.* CFTR Cl- channel function in native human colon correlates with the genotype and phenotype in cystic fibrosis. *Gastroenterology* **127,** 1085–1095 (2004).
50. Sousa, M. *et al.* Measurements of CFTR-Mediated Cl- Secretion in Human Rectal Biopsies Constitute a Robust Biomarker for Cystic Fibrosis Diagnosis and Prognosis. *PLoS One* **7,** (2012).
51. Crossley, J. R., Smith, P. A., Edgar, B. W., Gluckman, P. D. & Elliott, R. B. Neonatal screening for cystic fibrosis, using immunoreactive trypsin assay in dried blood spots. *Clin. Chim. Acta* **113,** 111–121 (1981).
52. Castellani, C. *et al.* Consensus on the use and interpretation of cystic fibrosis mutation analysis in clinical practice. **7,** 179–196 (2008).
53. Dequeker, E. *et al.* Best practice guidelines for molecular genetic diagnosis of cystic fibrosis and CFTR-related disorders – updated European recommendations. *Eur. J. Hum. Genet.* **17,** 51–65 (2009).
54. Sato, T. *et al.* Long-term expansion of epithelial organoids from human colon, adenoma, adenocarcinoma, and Barrett's epithelium. *Gastroenterology* **141,** 1762–1772 (2011).
55. Dekkers, J. F. *et al.* A functional CFTR assay using primary cystic fibrosis intestinal organoids. *Nat. Med.* **19,** 939–945 (2013).
56. Dekkers, J. F. *et al.* Optimal correction of distinct CFTR folding mutants in rectal cystic fibrosis organoids. *Eur. Respir. J.* **48,** 451–458 (2016).
57. Awatade, N. T. *et al.* Measurements of Functional Responses in Human Primary Lung Cells as a Basis for Personalized Therapy for Cystic Fibrosis. *EBioMedicine* **2,** 147–153 (2015).
58. Mou, H. *et al.* Dual SMAD signaling inhibition enables long-term expansion of diverse epithelial basal cells. *Cell Stem Cell* **19,** 217–231 (2016).

59. Zeitlin, P. L. *et al.* A cystic fibrosis bronchial epithelial cell line: immortalization by adeno-12-SV40 infection. *Am. J. Respir. Cell Mol. Biol.* **4,** 313–319 (1991).
60. Ehrhardt, C. *et al.* Towards an in vitro model of cystic fibrosis small airway epithelium: characterisation of the human bronchial epithelial cell line CFBE41o-. *Cell Tissue Res.* **323,** 405–415 (2006).
61. Han, S. T. *et al.* Residual function of cystic fibrosis mutants predicts response to small molecule CFTR modulators. *JCI Insight* **3,** (2018).
62. Botelho, H. M. *et al.* Protein Traffic Disorders: An Effective High-Throughput Fluorescence Microscopy Pipeline for Drug Discovery. *Sci. Rep.* **5,** 1–8 (2015).
63. Dekkers, J. F., van der Ent, C. K. & Beekman, J. M. Novel opportunities for CFTR-targeting drug development using organoids. *Rare Dis.* **1,** (2013).
64. Salomon, J. J. *et al.* The Cell Line NCl-H441 Is a Useful in Vitro Model for Transport Studies of Human Distal Lung Epithelial Barrier. *Mol. Pharm.* **11,** 995–1006 (2014).
65. Hunter, M. J. *et al.* Expression of wild-type CFTR suppresses NF-κB-driven inflammatory signalling. *PLoS One* **5,** (2010).
66. Dekkers, J. F. *et al.* Characterizing responses to CFTR-modulating drugs using rectal organoids derived from subjects with cystic fibrosis. *Sci. Transl. Med.* **8,** 13 (2016).
67. Terlizzi, V. *et al.* Clinical expression of patients with the D1152H CFTR mutation. *J. Cyst. Fibros.* **14,** 447–452 (2015).
68. Vankeerberghen, A. *et al.* Characterization of mutations located in exon 18 of the CFTR gene. *FEBS Lett.* **437,** 1–4 (1998).
69. Burgel, P. R. *et al.* Non-classic cystic fibrosis associated with D1152H CFTR mutation. *Clin. Genet.* **77,** 355–364 (2010).
70. Wang, X. R. & Li, C. Decoding F508del misfolding in cystic fibrosis. *Biomolecules* **4,** 498–509 (2014).
71. Vecchio-Pagán, B. *et al.* Deep resequencing of CFTR in 762 F508del homozygotes reveals clusters of non-coding variants associated with cystic fibrosis disease traits. *Hum. Genome Var.* **3,** 1–9 (2016).
72. Rapino, D. *et al.* Rescue of NBD2 mutants N1303K and S1235R of CFTR by small-molecule correctors and transcomplementation. *PLoS One* **10,** 1–17 (2015).
73. Cotellessa, M. *et al.* N1303K mutation and diabetes mellitus in cystic fibrosis. *Arch. Dis. Child.* **75,** 546 (1996).
74. Chillón, M. *et al.* Identification of a new missense mutation (P205S) in the first transmembrane domain of the CFTR gene associated with a mild cystic fibrosis phenotype. *Hum. Mol. Genet.* **2,** 1741–1742 (1993).
75. Sheppard, D. N., Travis, S. M., Ishihara, H. & Welsh, M. J. Contribution of proline residues in the membrane-spanning domains of cystic fibrosis transmembrane conductance regulator to chloride channel function. *J. Biol. Chem.* **271,** 14995–15001 (1996).
76. Bozon, D., Zielenski, J., Rininsland, F. & Tsui, L.-C. Identification of Four New Mutations in the Cystic Fibrosis Transmembrane Conductance Regulator Gene: I148T,L1077P,Y1092X, 2183AA>G. *Hum. Mutat.* **3,** 330–332 (1994).
77. De Braekeleer, M., Allard, C., Leblanc, J. P., Simard, F. & Aubin, G. Phenotypic variability in five cystic fibrosis patients compound heterozygous for the Y1092X mutation. *Hum. Hered.* **48,** 158–162 (1998).
78. Vankeerberghen, A. *et al.* Characterization of 19 Disease-Associated Missense Mutations in the Regulatory Domain of the Cystic Fibrosis Transmembrane Conductance Regulator. *Hum. Mol. Genet.* **7,** 1761–1769 (1998).
79. Castaldo, G. *et al.* Phenotypic discordance in three siblings affected by atypical cystic fibrosis with the F508del/D614G genotype. *J. Cyst. Fibros.* **5,** 193–195 (2006).
80. Highsmith, W. E. *et al.* A novel mutation in the cystic fibrosis gene in patients with pulmonary disease but normal sweat chloride concentrations. *N. Engl. J. Med.* **331,** 974–980 (1994).
81. Chiba-Falek, O., Parad, R. B., Kerem, E. & Kerem, B. Variable levels of normal RNA in different fetal organs carrying a cystic fibrosis transmembrane conductance regulator splicing mutation. *Am. J. Respir. Crit. Care Med.* **159,** 1998–2002 (1999).
82. Dörk, T. *et al.* Characterization of a novel 21-kb deletion, CFTRdele2,3(21 kb), in the CFTR gene: A cystic fibrosis mutation of Slavic origin common in Central and East Europe. *Hum. Genet.* **106,** 259–268 (2000).
83. Hull, J., Shackleton, S. & Harris, A. Abnormal messenger RNA Splicing Resulting from 3 Different Mutations in the CFTR Gene. *Hum Mol Genet* **2,** 689–692 (1993).
84. Witt, M., Pogorzelski, A., Zebrak, J. & Rutkiewicz, E. A cystic fibrosis patient homozygous for 621+1G→T mutation has a severe pulmonary disease, mild pancreatic insufficiency and a gastro-esophageal reflux. *Clin.Genet.* **50,** 149–151 (1996).
85. Sheppard, D. N. *et al.* Mutations in CFTR associated with mild-disease form Cl- channels with altered pore properties. *Nature* **362,** 160–164 (1993).

86. Varon, R. *et al.* Pancreatic insufficiency and pulmonary disease in German and Slavic cystic fibrosis patients with the R347P mutation. *Hum. Mutat.* **6,** 219–225 (1995).
87. Goor, F. Van, Yu, H., Burton, B. & Hoffman, B. J. Effect of ivacaftor on CFTR forms with missense mutations associated with defects in protein processing or function. *J. Cyst. Fibros.* **13,** 29–36 (2014).
88. Antiñolo, G. *et al.* Genotype-phenotype relationship in 12 patients carrying cystic fibrosis mutation R334W. *J. Med. Genet.* **34,** 89–91 (1997).
89. Highsmith, W. E. *et al.* Identification of a Splice Site Mutation (2789 + 5 G > A) Associated With Small Amounts of Normal CFTR mRNA and Mild Cystic Fibrosis. **338,** 332–338 (1997).
90. Beck, S. *et al.* Cystic fibrosis patients with the 3272-26A→G mutation have mild disease, leaky alternative mRNA splicing, and CFTR protein at the cell membrane. *Hum. Mutat.* **14,** 133–144 (1999).
91. Cormet-Boyaka, E. *et al.* Rescuing cystic fibrosis transmembrane conductance regulator (CFTR)-processing mutants by transcomplementation. *Proc. Natl. Acad. Sci.* **101,** 8221–8226 (2004).
92. Padoan, R. *et al.* First report of three cystic fibrosis patients homozygous for the 1717-1G>A mutation. *J Med Genet* **33,** 1052–1054 (1996).
93. Decaestecker, K. *et al.* Genotype/phenotype correlation of the G85E mutation in a large cohort of cystic fibrosis patients. *Eur. Respir. J.* **23,** 679–684 (2004).
94. Hamosh, A., Rosenstein, B. J. & Cutting, G. R. CFTR nonsense mutations G542X and W1282X associated with severe reduction of CFTR mRNA in nasal epithelial cells. *Hum. Mol. Genet.* **1,** 542–544 (1992).
95. Bienvenu, T., Beldjord, C., Fonknechten, N., Kaplan, J. C. & Lenoir, G. Severe cystic fibrosis in a child homozygous for the G542 nonsense mutation in the CFTR gene. *J Med Genet* **30,** 621–622 (1993).
96. Zielenski, J. *et al.* Analysis of CFTR transcripts in nasal epithelial cells and lymphoblasts of a cystic fibrosis patient with 621 + 1G→ T and 711 + 1G→ T mutations. *Hum. Mol. Genet.* **2,** 683 (1993).
97. Ramalho, A. S. *et al.* Five percent of normal cystic fibrosis transmembrane conductance regulator mRNA ameliorates the severity of pulmonary disease in cystic fibrosis. *Am. J. Respir. Cell Mol. Biol.* **27,** 619–627 (2002).
98. Cutting, G. R. Modifier genes in Mendelian disorders: the example of cystic fibrosis. *Ann N Y Acad Sci* 57–69 (2010).
99. Begenisich, T. *et al.* Physiological roles of the intermediate conductance, Ca2+-activated potassium channel Kcnn4. *J. Biol. Chem.* **279,** 47681–47687 (2004).
100. Van Goor, F. *et al.* Correction of the F508del-CFTR protein processing defect in vitro by the investigational drug VX-809. *Proc. Natl. Acad. Sci.* **108,** 18843–18848 (2011).
101. Guimbellot, J. S. *et al.* Nasospheroids permit measurements of CFTR-dependent fluid transport. *JCI Insight* **2,** (2017).
102. Lopes-Pacheco, M. CFTR modulators: Shedding light on precision medicine for cystic fibrosis. *Front. Pharmacol.* **7,** 1–20 (2016).

7. Appendices

Appendix I – CFTR structure

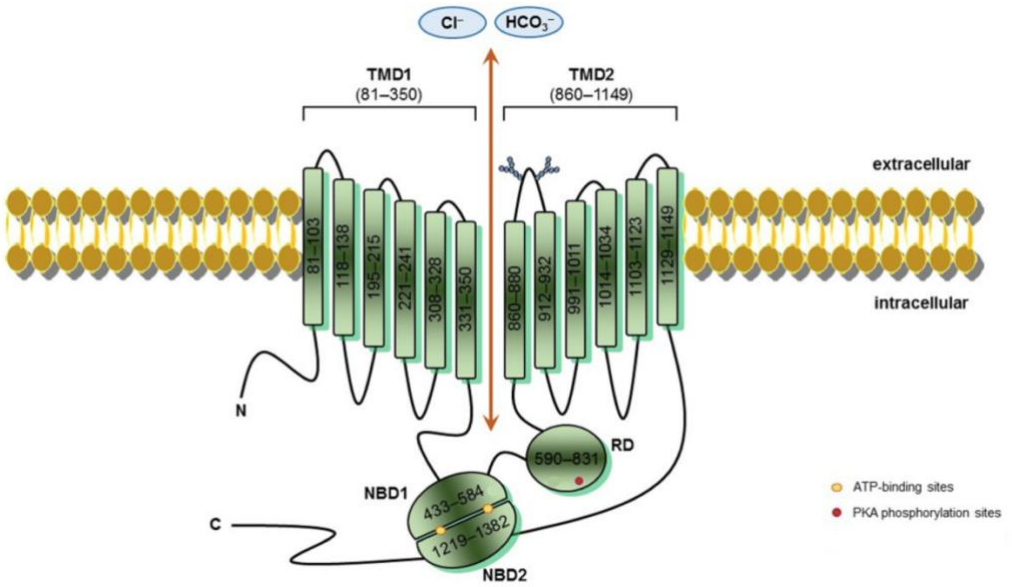

Figure 7.1 – Schematic structure of CFTR. Representative scheme of the CFTR protein structure. CFTR is a 1,480 amino-acids transmembrane glycoprotein belonging to the ABC superfamily. CFTR possesses two transmembrane domains (TMD1/2) that form the channel pore, each containing six hydrophobic alpha-helices which cross the cell surface lipid bilayer, joined by two intracellular loops and three extracellular loops, and with glycosylated residues linked in the forth extracellular loop; two nucleotide-binding domains (NBD1/2) with ATP-binding locations (yellow dots) where hydrolysis occurs; and one unique regulatory domain (RD) with protein kinase A phosphorylation sites (red dot). The numbers correspond to the first and last amino-acid position of each fragment represented within the CFTR protein. **Adapted from Lopes-Pacheco (2016)**[102]**.**

Appendix II – Results from patients' analyses: mild *CFTR* genotypes

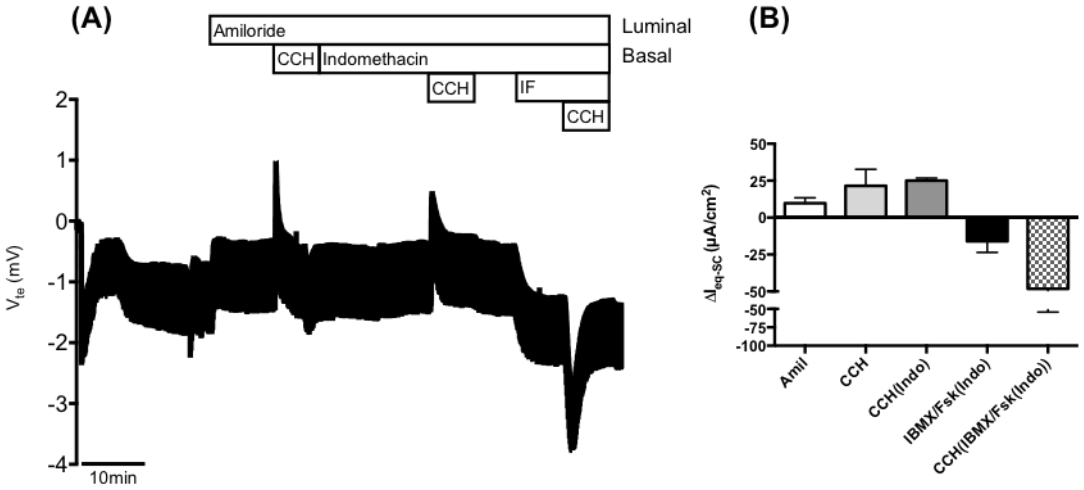

Figure 7.2 – Results from Ussing chamber measurements in rectal biopsies from patient CFL50 (D1152H/N1303K genotype). (A) Representative original recording of the effects of cholinergic (CCH, 100 µM, basolateral) and cAMP-dependent (IBMX/Fsk (I/F), 100 µM/2 µM, basolateral) activation on transepithelial voltage (V_{te}) in D1152H/N1303K rectal biopsies from patient CFL50. Experiments were performed in the presence of Amiloride (Amil, 20 µM, luminal) and/or Amiloride + Indomethacin (Indo, 10 µM, basolateral), as indicated in the figure. **(B)** Summary of activated equivalent short-circuit currents (ΔI_{eq-sc}) for Amil ($\Delta I_{eq-sc,Amil}$), basal CCH ($\Delta I_{eq-sc,CCH}$), CCH + Indo ($\Delta I_{eq-sc,CCH(Indo)}$), IBMX/Fsk + Indo ($\Delta I_{eq-sc,IBMX/Fsk(Indo)}$) and CCH following IBMX/Fsk application ($\Delta I_{eq-sc,CCH(IBMX/Fsk(Indo))}$); data represent the mean of measurements on three rectal biopsies ± SEM. $\Delta I_{eq-sc,IBMX/Fsk(Indo)}$ = -16.000 ± 7.571 µA/cm^2; $\Delta I_{eq-sc,CCH(IBMX/Fsk(Indo))}$ = -48.220 ± 6.139 µA/cm^2 (29.5% of WT CFTR function).

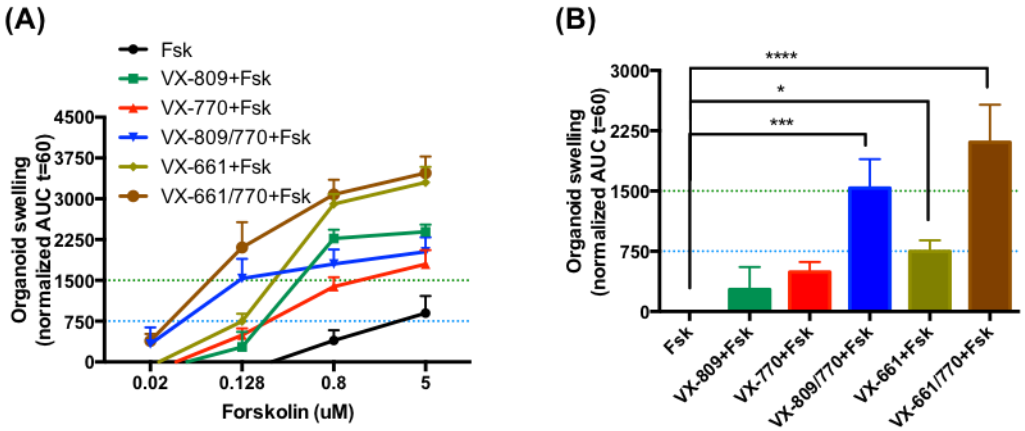

Figure 7.3 – Results from the forskolin-induced swelling (FIS) assay on intestinal organoids from patient CFL06 (P205S/Y1092X genotype). (A) Quantification of FIS in organoids for all treatments tested (Forskolin (Fsk) alone, VX-809 (3 µM) + Fsk, VX-770 (3 µM) + Fsk, VX-809/770 + Fsk, VX-661 (5 µM) + Fsk and VX-661/770 + Fsk) at the Fsk concentrations of 0.02, 0.128, 0.8 and 5 µM, expressed as the AUC of organoid surface area increase (baseline = 100%, t = 60 min). **(B)** Quantification of organoid swelling for all treatments at [Fsk] = 0.128 µM. The dashed blue and green lines represent the established thresholds for medium and high clinical benefit potential for treatments, respectively. Data represent the mean of measurements on 5-8 replicate wells per condition ± SEM. Asterisks (*) indicate degree of significant difference calculated by unpaired one-way ANOVA to control (Fsk) using Fisher's LSD test. [Experiments were performed in collaboration with Iris Silva and included with permission].

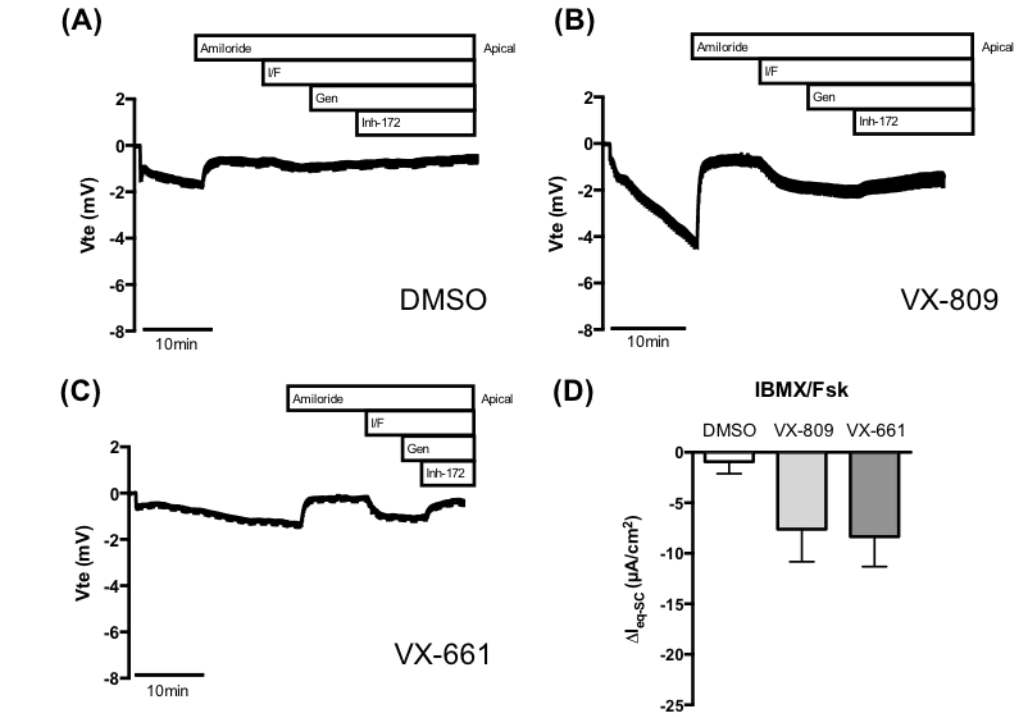

Figure 7.4 – Results from Ussing chamber measurements in human nasal epithelial cells (HNECs) from patient CFL06 (P205S/Y1092X genotype). Representative original recordings of the effects of cAMP-dependent (IBMX/Fsk (I/F), 100 µM/2 µM, apical) activation, CFTR potentiation (Genistein (Gen), 25 µM, apical) and CFTR-specific inhibition ($CFTR_{inh}$-172 (Inh-172), 30 µM, apical) on transepithelial voltage (V_{te}) in HNECs from patient CFL06 (P205S/Y1092X). Experiments were performed in the presence of Amiloride (Amil, 20 µM, apical) for **(A)** 0.05% DMSO **(B)** 3 µM VX-809 and **(C)** 5 µM VX-661 treated cells for 48 h. **(D)** Summary of activated equivalent short-circuit currents ($\Delta I_{eq\text{-}sc}$) upon IBMX/Fsk addition for all conditions. Data represent the mean of measurements on 3-4 replicates per condition ± SEM. No statistically significant differences were detected by unpaired one-way ANOVA to control (DMSO) using Fisher's LSD test.

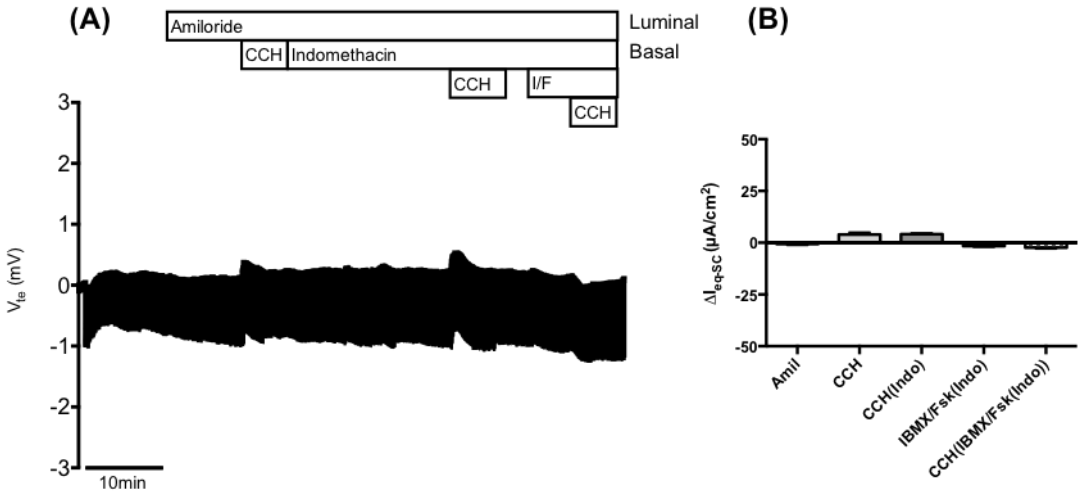

Figure 7.5 – Results from Ussing chamber measurements in rectal biopsies from patient CFL58 (3849+10kbC>T/F508del genotype). (A) Representative original recording of the effects of cholinergic (CCH, 100 µM, basolateral) and cAMP-dependent (IBMX/Fsk (I/F), 100 µM/2 µM, basolateral) activation on transepithelial voltage (V_{te}) in 3849+10kbC>T/F508del rectal biopsies from patient CFL58. Experiments were performed in the presence of Amiloride (Amil, 20 µM, luminal) and/or Amiloride + Indomethacin (Indo, 10 µM, basolateral), as indicated in the figure. **(B)** Summary of activated equivalent short-circuit currents ($\Delta I_{eq\text{-}sc}$) for Amil ($\Delta I_{eq\text{-}sc,Amil}$), basal CCH ($\Delta I_{eq\text{-}sc,CCH}$), CCH + Indo ($\Delta I_{eq\text{-}sc,CCH(Indo)}$), IBMX/Fsk + Indo ($\Delta I_{eq\text{-}sc,IBMX/Fsk(Indo)}$) and CCH following IBMX/Fsk application ($\Delta I_{eq\text{-}sc,CCH(IBMX/Fsk(Indo))}$); data represent the mean of measurements on three rectal biopsies ± SEM. $\Delta I_{eq\text{-}sc,IBMX/Fsk(Indo)}$ = -1.604 ± 0.503 µA/cm²; $\Delta I_{eq\text{-}sc,CCH(IBMX/Fsk(Indo))}$ = -2.380 ± 0.5816 µA/cm² (1.8% of WT CFTR function).

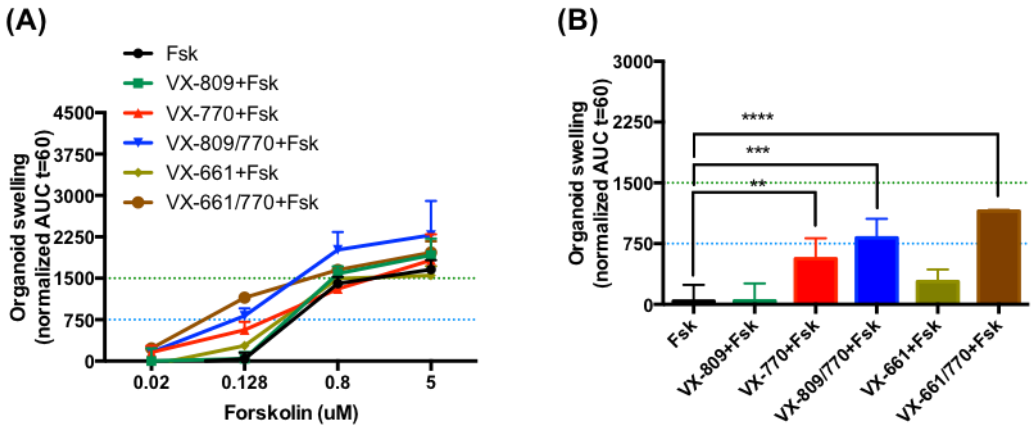

Figure 7.6 – Results from the forskolin-induced swelling (FIS) assay on intestinal organoids from patient CFL58 (3849+10kbC>T/F508del genotype). (A) Quantification of FIS in organoids for all treatments tested (Forskolin (Fsk) alone, VX-809 (3 µM) + Fsk, VX-770 (3 µM) + Fsk, VX-809/770 + Fsk, VX-661 (5 µM) + Fsk and VX-661/770 + Fsk) at the Fsk concentrations of 0.02, 0.128, 0.8 and 5 µM, expressed as the AUC of organoid surface area increase (baseline = 100%, t = 60 min). **(B)** Quantification of organoid swelling for all treatments at [Fsk] = 0.128 µM; The dashed blue and green lines represent the established thresholds for medium and high clinical benefit potential for treatments, respectively. Data represent the mean of measurements on 4-6 replicate wells per condition ± SEM. Asterisks (*) indicate degree of significant difference calculated by unpaired one-way ANOVA to control (Fsk) using Fisher's LSD test.

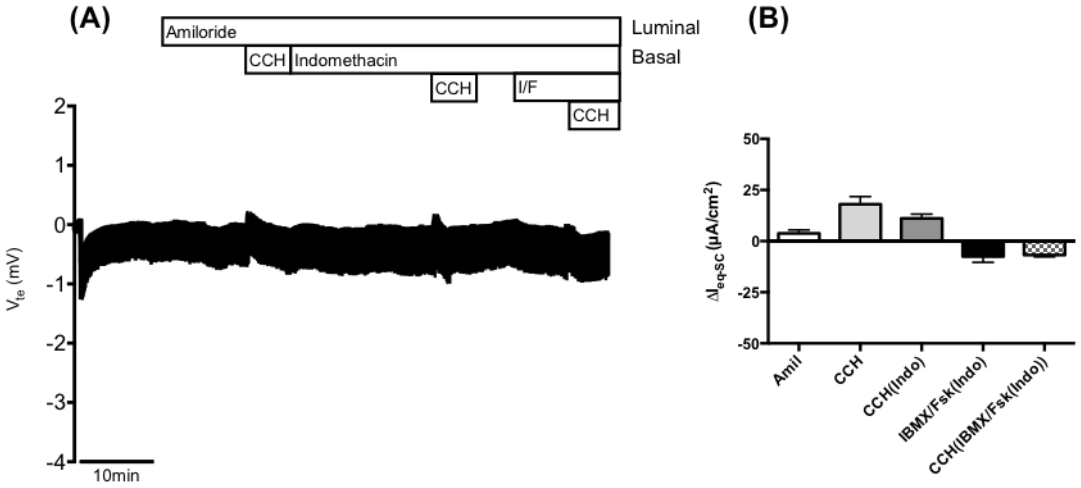

Figure 7.7 – Results from Ussing chamber measurements in rectal biopsies from patient CFL56 (3849+10kbC>T/621+1G>T genotype). (A) Representative original recording of the effects of cholinergic (CCH, 100 µM, basolateral) and cAMP-dependent (IBMX/Fsk (I/F), 100 µM/2 µM, basolateral) activation on transepithelial voltage (V_{te}) in 3849+10kbC>T/621+1G>T rectal biopsies from patient CFL56. Experiments were performed in the presence of Amiloride (Amil, 20 µM, luminal) and/or Amiloride + Indomethacin (Indo, 10 µM, basolateral), as indicated in the figure. **(B)** Summary of activated equivalent short-circuit currents ($\Delta I_{eq\text{-}sc}$) for Amil ($\Delta I_{eq\text{-}sc,Amil}$), basal CCH ($\Delta I_{eq\text{-}sc,CCH}$), CCH + Indo ($\Delta I_{eq\text{-}sc,CCH(Indo)}$), IBMX/Fsk + Indo ($\Delta I_{eq\text{-}sc,IBMX/Fsk(Indo)}$) and CCH following IBMX/Fsk application ($\Delta I_{eq\text{-}sc,CCH(IBMX/Fsk(Indo))}$); data represent the mean of measurements on two rectal biopsies ± SEM. $\Delta I_{eq\text{-}sc,IBMX/Fsk(Indo)}$ = -7.568 ± 2.804 µA/cm^2; $\Delta I_{eq\text{-}sc,CCH(IBMX/Fsk(Indo))}$ = -6.774 ± 0.947 µA/cm^2 (6.6% of WT CFTR function).

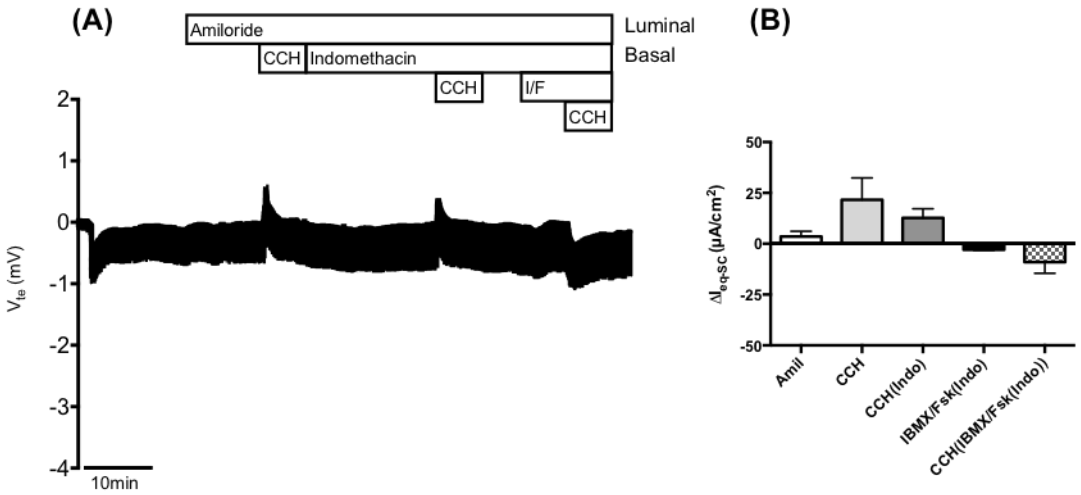

Figure 7.8 – Results from Ussing chamber measurements in rectal biopsies from patient CFL55 (2789+5G>A/F508del genotype). (A) Representative original recording of the effects of cholinergic (CCH, 100 µM, basolateral) and cAMP-dependent (IBMX/Fsk (I/F), 100 µM/2 µM, basolateral) activation on transepithelial voltage (V_{te}) in 2789+5G>A/F508del rectal biopsies from patient CFL55. Experiments were performed in the presence of Amiloride (Amil, 20 µM, luminal) and/or Amiloride + Indomethacin (Indo, 10 µM, basolateral), as indicated in the figure. **(B)** Summary of activated equivalent short-circuit currents (ΔI_{eq-sc}) for Amil ($\Delta I_{eq-sc,Amil}$), basal CCH ($\Delta I_{eq-sc,CCH}$), CCH + Indo ($\Delta I_{eq-sc,CCH(Indo)}$), IBMX/Fsk + Indo ($\Delta I_{eq-sc,IBMX/Fsk(Indo)}$) and CCH following IBMX/Fsk application ($\Delta I_{eq-sc,CCH(IBMX/Fsk(Indo))}$); data represent the mean of measurements on three rectal biopsies ± SEM. $\Delta I_{eq-sc,IBMX/Fsk(Indo)}$ = -2.961 ± 0.280 µA/cm^2; $\Delta I_{eq-sc,CCH(IBMX/Fsk(Indo))}$ = -9.054 ± 5.474 µA/cm^2 (5.5% of WT CFTR function).

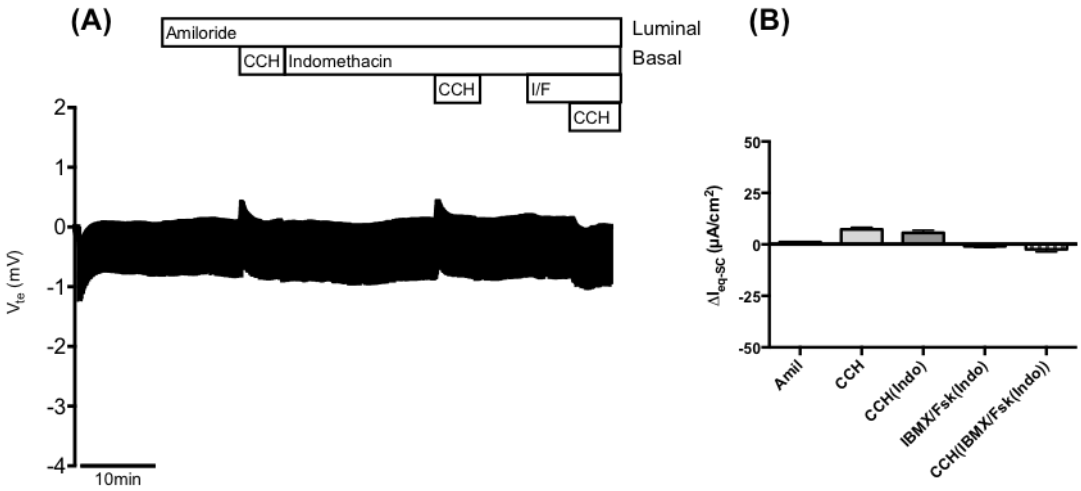

Figure 7.9 – Results from Ussing chamber measurements in rectal biopsies from patient CFL27 (2789+5G>A/F508del genotype). (A) Representative original recording of the effects of cholinergic (CCH, 100 µM, basolateral) and cAMP-dependent (IBMX/Fsk (I/F), 100 µM/2 µM, basolateral) activation on transepithelial voltage (V_{te}) in 2789+5G>A/F508del rectal biopsies from patient CFL27. Experiments were performed in the presence of Amiloride (Amil, 20 µM, luminal) and/or Amiloride + Indomethacin (Indo, 10 µM, basolateral), as indicated in the figure. **(B)** Summary of activated equivalent short-circuit currents (ΔI_{eq-sc}) for Amil ($\Delta I_{eq-sc,Amil}$), basal CCH ($\Delta I_{eq-sc,CCH}$), CCH + Indo ($\Delta I_{eq-sc,CCH(Indo)}$), IBMX/Fsk + Indo ($\Delta I_{eq-sc,IBMX/Fsk(Indo)}$) and CCH following IBMX/Fsk application ($\Delta I_{eq-sc,CCH(IBMX/Fsk(Indo))}$); data represent the mean of measurements on three rectal biopsies ± SEM. $\Delta I_{eq-sc,IBMX/Fsk(Indo)}$ = -0.982 ± 0.495 µA/cm^2; $\Delta I_{eq-sc,CCH(IBMX/Fsk(Indo))}$ = -2.383 ± 1.237 µA/cm^2 (1.5% of WT CFTR function).

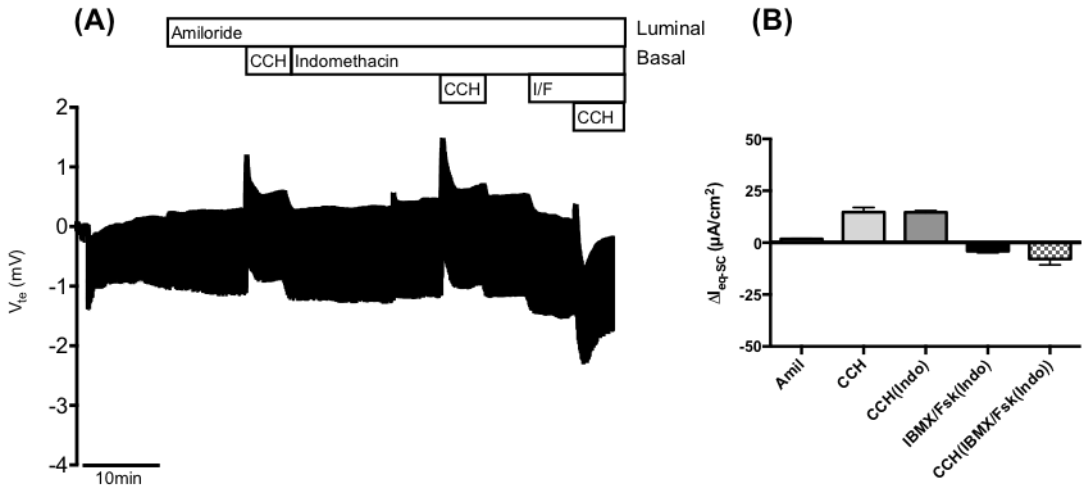

Figure 7.10 – Results from Ussing chamber measurements in rectal biopsies from patient CFL64 (3272-26A>G/F508del genotype). (A) Representative original recording of the effects of cholinergic (CCH, 100 µM, basolateral) and cAMP-dependent (IBMX/Fsk (I/F), 100 µM/2 µM, basolateral) activation on transepithelial voltage (V_{te}) in 3272-26A>G/F508del rectal biopsies from patient CFL64. Experiments were performed in the presence of Amiloride (Amil, 20 µM, luminal) and/or Amiloride + Indomethacin (Indo, 10 µM, basolateral), as indicated in the figure. **(B)** Summary of activated equivalent short-circuit currents (ΔI_{eq-sc}) for Amil ($\Delta I_{eq-sc,Amil}$), basal CCH ($\Delta I_{eq-sc,CCH}$), CCH + Indo ($\Delta I_{eq-sc,CCH(Indo)}$), IBMX/Fsk + Indo ($\Delta I_{eq-sc,IBMX/Fsk(Indo)}$) and CCH following IBMX/Fsk application ($\Delta I_{eq-sc,CCH(IBMX/Fsk(Indo))}$); data represent the mean of measurements on four rectal biopsies ± SEM. $\Delta I_{eq-sc,IBMX/Fsk(Indo)}$ = -4.165 ± 0.694 µA/cm^2; $\Delta I_{eq-sc,CCH(IBMX/Fsk(Indo))}$ = -7.845 ± 2.884 µA/cm^2 (5.5% of WT CFTR function).

Appendix III – Results from patients' analyses: severe *CFTR* genotypes

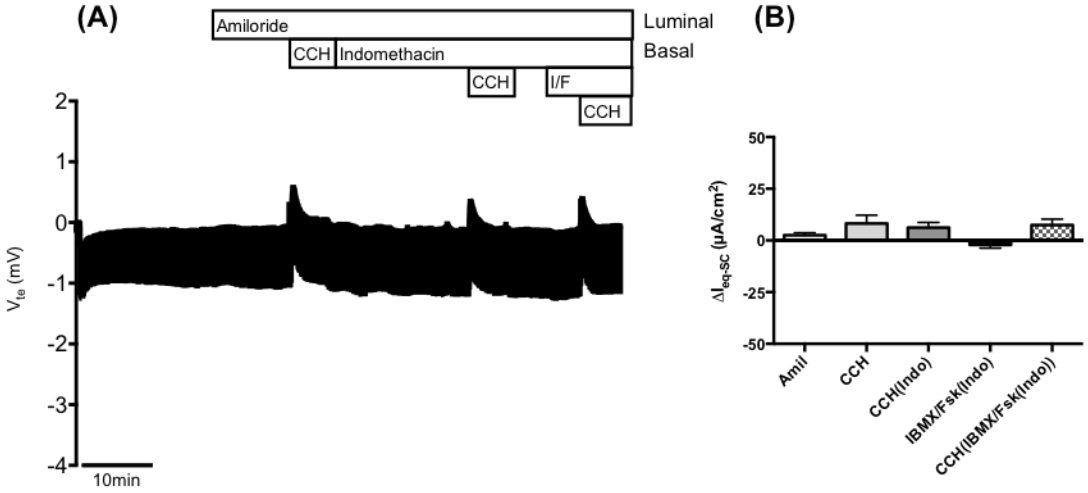

Figure 7.11 – Results from Ussing chamber measurements in rectal biopsies from patient CFL65 (F508del/F508del genotype). (A) Representative original recording of the effects of cholinergic (CCH, 100 µM, basolateral) and cAMP-dependent (IBMX/Fsk (I/F), 100 µM/2 µM, basolateral) activation on transepithelial voltage (V_{te}) in F508del/F508del rectal biopsies from patient CFL65. Experiments were performed in the presence of Amiloride (Amil, 20 µM, luminal) and/or Amiloride + Indomethacin (Indo, 10 µM, basolateral), as indicated in the figure. **(B)** Summary of activated equivalent short-circuit currents (ΔI_{eq-sc}) for Amil ($\Delta I_{eq-sc,Amil}$), basal CCH ($\Delta I_{eq-sc,CCH}$), CCH + Indo ($\Delta I_{eq-sc,CCH(Indo)}$), IBMX/Fsk + Indo ($\Delta I_{eq-sc,IBMX/Fsk(Indo)}$) and CCH following IBMX/Fsk application ($\Delta I_{eq-sc,CCH(IBMX/Fsk(Indo))}$); data represent the mean of measurements on three rectal biopsies ± SEM. $\Delta I_{eq-sc,IBMX/Fsk(Indo)}$ = -2.124 ± 1.553 µA/cm^2; $\Delta I_{eq-sc,CCH(IBMX/Fsk(Indo))}$ = 7.436 ± 2.862 µA/cm^2 (0% of WT CFTR function).

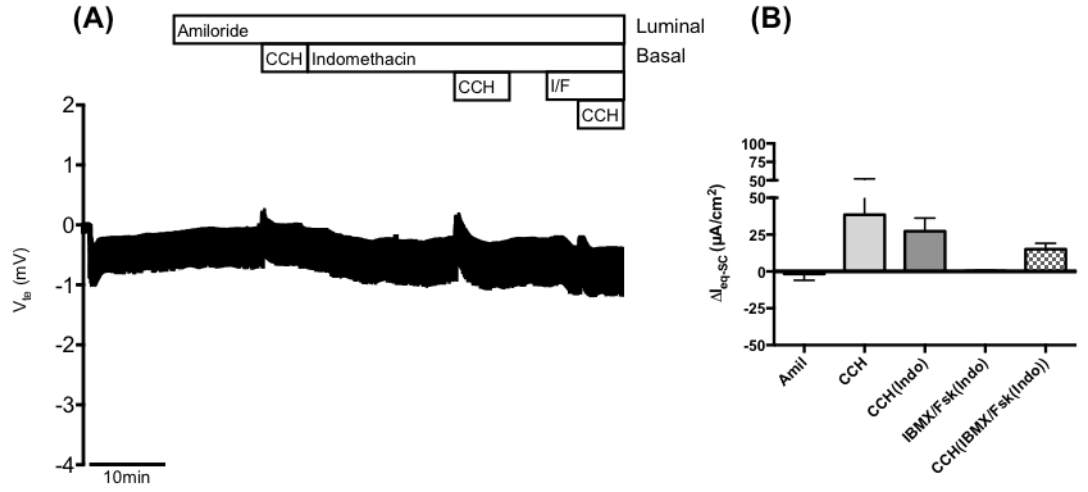

Figure 7.12 – Results from Ussing chamber measurements in rectal biopsies from patient CFL53 (F508del/G542X genotype). (A) Representative original recording of the effects of cholinergic (CCH, 100 µM, basolateral) and cAMP-dependent (IBMX/Fsk (I/F), 100 µM/2 µM, basolateral) activation on transepithelial voltage (V_{te}) in F508del/G542X rectal biopsies from patient CFL53. Experiments were performed in the presence of Amiloride (Amil, 20 µM, luminal) and/or Amiloride + Indomethacin (Indo, 10 µM, basolateral), as indicated in the figure. **(B)** Summary of activated equivalent short-circuit currents (ΔI_{eq-sc}) for Amil ($\Delta I_{eq-sc,Amil}$), basal CCH ($\Delta I_{eq-sc,CCH}$), CCH + Indo ($\Delta I_{eq-sc,CCH(Indo)}$), IBMX/Fsk + Indo ($\Delta I_{eq-sc,IBMX/Fsk(Indo)}$) and CCH following IBMX/Fsk application ($\Delta I_{eq-sc,CCH(IBMX/Fsk(Indo))}$); data represent the mean of measurements on four rectal biopsies ± SEM. $\Delta I_{eq-sc,IBMX/Fsk(Indo)}$ = 0.246 ± 0.452 µA/cm^2; $\Delta I_{eq-sc,CCH(IBMX/Fsk(Indo))}$ = 15.100 ± 4.010 µA/cm^2 (0% of WT CFTR function).

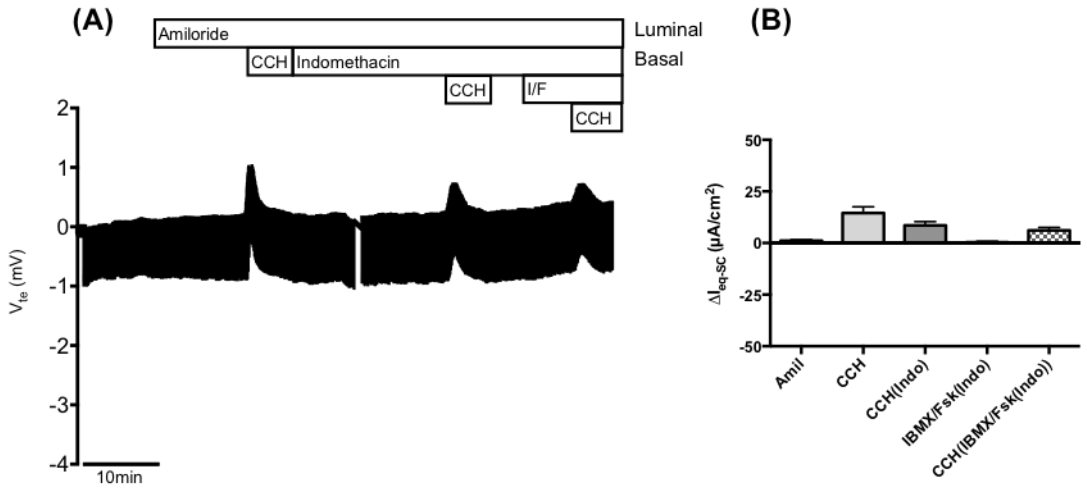

Figure 7.13 – Results from Ussing chamber measurements in rectal biopsies from patient CFL61 (F508del/G542X genotype). (A) Representative original recording of the effects of cholinergic (CCH, 100 µM, basolateral) and cAMP-dependent (IBMX/Fsk (I/F), 100 µM/2 µM, basolateral) activation on transepithelial voltage (V_{te}) in F508del/G542X rectal biopsies from patient CFL61. Experiments were performed in the presence of Amiloride (Amil, 20 µM, luminal) and/or Amiloride + Indomethacin (Indo, 10 µM, basolateral), as indicated in the figure. **(B)** Summary of activated equivalent short-circuit currents (ΔI_{eq-sc}) for Amil ($\Delta I_{eq-sc,Amil}$), basal CCH ($\Delta I_{eq-sc,CCH}$), CCH + Indo ($\Delta I_{eq-sc,CCH(Indo)}$), IBMX/Fsk + Indo ($\Delta I_{eq-sc,IBMX/Fsk(Indo)}$) and CCH following IBMX/Fsk application ($\Delta I_{eq-sc,CCH(IBMX/Fsk(Indo))}$); data represent the mean of measurements on four rectal biopsies ± SEM. $\Delta I_{eq-sc,IBMX/Fsk(Indo)} = 0.374 \pm 0.504$ µA/cm^2; $\Delta I_{eq-sc,CCH(IBMX/Fsk(Indo))} = 6.085 \pm 1.497$ µA/cm^2 (0% of WT CFTR function).

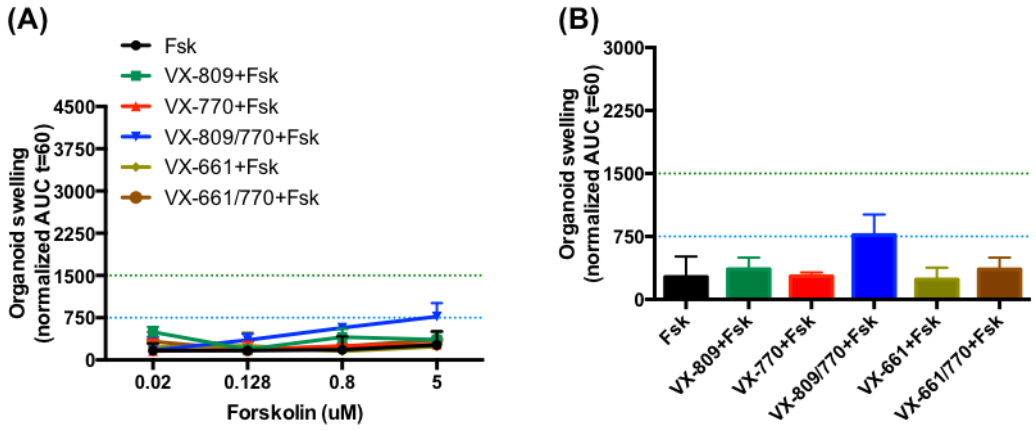

Figure 7.14 – Results from the forskolin-induced swelling (FIS) assay on intestinal organoids from patient CFL53 (F508del/G542X genotype). (A) Quantification of FIS in organoids for all treatments tested (Forskolin (Fsk) alone, VX-809 (3 µM) + Fsk, VX-770 (3 µM) + Fsk, VX-809/770 + Fsk, VX-661 (5 µM) + Fsk and VX-661/770 + Fsk) at the Fsk concentrations of 0.02, 0.128, 0.8 and 5 µM, expressed as the AUC of organoid surface area increase (baseline = 100%, t = 60 min). **(B)** Quantification of organoid swelling for all treatments at [Fsk] = 5 µM; The dashed blue and green lines represent the established thresholds for medium and high clinical benefit potential for treatments, respectively. Data represent the mean of measurements on 5-8 replicate wells per condition ± SEM. No statistically significant differences were detected by unpaired one-way ANOVA to control (Fsk) using Fisher's LSD test.

Appendix IV – Information on *CFTR* mutations found in patients under study

Table 7.1 – Information on *CFTR* mutations found in patients under study: variant names, Human Genome Variation Society (HGVS) nomenclature, cDNA names, localization in DNA (exon/intron) following legacy nomenclature, localization in CFTR (domain), allele frequency and clinical consequence reported in CFTR2[40] and functional classification based on data reported in current literature, discussed previously. NA = not available. ? = unknown/unclear.

Variant	HGVS nomenclature	cDNA name	Exon/ Intron	CFTR Domain	Allele frequency	Clinical consequence	Class
1717-1G>A	No protein name	c.1585-1G>A	In.10	-	0.00856	CF-causing	VII
2789+5G>A	No protein name	c.2657+5G>A	In.14b	-	0.00723	CF-causing	V
3272-26A>G	No protein name	c.3140-26A>G	In.17a	-	0.00331	CF-causing	V
3849+10kbC>T	No protein name	c.3718-2477C>T	In.19	-	0.00815	CF-causing	V
621+1G>T	No protein name	c.489+1G>T	In.4	-	0.00931	CF-causing	I/VII?
711+1G>T	No protein name	c.579+1G>T	In.5	-	0.00193	CF-causing	I/VII?
711+5G>A	No protein name	c.579+5G>A	In.5	-	0.00042	CF-causing	V?
D1152H	p.Asp1152His	c.3454G>C	Ex.18	Linker 3	0.00402	Varying	IV
D614G	p.Asp614Gly	c.1841A>G	Ex.13	RD	0.00012	Varying	?
dele2,3(21kb)	p.Ser18ArgfsX16	c.54-5940_273+10250del21kb	In.1-3	-	0.00294	CF-causing	VII
F508del	p.Phe508del	c.1521_1523del	Ex.10	NBD1	0.69744	CF-causing	II
G542X	p.Gly542X	c.1624G>T	Ex.11	NBD1	0.02542	CF-causing	I
G85E	p.Gly85Glu	c.254G>A	Ex.3	TMD1	0.00434	CF-causing	II
N1303K	p.Asn1303Lys	c.3909C>G	Ex.21	NBD2	0.01581	CF-causing	II
P205S	p.Pro205Ser	c.613C>T	Ex.6a	TMD3	0.00023	CF-causing	II
R334W	p.Arg334Trp	c.1000C>T	Ex.7	TMD6	0.00302	CF-causing	IV
R347P	p.Arg347Pro	c.1040G>C	Ex.7	TMD6	0.00375	CF-causing	IV
S955P	p.Ser955Pro	c.2863T>C	Ex.15	ICL4	NA	NA	?
W57G	p.Trp57Gly	c.169T>G	Ex.3	*N*-term	0.00007	CF-causing	II
Y1092X(C>A)	p.Tyr1092X	c.3276C>A	Ex.17b	ICL5	0.00158	CF-causing	I/VII?

Appendix V – Patient data used for correlation analyses between different CFTR function parameters, established CF biomarkers and clinical data

Table 7.2 – Summary of data from all patients studied used for correlation analyses: *CFTR* genotypes, patient codes, activated equivalent short circuit currents measured in Ussing chamber analyses of rectal biopsies under IBMX/Fsk ($\Delta I_{eq\text{-}sc}$(I/F)), CCH after I/F ($\Delta I_{eq\text{-}sc}$(CCH(I/F))) and the sum of these two currents, corresponding to the maximal CFTR activation ($\Delta I_{eq\text{-}sc}$(max)) (µA/cm^2), sweat [Cl$^-$] (mmol/L), forced expiratory volume in 1 sec in percentage predicted (FEV_1,%), fecal elastase E1 values (FEE, µg/g stool) and intestinal organoid forskolin-induced swelling (FIS, expressed as the AUC of organoid surface area increase (baseline = 100%, t = 60 min)) for [Fsk] = 0.02, 0.128, 0.8 and 5 µM, from all patients studied. NA = not available.

***CFTR* Genotype**	**Patient code**	**$\Delta I_{eq\text{-}sc}$ (I/F)**	**$\Delta I_{eq\text{-}sc}$ (CCH(I/F))**	**$\Delta I_{eq\text{-}sc}$ (max)**	**Sweat [Cl$^-$]**	**FEV_1**	**FEE**	**FIS 0.02**	**FIS 0.128**	**FIS 0.8**	**FIS 5**
D1152H/F508del	CFL26	-14,380	-62,860	-77,240	51.0	61	NA	-145,7	286,6	2881,8	2913,0
D1152H/N1303K	CFL50	-16,000	-48,220	-64,220	20.0	124	497,3	NA	NA	NA	NA
D1152H/N1303K	CFL51	-18,060	-68,180	-86,240	33.0	111	1036,7	NA	NA	NA	NA
F508del/S995P	CFL59	-6,421	-9,877	-16,298	56.5	95	500	306,7	399,3	1189,7	1635,5
P205S/Y1092X	CFL05	-9,882	-24,150	-34,032	91.5	NA	NA	-76,5	-69,1	126,6	249,8
P205S/Y1092X	CFL06	-9,882	-24,150	-34,032	89.5	NA	NA	-280,5	-187,8	397,1	897,5
D614G/F508del	CFL44	-15,550	-36,200	-51,750	NA	NA	NA	-36,4	133,7	1909,0	2504,7
3849+10kbC>T/F508del	CFL57	-1,236	-7,796	-9,032	43.5	72	573	-84,1	309,2	2059,0	3116,7
3849+10kbC>T/F508del	CFL58	-1,604	-2,380	-3,984	36.0	47	NA	-52,5	40,7	1405,7	1660,0
3849+10kbC>T/dele2,3(21kb)	CFL49	-5,167	-12,020	-17,187	60.0	75	479	NA	NA	NA	NA
3849+10kbC>T/621+1G>T	CFL56	-7,568	-6,774	-14,342	81.5	41	NA	NA	NA	NA	NA
F508del/R334W	CFL69	NA	NA	NA	112.5	95	NA	-24,4	66,1	905,1	1507,3
F508del/R347P	CFL54	-2,473	-7,509	-9,982	84.6	64	351	NA	NA	NA	NA
2789+5G>A/F508del	CFL55	-2,961	-9,054	-12,015	91.0	52	371	NA	NA	NA	NA
2789+5G>A/F508del	CFL27	-0,982	-2,383	-3,365	78.0	80	NA	NA	NA	NA	NA
2789+5G>A/dele2,3(21kb)	CFL62	-1,451	-2,952	-4,403	100.5	93	NA	NA	NA	NA	NA
3272-26A>G/W57G	CFL63	-13,410	-5,851	-19,261	89.2	89	NA	NA	NA	NA	NA
3272-26A>G/F508del	CFL64	-4,165	-7,845	-12,010	88.3	88	NA	NA	NA	NA	NA

CFTR Genotype	Patient code	$\Delta I_{eq\text{-}sc}$ (I/F)	$\Delta I_{eq\text{-}sc}$ (CCH(I/F))	$\Delta I_{eq\text{-}sc}$ (max)	Sweat [Cl^-]	FEV_1	FEE	FIS 0.02	FIS 0.128	FIS 0.8	FIS 5
1717-1G>A/G85E	CFL41	-3,899	18,767	14,868	90.0	80	NA	-200,4	-165,2	-237,7	27,6
F508del/F508del	CFL66	0,242	4,629	4,871	113.0	108	NA	-159,5	-52,7	-32,6	1,5
F508del/F508del	CFL65	-2,124	7,436	5,312	117.0	89	NA	NA	NA	NA	NA
F508del/G542X	CFL52	-1,298	12,640	11,342	84.7	80	40	7,5	-3,1	-11,0	-104,1
F508del/G542X	CFL53	0,246	15,100	15,346	78.9	64	10	167,0	166,2	180,2	268,0
F508del/G542X	CFL61	0,374	6,085	6,459	82.7	95	1	NA	NA	NA	NA
711+5G>A/F508del	CFL60	-0,537	11,790	11,253	84.3	102	50	NA	NA	NA	NA
711+1G>T/F508del	CFL68	NA	NA	NA	NA	105	NA	-178,2	-145,1	-46,9	-151,4

Appendix VI – CFTR correctors' effect on other epithelial channels

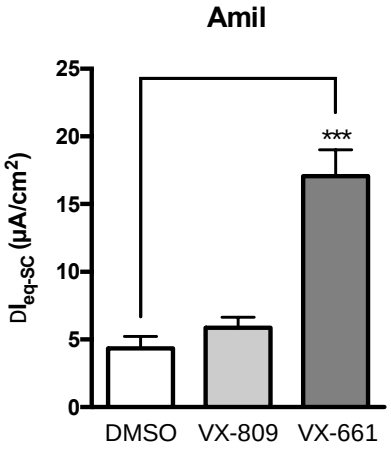

Figure 7.15 – Results from Ussing chamber measurements of Amiloride responses in human nasal epithelial cells (HNECs) from patient CFL05 (P205S/Y1092X genotype). Summary of activated equivalent short-circuit currents upon Amiloride addition ($\Delta I_{eq\text{-}sc,Amil}$) (Amil, 20 µM, apical) in HNECs from patient CFL05 (P205S/Y1092X) treated with 0.05% DMSO, 3 µM VX-809 or 5 µM VX-661. Data represent the mean of measurements on 3-5 replicates per condition ± SEM. Asterisks (*) indicate degree of significant difference calculated by unpaired one-way ANOVA to control (DMSO) using Fisher's LSD test.

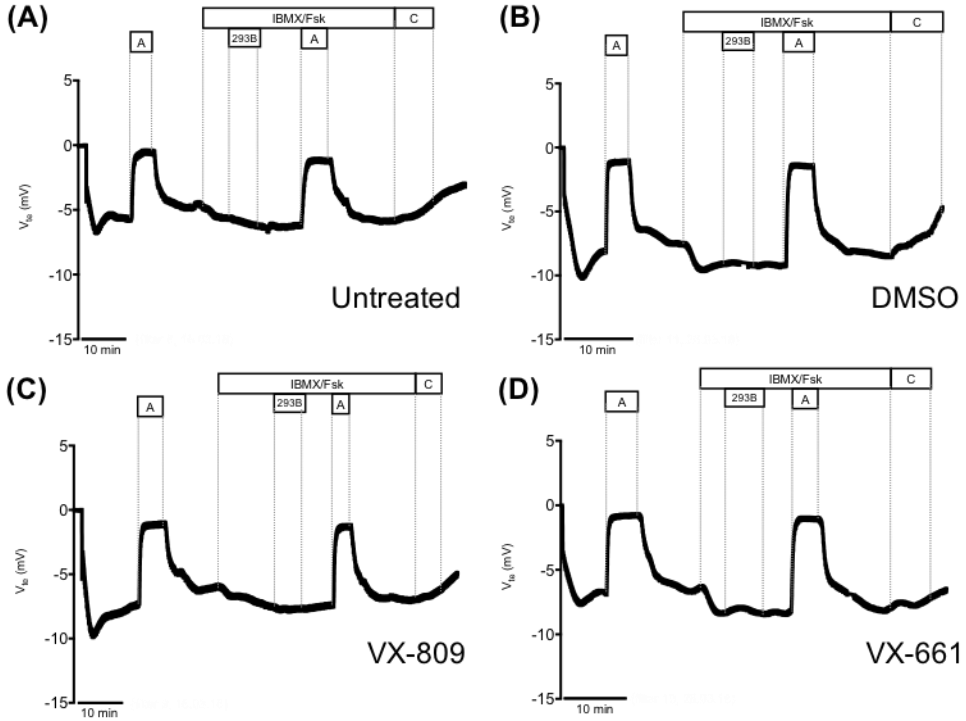

Figure 7.16 – Results from Ussing chamber measurements in NCI-H441 cells. Representative original recordings of the effects of ENaC inhibition (Amil (A), 20 µM, apical), cAMP-dependent activation (IBMX/Fsk, 100 µM/2 µM, basolateral), KCNQ1 channels inhibition (293B, 10 µM, basolateral) and ENaC inhibition after c-AMP activation and KCNN4/SK4 channels inhibition (Clotrimazole (C), 10 µM, basolateral) on transepithelial voltage (V_{te}) in NCI-H441 cells **(A)** untreated or treated with **(B)** 0.05% DMSO, **(C)** 3 µM VX-809 and **(D)** 5 µM VX-661 for 48 h. 7 replicates were measured per condition.